RIGA TECHNICAL UNIVERSITY

Faculty of Computer Science and Information Technology

Department of Engineering Mathematics

IMAD CHADDAD

Ph.D student of the Mathematical Modeling program

THE INFLUENCE OF SURFACE ROUGHNESS ON THE STRUCTURE OF MAGNETOHYDRODYNAMIC FLOWS AND STABILITY OF SHALLOW WATER FLOWS

Scientific supervisors :

Dr. habil.phys ,

Professor M.Ya.Antimirov

(Till 20.03.2005)

Dr. Math Professor Kolishkin.A

RIGA 2008

ABSTRACT

The main topic of the PhD thesis is the analysis of the factors that influence the structure and stability of magnetohydrodynamic (MHD) flows and shallow water flows. In particular, we shall concentrate on the effect of roughness of the boundary. Methods of analysis are based on analytic solutions which are found for some MHD flows over roughness elements in strong magnetic fields in rectangular ducts. The MHD solutions described in our work facilitate the investigation of the redistribution of the fluid in a region where the magnetic field is strong (the Hartmann number is large). The analysis of the behavior of MHD flows at high Hartmann numbers is a topic of increasing interest since it is mainly applicable to MHD devices such as pumps, and MHD generators. The main features of MHD liquid-metal flows at large Hartmann number are as follows: A ‘ flat’ velocity profile in the core of a channel and thin boundary layers near the boundaries. Electric currents induced in the fluid modify the structure of the flow. Knowing the path of these currents it is possible to predict the flow structure. In our analytical solution of the MHD problems where wall roughness is taken into account, the length of the sidewalls of the channel is considered to be infinitely long and the Hartmann number (Ha) is taken to be sufficiently large and even sometimes the boundary limits approach $+\infty$.

Hydraulic engineers are effectively using Chezy formula to estimate the “lumped” effect of friction in turbulent flows for computations of flow rate and losses in channels or pipes as well as for design of open channels. Roughness of the boundary is taken care of by using empirical friction coefficients. These coefficients are related to the Reynolds number of the flow and roughness of the boundary by means of several empirical formulas. The coherent structures in wake flows (flows behind obstacles such as islands) are believed to appear as a final product of hydrodynamic instability of the flow. Methods of weakly nonlinear theory have been applied in the past to different flows and usually lead to amplitude evolution equations for the most unstable mode. One of such equations is the complex Ginzburg-Landau equation. Weakly nonlinear theory is applied to quasi-two-dimensional flows in [22] with Rayleigh friction (internal friction is assumed to be linearly related to the velocity distribution). It is shown in [22] that the coefficients of the Ginzburg-Landau equation for the case where the internal friction is represented by a linear function of the velocity strongly depend on the shape of the base flow profile. As a result it was concluded in [22] that weakly nonlinear models cannot be used for such cases since it is impossible to determine experimentally the base flow velocity distribution with high accuracy and, therefore, one cannot use reliable values of the coefficients of the Ginzburg-Landau equation in the analysis. However, in Chapter 5 of our work we show that small variations of linear stability characteristics do not lead to large changes in the Landau

constant (the Landau constant is the real part of one of the coefficients of the Ginzburg-Landau equation) when a nonlinear Chezy formula is used to model bottom friction.

This work consists of five chapters. All of the chapters are theoretical while Chapter 4 is practical dealing with corrosion of EUROFER steel in the Pb17Li flow and its application to D-T (Deutrium-tritium) plasma confinement in a reactor.

Literature review is presented in the Chapter 1. In addition, the structure of the thesis and the main results are presented.

In Chapter 2 we state the principles of MHD flows and the governing equations that describe the influence of surface roughness on the MHD flow of a conducting liquid metal. Since MHD flow problems are widely studied in channels of various forms under different boundary conditions, the results of such studies have direct applications in different fields of magnetohydrodynamics [29], [38], and [58]. Since magnetohydrodynamics studies the motion of electrically conducting fluids in the presence of magnetic fields, it is obvious that the magnetic field influences the fluid motion. Usually in MHD problems electromagnetic force is added to the equation of motion and the magnetic field (through Ohm's law) changes the fluid motion. We analyze some MHD flow problems in ducts over roughness elements in a strong magnetic field. Analytical solutions of such problems are obtained using the Dirac delta function (see [2], [5], [6], [7], [12] and [13]).

Asymptotic analysis of these problems is performed for the case of strong magnetic fields and graphs of the z-components of the current are shown for different Hartmann numbers. Different boundary layers for the fluid velocity and for the z-components of the currents at large Hartmann numbers are analyzed. The MHD problem for fully developed flow is solved for the cases of a uniform and non-uniform external magnetic field where the surface roughness is taken into account. The distribution of fluid velocity, induced current and its potential and induced magnetic field are derived (see the following references for the analysis of similar problems [2], [5], [11]-[13], [17], [18], [30], [31], [42], [50], [53], [54], [57], [59], [65], [69], and [71]).

In addition, we examine in Chapter 2 the profiles of induced magnetic fields in order to get a clearer idea about the behavior of such flows of an electrically conducting fluid through channels (or ducts). In fact, this problem is directly applicable to other MHD problems such as MHD generators, pumps, accelerators, and flow meters (in a flow meter, a conducting fluid passes through an insulating pipe (duct) across which a uniform magnetic field is applied). A potential gradient is created and it can be measured by probes embedded in the walls of the pipe (this technique is used to measure the flow of blood in human bodies). In addition, the influence of the surface roughness on the MHD flow of a conducting liquid metal may be useful for the

techniques used to set up the cooling system of the Tokamak reactor (Tokamak is an acronym from the Russian words for toroidal magnetic confinement) .

Chapter 3 of our work is devoted to the calculation of some classes of improper oscillatory integrals. It is shown that oscillatory integrals in some cases can be transformed to integrals of non-oscillating functions. Such integrals have direct applications to MHD flows analyzed in the thesis. These results are applied in order to transform the solution of some MHD problems arising in half space $z \geq 0$ with roughness of the surface z=0 (see [3], [4], [6], [7], [17], [21]).

During my seven year stay in Riga, Latvia (one the main MHD application centers in Europe), I had the opportunity to visit some interesting sites related to MHD study such as the Physics Institute in Salaspils where I have seen the three recently planned experimental sessions (each 2000 hours long) which have been successfully completed. Results gained in these investigations demonstrated essential influence of magnetic field on the corrosion processes both in the intensity of corrosion and its character. New results concerning the profile of corrosion are obtained in [55] and [56]. Such studies have an important implication on how to confine and control the burning D-T plasmas by a strong drag of magnetic fields inside a reactor [1], [9], [55], [56], [70] and [73]. In addition, I had the opportunity to participate in some PAMIR MHD International Conferences (4^{th} , 5^{th} and 7^{th} PAMIR International Conferences) . As a result of these activities Chapter 4 of the thesis describing practical aspects related to the effect of surface roughness on MHD flows ([1], [9], [32]-[37], [39], [40], [48], [49], [55]-[57], [60], [64], [68], [70] and [73]) was written.

Chapter 5 is devoted to the analysis of shallow water flow in a weakly nonlinear regime using the complex Ginzburg-Landau equation (CGLE). It is shown in the previous studies [22] related to weakly nonlinear analysis of quasi-two-dimensional flows (shallow water flow is one of the examples considered in [22]) that the values of the Landau's constant differ by a factor of 3 for two different velocity profiles with linear stability characteristics differing by not more that 20%. In other words, the Landau's constant was found to be quite sensitive to the shape of the base flow profile. In Chapter 5 of the thesis the bottom friction is modeled by a nonlinear Chezy formula [66]. The analysis of data presented in Table 3 and Table 4 shows that for a one-parametric family of shallow wake flows the changes in the linear stability characteristics resulted in even smaller changes in the coefficients of the CGLE. As a result, it is plausible to conclude that the complex Ginzburg-Landau equation can be used for the analysis of shallow

wake flows in a weakly nonlinear regime (see [8], [10], [14]-[16], [19], [20], [22], [24], [26], [43]-[47], and [67]) as one of the application of weakly nonlinear models to different flows in fluid mechanics.

ANOTĀCIJA

Promocijas darba galvenais uzdevums ir analizēt faktorus, kuri ietekmē magnētohidrodinamisku (MHD) un seklu ūdens plūsmu struktūru un stabilitāti. Īpaša uzmanība ir veltīta negluduma efektiem uz apgabala robežām. Dažām MHD problēmām ar negluduma elementiem stipros magnētiskos laukos taisnstūrveida kanālos ir konstruēti analītiskie atrisinājumi. Iegūto problēmu atrisinājumi palīdz labāk saprast šķidruma plūsmas sadalījumu apgabalos, kuros magnētisks lauks ir stiprs (Hartmaņa skaitlis ir liels). MHD plūsmu analīze gadījumos, kad Hartmaņa skaitlis ir liels, izraisa lielu interesi sakarā ar pielietojumiem MHD sūkņu un MHD ģenerātoru dizainā un ekspluatēšanā.

Šķidra metāla MHD plūsmas struktūru lielo Hartmaņa skaitļa gadījumā var raksturot šādi: vienmērīgs šķidruma ātruma sadalījums kanāla kodolā un plāni robežslāņi pie apgabala robežām.

Elektriskās strāvas, kas ir inducētas šķidrumā, maina plūsmas struktūru. Ja šo strāvu sadalījums ir zināms, tad plūsmas struktūru var aprakstīt. Analītiskie atrisinājumi MHD problēmām, kurām kanāla sienas negludums ir ņemts vērā, ir konstruēti gadījumā, kad kanāla sānu sienu garums ir bezgalīgi liels.

Hidraulikā inženieri efektīvi izmanto Čezī formulu, lai raksturotu "integrētu" berzes efektu turbulentās plūsmās ar mērķi aprēķināt šķidruma plūsmu caur kanāla šķērsgriezumu vai novērtēt zudumus kanālos un caurulēs, kā arī atklāto kanālu dizainā. Sienas negludums ir ņemts vērā, izmantojot empīriskus berzes koeficientus. Šos koeficientus ar plūsmas Reinoldsa skaitli un sienas negludumu saista dažādas empīriskas formulas.

Kogerentas struktūras plūsmās aiz šķēršļiem (piemēram, aiz salām) rodas kā plūsmas hidrodinamiskās stabilitātes gala products.

Vāji nelineārās stabilitātes teorijas metodes tika pielietotas dažādām plūsmām un parasti noveda pie amplitūdas evolucionāriem vienādojumiem, kuri apraksta visnestabilākās perturbācijas attistību. Viens no šiem vienādojumiem ir kompleksais Ginzburga-Landau vienādojums. Vāji nelineārā teorija ir pielietota rakstā [22] kvazi-divu dimensiju plūsmām ar Releja berzes modeli (ir pieņemts, ka iekšējā berze ir lineāri atkarīga no šķidruma ātruma sadalījuma). Rakstā [22] ir parādīts, ka Ginzburga-Landau vienādojuma koeficienti gadījumā, kad iekšējā berze ir lineāri saistīta ar šķidruma ātruma sadalījumu, ir ievērojami atkarīgi no bāzes plūsmas šķidruma ātruma sadalījuma. Rezultātā rakstā [22] autori secina, ka vāji nelineārus modeļus nedrīkst lietot šajā gadījumā, tāpēc ka nav iespējams eksperimentāli noteikt bāzes plūsmas ātrumu sadalījumu ar

augstu precizitāti. Tas nozīme, ka nav iespējams izmantot ticamas Ginzburga-Landau koeficientu vērtības analīzē.

Promocijas darbā 5. nodaļā ir parādīts, ka mazas izmaiņas lineārās stabilitātes raksturotāju vērtībās nenoved pie lielām izmaiņām (Landau konstante ir viena no Ginzburga-Landau vienādojuma koeficientiem reālā daļa), ja nelineārā Čezī formula ir izmantota, lai modelētu berzi.

Darbs sastāv no piecām nodaļām. Visas nodaļas (izņemot ceturto) ir teorētiskās. 4. nodaļai ir praktisks raksturs, kurā aplūkota korozija EUROFER teraudā Pb17Li plūsmā ar pielietojumiem, kas ir saistīti ar plazmas uzturēšanu reaktorā. 1. nodaļa ir ievada daļa, kurā ir aplūkots literatūras apraksts, kā arī analizēta promocijas darba struktūra un galvenie rezultāti.

2. nodaļā ir formulēti MHD plūsmu pamatprincipi un atbilstošie veinādojumi. Ir analizēta virsmas negluduma ietekme uz vadoša šķidra metāla MHD plūsmu.

Problēmas par MHD plūsmām ir bieži analizētas dažādu viedu kanālos ar dažādiem robežnosacījumiem, tāpēc šo pētījumu rezultātus var izmantot magnētiskās hidrodinamikas pielietojumos [29], [38], [58]. Tā kā magnētiskā hidrodinamika pēta elektrību vadošā šķidruma plūsmu magnētiskā laukā, ir acīmredzams, ka magnētisks lauks ietekmē šķidruma kustības struktūru. MHD problēmās kustības vienādojumam ir pievienots elektromagnētisko spēku raksturojošs loceklis un magnētisks lauks (caur Oma likumu) maina šķidruma kustību. Promocijas darbā analizētas dažas MHD plūsmu problēmas kanālos ar negluduma elementiem stiprā magnētiskā laukā. Šādu problēmu analītiskie atrisinājumi ir konstruēti, izmantojot Diraka delta-funkciju (sk. [2], [5], [6], [7], [12] un [13]). Darbā analizēti šo problēmu asimptotiskie atrisinājumi stiprā magnētiskā laukā un konstruēti strāvas z-komponentes grafiki dažādiem Hartmaņa skaitļiem. Ir analizēti daži robežslāņi šķidruma ātruma sadalījumam un strāvas z-komponentes sadalījumam gadījumā, kad Hartmaņa skaitlis ir liels. MHD problēma pilnīgi attistītai plūsmai ir atrisināta homogēna un nehomogēna magnētisko lauku gadījumā, ņemot vērā sienas negludumu. Ir aprēķināts šķidruma ātruma sadalījums, inducētas strāvas sadalījums kopā ar potenciālu un inducēts magnētisks lauks (lidzīgas problēmas ir analizētas rakstos [2], [5], [11]-[13], [17], [18], [30], [31], [42], [50], [53], [54], [57], [59], [65], [69] un [71]).

1. nodaļā analizēti arī inducēta magnētiska lauka profile, kas ļauj labāk saprast elektriski vadošas plūsmas struktūru kanālos (vai caurulēs). Šīs problēmas analīze var palīdzēt citu MHD problēmu analīzei, piemēram, MHD plūsmas ģenerātoros, sūkņos, paātrinātājos vai plūsmas skaitītājos (plūsmas skaitītājā vadošs šķidrums tek caur izolētu cauruli (vai kanālu) homogēnā magnētiskā laukā). Tas izraisa potenciāla gradientu, kuru var novērtēt ar caurules sienā iebūvētu skaitītāja palīdzību (šo metodi izmanto arī, lai analizētu asins plūsmu cilvēka ķermenī).

Virsmu negluduma ietekme uz MHD šķidra metāla plūsmu ir svarīga pielietojumos (piemēram, atvēsināšanas sistēmas dizains reaktorā Tokamak).

Promocijas darbā 3. nodaļa ir veltīta vienas klases ascilējošo integrāļu aprēķināšanai. Ir parādīts, ka dažos gadījumos oscilējošo integrāli var pārveidot par integrāli, kuram zemintegrāļa funkcija nav oscilējoša. Šāda veida integrāļus var izmantot pielietojumos (viens no tiem ir aplūkots promocijas darbā un atticas uz MHD plūsmām). Iegūtos rezultātus var pielietot, lai transformētu dažu MHD problēmu risinājumu pusplaknē $z \geq 0$ ar negludumu uz robežas $z = 0$ (sk. [3], [4], [6], [7], [17], [21]).

Septiņu gadu laikā, kad es studēju Rīgā (vienā no galvenajiem MHD pētījumu centriem Eiropā), man bija iespēja apmeklēt dažas vietas, kas ir saistītas ar MHD pētījumiem (piemēram, Fizikas Institūts Salaspilī), kur es redzēju trīs eksperimentus (katrs ir 2000 stundu garš), kuri ir jau veiksmīgi pabeigti. Šo eksperimentu rezultāti rāda, ka magnētisks lauks ietekmē gan korozijas intensitāti, gan arī korozijas raksturu. Jaunie rezultāti, kas ir saistīti ar korozijas paraugiem, ir iegūti rakstos [55] un [56]. Šāda veida pētījumi ir svarīgi pielietojumos (piemēram, kā kontrolēt D-T plazmas degšanas procesu reaktorā (sk. [1], [9], [55], [56], [70], [73])). Es arī piedalījos PAMIR MHD starptautiskajās konferencēs (4., 5. un 7. PAMIR konferencēs). Šo aktivitāšu rezultātā ir uzrakstīta darba 4. nodaļa, kas raksturo praktiskus aspektus, saistītus ar sienu negluduma efektu uz MHD plūsmām (sk. [1], [9], [32]-[37], [39], [40], [48], [49], [55]-[57], [60], [64], [68], [70] un [73]).

5. nodaļā ir analizēta sekla ūdens plūsma vāji nelineārā režīmā, izmantojot kompleksā Ginzburga-Landau vienādojumu (KGLV). Rakstā [22] ir parādīts, ka izmantojot vāji nelineāro analīzi kvazi-divu dimensiju plūsmām (sekla ūdens plūsma ir viens no piemēriem, kas ir aplūkots rakstā [22]), Landau konstantes vērtība diviem šķidruma sadalījuma profiliem atšķiras par rezinātāju 3, ja divu profiļu lineārās stabilitātes raksturotāji atšķiras ne vairāk kā par 20%. Citiem vārdiem sakot, Landau konstante ir diezgan jūtīga attiecībā pret bāzes plūsmas šķidruma sadalījuma ātruma izmaiņām.

Promocijas darba 5. nodaļā berzes spēks ir modelēts ar nelineāro Čezī formulu [66]. Datu analīze tabulās 3 un 4 rāda, ka viena parametra sekla ūdens plūsmas saimei lineārās stabilitātes raksturotāju izmaiņas izraisa vēl mazākas izmaiņas KGLV koeficientos.

Rezultātā var secināt, ka KGLV var izmantot sekla ūdens plūsmas analīzei aiz šķēršļiem vāji nelineārā režīmā (sk. [8], [10], [14]-[16], [19], [20], [22], [24], [26], [43]-[47] un [67]) kā vienu no vāji nelineāru modeļu pielietojumiem šķidruma mehānikā.

CONTENTS

Chapter 1

Introduction

Magnetohydrodynamics is a part of fluid mechanics which analyzes the dynamics of electrically conducting fluids and their interactions with magnetic fields. Examples of such fluids include plasmas and liquid metals.

The main set of equations which describes magnetohydrodynamics (MHD) is a combination of the Navier-Stokes equations of fluid dynamics and Maxwell's equations of electromagnetism (see [28], [50], [53], [54]). The corresponding differential equations have to be solved simultaneously. In fact, this is too complex to be done symbolically at all, except for the most trivial cases. For real world problems, numerical solutions are found using super computers. Since MHD is a fluid theory, it cannot treat kinetic phenomena (see [50], [53]). The interaction of a flow of an electrically conducting fluid with external magnetic field results in changes in the flow characteristics. These changes depend on the structure of the flow, the presence of conducting or non-conducting walls, the orientation of the magnetic field with respect to the flow and some other factors. For example, the presence of a magnetic field leads to larger pressure losses since in this case the pressure drop depends mainly on the Hartmann number (see [28], [53], [54]).

Some studies of MHD problems in liquid metal flows have concentrated on the determination of the pressure drop in the flows in straight pipes perpendicular to the magnetic field (see [50], [59]). One of the main problems in MHD that is important in applications is the estimation of pressure losses in pipe bends. Some local variations in pipe bend and special conditions of fluids are used to reduce such pressure losses (see [50], [53], and [59]).

It is known that the velocity distribution in a liquid metal blanket exerts a decisive influence on heat and mass transport. Therefore, since knowledge of this distribution is required, studies in the corrosion and tritium transport field have been conducted (see [1], [55] and [56]). We mention here the latest study of MHD problems in liquid metal blankets of fusion reactor done by I. Micheal [52] and the very recent one done by the European Fusion Development Agreement (EFDA) concerning the European fusion research programme that outlooks the infra-structures needed towards DEMO [37].

Other experiments were conducted to investigate the single phase convective heat transfer in a compact heat sink consisting of 26 rectangular microchannels of 300 μ m width and 800 μ m depth. The relative roughness is estimated to be 4-6 %. Dionized water was used as the working fluid. Tests were performed with the Reynolds number range of 162 and 1257. The inlet liquid temperature of 30, 50, and 70ºC and the heating powers of 140 to 450 w were investigated

(see [57] and [65]). The platform area was $5.0 \times 1{,}53\,\mathrm{cm}^2$. It is found that the friction factors significantly depart from those of conventional theories, possibly attributable to the surface roughness. The temperature is actually dependent on the fluid physical properties which also influences the heat transfer characteristics to some extent. Correlations were provided for the friction factors. Such pressure losses have also been analyzed in pipe bends and in magnetic field subject to local variations. For instance, in both of the papers [57] and [65] channel flows with transverse magnetic field were considered. As can be seen from the cited references, it is important to know the influence of surface roughness on the structure of MHD flows.

The main results obtained in this thesis are briefly summarized below. The principles of MHD flows are described in Chapter 2. The governing equations are presented for the case of a conducting fluid moving in a magnetic field perpendicular to the flow of the form:

$$\vec{B}^e = B_0 \vec{e}_z \tag{1.1}$$

with the boundary $\tilde{z} = 0$ along with the governing equations of magnetohydrodynamics (MHD). These equations represent a combination of the Navier-Stokes equations of fluid dynamics and the Maxwell's equations of electrodynamics:

$$\frac{\partial \vec{v}}{\partial t} + (\vec{v}\nabla)\vec{v} = -\frac{1}{\rho}\nabla p + \nu \Delta \vec{v} + \frac{1}{\rho}\left(\vec{j} \times \vec{B}\right) \tag{1.2}$$

$$\frac{\partial \vec{B}}{\partial t} = curl\left(\vec{v} \times \vec{B}\right) + \nu_m \Delta \vec{B} \tag{1.3}$$

$$div\,\vec{v} = 0 \tag{1.4}$$

$$div\vec{B} = 0 \tag{1.5}$$

Previous works concerning linear approximation to the flow over roughness elements in a strong magnetic field [28], [50] are generalized in [2] for the case of the roughness of the surface considered in the form

$$\tilde{z} = \tilde{\chi}_0 \cos(\pi \tilde{x} / 2L) \tag{1.6}$$

where the conducting fluid is located in the half space $\tilde{z} > 0, -\infty < \tilde{x}, \tilde{y} < +\infty$ and the external magnetic field is of the form $B^c = B_0 e_z$ and the boundary $\tilde{z} = 0$ is non conducting. We assume a steady current flow with the density $\tilde{\vec{j}} = j_0 \vec{e}_x$ in the direction of the x-axis. In this case, if the surface $\tilde{z} = 0$ is ideally smooth then the flow is absent because electromagnetic force $\vec{F} = \tilde{\vec{j}} \times \vec{B}$ is constant and $rot\vec{F} = 0$. Suppose that roughness on the surface $\tilde{z} = 0$ has the rectangular form:

$$\tilde{z} = \tilde{\chi}_0 \ \tilde{f}(\tilde{x}) = \tilde{\chi}_0 \left[\eta(\tilde{x} + L) - \eta(\tilde{x} - L)\right] = \begin{cases} \tilde{\chi}_0, & -L < \tilde{x} < L, \\ 0, & |\tilde{x}| > L, \end{cases} \tag{1.7}$$

In the beginning of Chapter 1 of our work we describe the result obtained in monograph [75] where MHD flow of an incompressible fluid in an infinitely long plane channel with the constant cross section with the walls parallel to the y-axis is considered. The problem discussed in [75] is generalized in our work for the case of surface roughness of the form:

$$\widetilde{z} = \begin{cases} \widetilde{f}(\widetilde{x}), -L \le \widetilde{x} \le L, -\infty < \widetilde{y} < +\infty, \\ 0, \widetilde{x} \notin (-L, L). \end{cases} \tag{1.8}$$

It is shown in Chapter 2 that dimensionless MHD equations for the fluid velocity $V_y(y,z)$, and the potential for the induced current $\Phi(y,z)$ have the form:

$$\Delta V_y - Ha^2 V_y + Ha \frac{\partial \Phi}{\partial x} = 0, \tag{1.9}$$

$$\Delta \Phi = Ha \frac{\partial V_y}{\partial x}, \tag{1.10}$$

where Ha denotes the Hartmann number.

A fully developed MHD flow is considered in the direction of the y-axis while the external magnetic field and the given external current have only x and z components which do not depend on the y variable. In fact, it is proved in Chapter 2 that if the external magnetic field has the form (1.1) and the flow is fully developed with the velocity

$$\vec{V}_y = \widetilde{V}_y(\widetilde{y}, \widetilde{z})\vec{e}_y \tag{1.11}$$

then the induced magnetic field is of the form

$$\vec{\widetilde{B}}^i = \widetilde{B}^i(\widetilde{x}, \widetilde{z})\vec{e}_y \tag{1.12}$$

Roughness in the form of an infinitely long prism is considered in the thesis. An analytical solution of the problem about MHD flow of a conducting fluid in the half space (z > 0) with a special form of roughness on the boundary $z = 0$ is obtained (see [2], [12], [13]). Besides, the results of numerical calculations and streamlines of induced current are presented. We investigate the asymptotic of the functions $V_y(x,z)$, $j_x(x,z)$ $j_z(x,z)$ in more detail. As a result, several boundary layers for the functions $V_y(x,z)$ and $j_z(x,z)$ as $Ha \to \infty$ are obtained. The results obtained by exact formula and asymptotic formula for the distribution of the component $j_z(x,z)$ are compared for different Hartmann numbers. For Hartmann numbers $Ha \ge 10$ the results obtained by exact formula and asymptotic formula practically coincide. The calculations are done with “Mathematica”.

The streamlines of the current $j(x,z)$ are calculated by the formula:

$$\frac{dz}{dx} = \frac{j_z(x,z)}{j_x(x,z)} \qquad (1.13)$$

Calculations are done for the Hartmann numbers $Ha = 5$ and $Ha = 10$ and for various values of initial conditions $z(0)$.

The solutions of certain problems in MHD flow of a conducting fluid in the half space ($z > 0$) are expressed in terms of improper integrals of the product of some meromorphic function and the function $\exp(-a\sqrt{\lambda^2 + b^2}\cos\lambda\cos\lambda x)$ where $a > 0$, $b > 0$ and $x > 0$. It is difficult to calculate these integrals numerically since the integrands are strongly oscillating at the large x. Methods of calculation of such integrals are discussed in Chapter 3 of our work.

We consider the improper integral having the form:

$$\int_0^\infty \frac{P_n(\lambda^2)}{Q_m(\lambda^2)} e^{-a\sqrt{\lambda^2+b^2}} \frac{\cos\lambda\cos\lambda x}{\lambda^2 - \frac{\lambda^2}{4}} d\lambda \qquad (1.14)$$

It is assumed that all the zeros of the polynomial $Q(\lambda^2)$ are simple and have the form:

$$\lambda_k{}^2 = -a_k{}^2,\ k = 1, 2, \cdots 3, ..., n. \qquad (1.15)$$

The following theorem (see [4]) is used to calculate the integral.

Theorem.

If $F_c(\lambda)$ and $\Phi_c(\lambda)$ are the Fourier cosine transforms of functions $f(x)$ and $\varphi(x)$, respectively, then

$$\int_0^\infty F_c(\lambda)\Phi_c(\lambda)\cos\lambda x d\lambda = \frac{1}{2}\int_0^\infty \varphi(\xi)\left[f(|x-\xi|) + f(x+\xi)\right]d\xi . \qquad (1.16)$$

The functions $\Phi_c(\lambda)$ and $F_c(\lambda)$ are defined by the formulas

$$\frac{P_n(\lambda^2)}{Q_m(\lambda^2)} \frac{\cos\lambda}{\lambda^2 - \frac{\pi^2}{4}} = \Phi_c(\lambda), \quad e^{-a\sqrt{\lambda^2+b^2}} = F_c(\lambda). \qquad (1.17)$$

The inverse Fourier cosine transforms of the functions $\Phi_c(\lambda)$ and $F_c(\lambda)$ are given by

$$I_1 = \sqrt{\frac{2}{\pi}}\int_0^\infty \frac{P_n(\lambda^2)}{Q_m(\lambda^2)} \frac{\cos\lambda\cos\lambda x\, d\lambda}{\lambda^2 - \frac{\pi^2}{4}} = \varphi(x),$$

$$I_2 = \sqrt{\frac{2}{\pi}}\int_0^\infty e^{-a\sqrt{\lambda^2+b^2}}\cos\lambda x\, d\lambda = \sqrt{\frac{2}{\pi}}\frac{K_1(b\sqrt{a^2+x^2})}{\sqrt{a^2+x^2}} = f(x) . \qquad (1.18)$$

Each of the integrals in (1.18) is evaluated separately and then formula (1.16) is used to transform the integral of oscillatory function to the integral of a monotonic function.

Hence, it is shown in Chapter 3 of the thesis that integrals (1.14) are transformed into integrals of monotone functions using the convolution theorem for product of two Fourier cosine transforms

and the formulas (1.17) and (1.18). Such a transformation is quite useful in solving some MHD problems (see [6], [7], [13] and [17]).

Linear approximation to the flow over roughness elements in a strong magnetic field is a subject of increasing interest nowadays especially due to the fact that this study is directly linked to other MHD phenomena such as the MHD studies on the EUROFER corrosion of Pb17-Li at 550°C. Three experimental sessions had been recently completed in the Physics Institute in Salaspils. The surface of the corroded metal on the wall is described by a simplest periodic structure of the form

$$Z = Z(y) = \chi_0 \cos(\pi y / L) \tag{1.19}$$

where χ_0 and L represent the scales of the considered roughness ([2], [13], [55] and [56]). Results gained in these investigations demonstrated essential influence of magnetic field on the corrosion processes both in the intensity of corrosion and its character. New results concerning the profile of corrosion are obtained [55], [56]. Note that the results of this study can be used to decide how to control the Deuterium-Tritium (D-T) burning plasmas by a strong magnetic field drag inside of a reactor [1], [55], [56], [70] and [73]. Recent results are reported in Chapter 4 of this work.

The Deuterium-Tritium (D-T) cycle is described by the relationship

$$D + T \rightarrow n + \alpha + 17.58MeV \tag{1.20}$$

The components of this equation are briefly explained in the following papers ([1], [9], [28] ,[32]-[37], [40], [49], [56], [64], [70] and [73]).

Many works and experiments were done with the purpose of reducing pressure losses in MHD duct flows. Two concepts are considered ideally practical for diminishing the pressure losses. The first is determined by an advantageous channel routing and the other relies on the reduction of the electrical conductivity of the channel. Because of the fact that an advantageous channel routing is depending mainly on the corrosion rate of the channel's wall, for this reason in Chapter 4 of our work we consider the investigation of corrosion phenomena in EUROFER steel in Pb17-Li stationary flow exposed to a magnetic field as for being one of the candidate materials used for fusion reactors (see [1], [9], [28], [32]-[37] , [40] , [49] , [51], [55], [56] , [62], [70] and [73]).

Chapter 5 is devoted to the analysis of shallow water flow in a weakly nonlinear regime using the Ginzburg-Landau equation (CGLE). One of the major reasons that led to the study of this part is the analysis performed in [22] for different quasi-two-dimensional flows (one of the examples of such flows is shallow water flow). Calculations presented in [22] showed that the values of the Landau's constants differ by a factor of 3 for two different velocity profiles with very similar linear stability characteristics. The analysis in [22] is performed under the

assumption that the internal friction is a linear function of the velocity. In particular, for quasi-two-dimensional flows the internal friction was modelled in [22] by means of the Rayleigh's formula

$$\vec{f}_R = -\lambda_R \vec{u} \tag{1.21}$$

In our work we show that for the case where the friction force is a nonlinear function of the velocity the changes in the linear stability characteristics resulted in even smaller changes in the coefficients of the CGLE. As a result, it is plausible to conclude that the complex Ginzburg-Landau equation can be used for the analysis of shallow wake flows in a weakly nonlinear regime ([8], [10], [14], [15], [16], [19], [20], [26], [43]-[47], [67]).

It is assumed here that the CGLE can be used to describe spatio-temporal dynamics of shallow wake flows. We consider the base flow of the form

$$\vec{U} = (U(y),0) \tag{1.22}$$

where

$$U(y) = 1 - \frac{2R}{1-R}\frac{1}{\cosh^2(\alpha y)}. \tag{1.23}$$

The profile of the base flow which is described in [19] after careful analysis of available experimental data for deep water flows behind circular cylinders is adopted in the present study.. The parameter R is the velocity ratio: $R = (U_m - U_a)/(U_m + U_a)$, where U_m is the wake centerline velocity and U_a is the ambient velocity, and $\alpha = \sinh^{-1}(1)$. It is shown in [19] that under the rigid-lid assumption the linear stability of wake flows in shallow water is described by the following eigenvalue problem:

$$\varphi_1''(U - c + SU) + SU_y\varphi_1' + \left(k^2 - U_{yy} - k^2U - \frac{S}{2}kU\right)\varphi_1 = 0 \tag{1.24}$$

$$\varphi_1(\pm\infty) = 0, \tag{1.25}$$

where the perturbed stream function of the flow, $\psi(x,y,t)$, is assumed to be of the form

$$\psi(x,y,t) = \varphi_1(y)\exp[ik(x-ct)] + c.c. \tag{1.26}$$

We use the collocation method based on Chebyshev polynomials to solve (1.24) – (1.25) numerically.

The collocation points r_j are

$$r_j = \cos\frac{\pi j}{N},\ j = 0,1,...,N. \tag{1.27}$$

Applying the collocation method we obtain the following equation:

$$(B - \lambda C)a = 0 \tag{1.28}$$

where B and C are complex-valued matrices and

$a = (a_1 a_2 ... a_N)^T$.

The generalized eigenvalue problem (1.28) is solved numerically by means of the IMSL routine DGVCCG. The critical values of the stability parameters k, S and c for different values of R are given in Table 3 (here $S_c = \max_k S$). Next, we perform weakly nonlinear analysis in the neighborhood of the critical point. As a result, calculations presented in our paper demonstrate that the coefficients of the CGLE are not so sensitive to the variation of the parameter R of the base flow and not only the Landau constant is not so sensitive to the changes in the profile but all the coefficients of the CGLE do not vary too much. The results that support such conclusions are shown in Tables 3 and 4. Our results contradict the conclusions in [22] that it would be impossible to apply methods of weakly nonlinear theory in practice since the base flow profile cannot be determined very precisely in experiments, and the coefficients of the CGLE are found to be quite sensitive to the variation of the base flow profile.

Chapter 2

FLOW OVER ROUGHNESS ELEMENTS IN A STRONG MAGNETIC FIELD

2.1 PRINCIPLES OF MHD FLOWS

The main MHD equations can be derived from the Navier-Stokes equations of fluid dynamics and the Maxwell equations. These MHD equations describe the complex couplings between the flow variables, i.e. the density, the velocity, the total energy, the pressure tensor, the gravitational force, and the magnetic field. As a matter of fact, MHD (magnetohydrodynamics) has a vast range of practical applications such as control over motion of liquid metal in ducts and creation of new MHD pumps which do not contain movable elements. In addition to that, MHD has also important applications in astrophysics for the explanation of the nature of the earth's magnetic field [21].

The main principles that govern MHD flows are:

1. Electric eddy currents flow in a plane perpendicular to the main direction of the flow. They cause the thickness of the wall boundary layer to decrease and wall friction to increase, i.e. the Hartmann effects.
2. If the channel wall is electrically conducting, the eddy currents are back-circuited via this wall. This gives rise to the electromagnetic volume forces contracting the fluid motion. Note that electrically insulating walls are considered in our work.
3. When the channel flow enters and leaves the homogeneous magnetic field zone, i.e., the field boundary zones, eddy currents are generated which likewise cause pressure losses counteracting the flow.
4. Another effect occurring both in the fluid flowing transversally and in the fluid flowing parallel to the magnetic field causes turbulence suppression. This laminarization leads to a big increase in the critical Reynolds number. Here we add some comments on how to reduce the MHD pressure losses.

The first concept is guaranteed when the coolant flow is transformed from the poloidal flow direction characterized by slow velocity to a toroidal flow in narrower channels surmounting the original channels and characterized by a higher velocity . The flow in the poloidal direction is almost perpendicular to the direction of the magnetic flux density of the plasma holding field and is associated with MHD pressure losses. The higher flow velocity guarantees a good heat transfer. The abrupt change of flow direction (poloidal-toroidal-poloidal) in the magnetic field has two characteristics. Firstly, this elbow constitutes the point of the maximum loading of the first wall. Secondly, the sharp deflection in the elbow might cause de-attachement of flow

accompanied by the formation of hot spots. To counteract this process, guide plates of baffles could be installed in the deflection zone (see [29], [57] and [65]).

The second concept is based on insulation between liquid and wall. Both the required pumping power and the mechanical stresses in the channel wall might become inadmissibly high. Reduction in stress by increasing the wall thickness is not possible because in non-insulated walls the pressure loss in a first approximation increases linearly with the wall thickness. A way out of this problem could consist in providing an electric insulation between the liquid metal and the supporting wall. Two methods are eligible. The most obvious idea would be to coat the inner side of the channel wall with an insulating material. However, no suitable material and coating technique have been found till this day to achieve an adequate service life if wall is in contact with the liquid metal. Therefore, the second method is more promising under which the wall is given a sandwich structure. The liquid metal is in contact with a thin (about 1 mm thick) wall supported via an electric insulator by the load carrying channel wall. This technique is applied above all for the supply and return manifolds of the blanket because the radiation exposure of the insulator is negligibly small in these manifolds. Two mathematical models for MHD-flows in a fusion reactor blanket have been considered. The first one describes fully-developed flows and the second governs non-uniform and non-steady-state flows. This model is derived from 3-D Navier-Stokes-Maxwell equations by their integration along the direction of the applied magnetic field (see [1], [29], [55], [56], [57] and [65]) .

2.2 THE FORM OF MAGNETIC FIELD AND MHD EQUATIONS FOR FULLY DEVELOPED MHD FLOW CAUSED BY ROUGHNESS OF THE BOUNDARY

The MHD flow of an incompressible fluid in an infinitely long channel with the constant cross section when the wall is taken parallel to the $\tilde{y}$ axis is considered in [5]. It is proved that the velocity of a fully developed flow in such channel is:

$$\vec{V} = V_y(x,z)\vec{e}_y, \tag{2.1}$$

and the magnetic field $\vec{B}$ is of the form

$$\vec{B} = \vec{B}_\perp(x,z) + B_y(x,y,z)\vec{e}_y, \tag{2.2}$$

where

$$\vec{B}_\perp(x,z) = B_x(x,z)\,\vec{e}_x + B_z(x,z)\vec{e}_z \tag{2.3}$$

Substituting (2.2) into the equation div $\vec{B} = 0$, we obtain

$$\frac{\partial B_y}{\partial y} = \theta \text{ , i.e. } B_y = B_y(x,z) = b(x,z) + y\theta(x,z) \tag{2.4}$$

at the condition that

$$div\,\vec{B}_\perp = -\theta(x,z) \tag{2.5}$$

Further analysis shows that

$$\theta(x,z) = C = const, \quad C = 0 \text{ or } C \neq 0 \tag{2.6}$$

and that $B_y(x,z)\vec{e}_y$ is the induced magnetic field, $\vec{B}_\perp(x,z)$ is the given external magnetic field. We consider a similar problem about the MHD flow in half-space $\tilde{z} \geq 0$ caused by roughness of the boundary $\tilde{z} = 0$. In contrast to what is done in monograph [75] it is assumed here at the first that the induced magnetic field $\vec{B}^i$ has the x, y and z components. After that the symmetry of the flow is used and it is proved that the induced magnetic field has a single y-component, i.e. has the form (2.4) with $\theta = 0$. We consider uniform external magnetic field in subsection 2.2.1 and non uniform magnetic field in subsection 2.2.2.

2.2.1 THE PROBLEM IN THE CASE OF A UNIFORM EXTERNAL MAGNETIC FIELD

The geometry of the flow is given in Fig. 1.

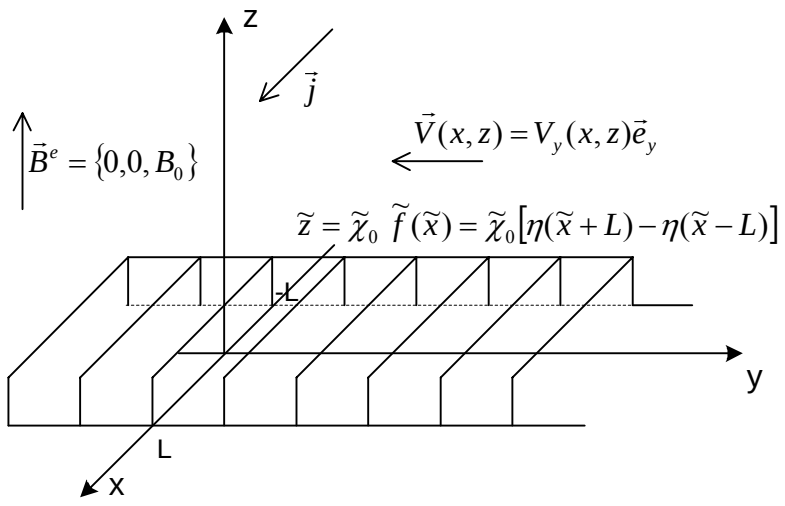

Figure 1. The geometry of the flow.

The conducting fluid is located in the half-space $\tilde{z} > 0$, $-\infty < \tilde{x}, \tilde{y} < +\infty$. The external magnetic field is of the form :

$$\vec{B}^e = B_0 \vec{e}_z \ . \tag{2.7}$$

A steady current flows with the density $\vec{j}_0 = j_0 \vec{e}_x$ in the direction of the x-axis. If the surface $\tilde{z} = 0$ is ideally smooth, then the flow is absent because the electromagnetic force $\vec{F} = \vec{j} \times \vec{B}^e$ is constant and rot $\vec{F} = 0$. Suppose further that roughness of the surface $\tilde{z} = 0$ is of the form :

$$\tilde{z} = \begin{cases} \tilde{f}(\tilde{x}), -L \le \tilde{x} \le L, -\infty < \tilde{y} < +\infty, \\ 0, \tilde{x} \notin (-L, L). \end{cases} \tag{2.8}$$

In this case the full current is equal to $\vec{j} = \vec{j}_0 + \vec{j}(\tilde{x}, \tilde{z})$ and the flow of the fluid with velocity

$$\vec{V}_y = \tilde{V}_y(\tilde{y}, \tilde{z}) \vec{e}_y \tag{2.9}$$

arises in the direction opposite to the $\tilde{y}$ -axis (see Fig.1).

We will prove that the induced magnetic field $\vec{B}^i$ in this case has the form

$$\tilde{\vec{B}}^i = \tilde{B}^i(\tilde{x}, \tilde{z}) \vec{e}_y \tag{2.10}$$

and the MHD equations for the fluid velocity $V_y(y, z)$ and for the potential of the induced current $\Phi(y, z)$ have the following dimensionless form

$$\Delta V_y - Ha^2 V_y + Ha \frac{\partial \Phi}{\partial x} = 0, \tag{2.11}$$

$$\Delta \Phi = Ha \frac{\partial V_y}{\partial x}, \tag{2.12}$$

where $\Delta = \partial^2 / \partial x^2 + \partial^2 / \partial z^2$, $Ha = B_0 L \sqrt{\sigma / \rho \nu}$ is the Hartmann number and σ, ρ, ν are, respectively, the conductivity, the density and the viscosity of the fluid. We use the MHD equation of incompressible fluid and the Ohm's law (see [29], [50] and [58]) :

$$\left(\tilde{\vec{V}} \nabla\right) \tilde{\vec{V}} = -\frac{1}{\rho} grad \tilde{P} + \nu \Delta \tilde{\vec{V}} + \frac{1}{\rho} \left(\tilde{\vec{j}} \times \tilde{\vec{B}} \right), \tag{2.13}$$

$$\vec{\tilde{j}} = \sigma\left(\vec{\tilde{E}} + \vec{\tilde{V}} \times \vec{\tilde{B}}\right) = \sigma\left(-grad\tilde{\Phi} + \vec{\tilde{V}} \times \vec{\tilde{B}}\right), \tag{2.14}$$

where $\Delta = \frac{\partial^2}{\partial \tilde{x}^2} + \frac{\partial^2}{\partial \tilde{y}^2} + \frac{\partial^2}{\partial \tilde{z}^2}$, $\quad \vec{\tilde{V}}\nabla = V_x \frac{\partial}{\partial \tilde{x}} + V_y \frac{\partial}{\partial \tilde{y}} + V_z \frac{\partial}{\partial \tilde{z}}$.

In our case

$$\vec{\tilde{V}} = \tilde{V}_y(x,z)\vec{e}_y, \tag{2.15}$$

$$\vec{B} = \vec{\tilde{B}}^i(\tilde{x},\tilde{z}) + \vec{B}^e, \tag{2.16}$$

where $\vec{\tilde{B}}^i$ is the induced magnetic field.

First , we prove that

$$\vec{\tilde{B}}^i(\tilde{x},\tilde{z}) = B^i(\tilde{x},\tilde{z})\vec{e}_y \tag{2.17}$$

at the condition that the vector of the induced current has the form

$$\vec{\tilde{j}}(\tilde{x},\tilde{z}) = j_x(\tilde{x},\tilde{z})\vec{e}_x + j_z(\tilde{x},\tilde{z})\vec{e}_z. \tag{2.18}$$

It will be shown as the corollary that the vector of fluid velocity is given by (2.15). For this purpose we use the Bio-Savare's law, according to which the induced magnetic field vector $d\vec{B}$ created by an element $d\vec{l}$ of infinitely thin wire directed along the current $\vec{I}$ is equal to

$$d\vec{\tilde{B}} = I\frac{d\vec{l} \times \vec{r}_{M'M}}{\left|\vec{r}_{M'M}\right|^3}, \tag{2.19}$$

where $\vec{r}_{M'M}$ is a radius vector connecting the point $M'(\tilde{x}',\tilde{y}',\tilde{z}') \in d\vec{l}$ and the point of observation $M(\tilde{x},\tilde{y},\tilde{z})$ (see Fig. 2):

$$\vec{r}_{M'M} = (\tilde{x} - \tilde{x}')\vec{e}_x + (\tilde{y} - \tilde{y}')\vec{e}_y + (\tilde{z} - \tilde{z}')\vec{e}_z. \tag{2.20}$$

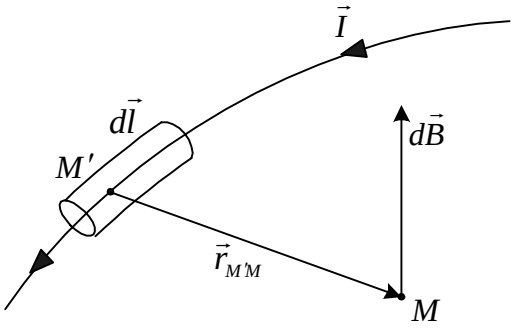

Figure 2. Magnetic induction $d\vec{B}$ caused by elementary current $Id\vec{l}$.

Without loss of generality we can choose the point of observation *M (0, 0, 0)* in the origin. For each point $M'(\tilde{x}', \tilde{y}', \tilde{z}')$ in the fluid we always can choose the symmetric point $N'(\tilde{x}', -\tilde{y}', \tilde{z}')$ with respect to point *M (0, 0, 0).* We consider the magnetic induction $d\vec{B}$ caused by elementary current $Id\vec{l}$ passing through the point $M'(\tilde{x}', \tilde{y}', \tilde{z}')$ and by elementary current $I_1 d\vec{l}$ passing through the symmetric point $N'(\tilde{x}', -\tilde{y}', \tilde{z}')$ (see Fig. 3). Here $\vec{I}$ and $\vec{I}_1$ are the currents with density $\tilde{\tilde{j}}(\tilde{x}, \tilde{z})$ given by formula (2.18).

Since vector $\tilde{\tilde{j}}(\tilde{x}, \tilde{z})$ does not depend on variable $\tilde{y}$ we have $\vec{I}_1 = \vec{I}$.

Using formula(2.19) we obtain

$$d\vec{B}\Big|_M = Dd\vec{l} \times \left(\vec{r}_{M'M} + \vec{r}_{N'M}\right) \tag{2.21}$$

where $D = I\left|r_{MM'}\right|^{-3}$, $d\vec{l} = dl_x \vec{e}_x + dl_z \vec{e}_z$, (2.22)

$$\vec{r}_{M'M} = -\left(\tilde{x}'\vec{e}_x + \tilde{y}'\vec{e}_y + \tilde{z}'\vec{e}_z\right),\ \vec{r}_{N'M} = -\left(\tilde{x}'\vec{e}_x - \tilde{y}'\vec{e}_y + \tilde{z}'\vec{e}_z\right). \tag{2.23}$$

Substituting (2.22), (2.23) into (2.21) we obtain:

$$d\vec{B} = -D\left(dl_x \vec{e}_x + dl_z \vec{e}_z\right) \times \left(2\tilde{x}'\vec{e}_x + 2\tilde{z}'\vec{e}_z\right)$$

or

$$d\vec{B} = D\left(2\tilde{z}'dl_x - 2\tilde{x}'dl_z\right)\vec{e}_y . \tag{2.24}$$

Summing formula (2.24) over the whole elements $d\vec{l}$ in the fluid we obtain formula (2.17),

which completes the proof.

In order to obtain equations (2.11), (2.12) we substitute vectors $\vec{\tilde{V}}$ and $\vec{\tilde{B}}^i$ from (2.15), (2.16) and (2.17) into equations (2.13) and (2.14). We have :

$$\vec{\tilde{V}} = \tilde{V}_y(x,z)\vec{e}_y\,,\quad \vec{\tilde{B}}(\tilde{x},\tilde{z}) = B_0\vec{e}_z + \tilde{B}^i(\tilde{x},\tilde{z})\vec{e}_y\,. \tag{2.25}$$

Consequently,

$$\vec{\tilde{V}} \times \vec{\tilde{B}} = \tilde{V}_y(x,z)\vec{e}_y \times \left(B_0\vec{e}_z + \tilde{B}^i(\tilde{x},\tilde{z})\vec{e}_y\right) = B_0\tilde{V}_y(x,z)\vec{e}_x\,, \tag{2.26}$$

$\vec{\tilde{j}} \times \vec{\tilde{B}} = \sigma\left(-\,grad\tilde{\Phi} + B_0\tilde{V}_y\vec{e}_x\right)\times\left(B_0\vec{e}_z + \tilde{B}^i\vec{e}_y\right)$, i.e.

$$\vec{\tilde{j}} \times \vec{\tilde{B}} = \sigma\left\{B_0\frac{\partial\tilde{\Phi}}{\partial\tilde{x}}\vec{e}_y - \frac{\partial\tilde{\Phi}}{\partial\tilde{x}}\tilde{B}^i\vec{e}_z + \frac{\partial\tilde{\Phi}}{\partial\tilde{z}}\tilde{B}^i\vec{e}_x - {B_0}^2\tilde{V}_y\vec{e}_y + B_0\tilde{V}_y\tilde{B}^i\vec{e}_z\right\}, \tag{2.27}$$

$$\left(\vec{\tilde{V}}\nabla\right)\vec{\tilde{V}} = 0\,. \tag{2.28}$$

Substituting (2.27) and (2.28) into (2.13) and projecting the resulting equation on the y axis we

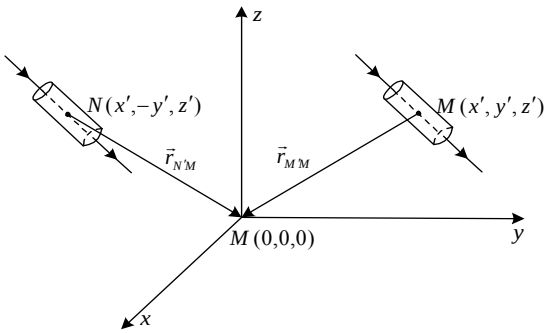

Figure 3. Symmetric representation needed to the proof of formula (2.24).

obtain

$$0 = -\frac{1}{\rho}\frac{\partial\tilde{P}(\tilde{x},\tilde{y},\tilde{z})}{\partial\tilde{y}} + \nu\left(\frac{\partial^2}{\partial\tilde{x}^2} + \frac{\partial^2}{\partial\tilde{z}^2}\right)\tilde{V}_y(\tilde{x},\tilde{z}) + \frac{\sigma}{\rho}\left[B_0\frac{\partial\tilde{\Phi}(\tilde{x},\tilde{z})}{\partial\tilde{x}} - B_0^2\tilde{V}_y(\tilde{x},\tilde{z})\right]. \tag{2.29}$$

Since all of the terms in equation (2.29) except the term $\partial\tilde{P}/\partial\tilde{y}$ do not depend on the variable $\tilde{y}$ then the term $\partial\tilde{P}/\partial\tilde{y}$ also does not depend on the variable $\tilde{y}$, i.e.

$$\frac{\partial\tilde{P}}{\partial\tilde{y}} = F_1(\tilde{x},\tilde{z}) \Rightarrow \tilde{P} = F_1(\tilde{x},\tilde{z})\tilde{y} + F_2(\tilde{x},\tilde{z}), \tag{2.30}$$

where F_1 and F_2 are arbitrary functions.

Substituting (2.30) and (2.27) into (2.13) and projecting the resulting equation on the x and z axes we obtain the following two equations:

$$0 = -\frac{\tilde{y}}{\rho}\frac{\partial F_1}{\partial \tilde{x}} - \frac{1}{\rho}\frac{\partial F_2}{\partial \tilde{x}} + \frac{\sigma}{\rho}\frac{\partial \tilde{\Phi}}{\partial \tilde{z}}B^i, \tag{2.31}$$

$$0 = -\frac{\tilde{y}}{\rho}\frac{\partial F_1}{\partial \tilde{z}} - \frac{1}{\rho}\frac{\partial F_2}{\partial \tilde{z}} + B^i\left(-\frac{\partial \tilde{\Phi}}{\partial \tilde{x}} + B_0 V_y\right). \tag{2.32}$$

Since all the terms on the right hand sides of equations (2.31) and (2.32) except the first ones do not depend on $\tilde{y}$, then the first terms in these equations also do not depend on $\tilde{y}$, i.e.

$$\frac{\partial F_1}{\partial \tilde{x}} = 0, \quad \frac{\partial F_1}{\partial \tilde{z}} = 0 \Rightarrow \quad F_1 = C = const. \tag{2.33}$$

Consequently, equations (2.30)-(2.32) are of the form:

$$\frac{\partial \tilde{P}}{\partial \tilde{y}} = C \ \ (C \text{ is a constant}) \tag{2.34}$$

$$\Rightarrow \tilde{P}(\tilde{x}.\tilde{z}) = C\tilde{y} + F_2(\tilde{x}.\tilde{z}), \tag{2.35}$$

$$\frac{\partial F_2(\tilde{x},\tilde{z})}{\partial \tilde{x}} = \sigma\frac{\partial \tilde{\varphi}}{\partial \tilde{z}}B^i, \tag{2.36}$$

$$\frac{\partial F_2(\tilde{x},\tilde{z})}{\partial \tilde{z}} = \rho B^i\left(\frac{\partial \tilde{\Phi}}{\partial \tilde{x}} - B_0\tilde{V}_y\right). \tag{2.37}$$

In our problem the external pressure gradient is absent. As a result, then it follows from (2.34) and (2.35) that

$$\text{C} = 0, \ \tilde{P}(\tilde{x},\tilde{z}) = F_2(\tilde{x},\tilde{z}). \tag{2.38}$$

Thus, equation (2.29) can be written as follows:

$$\nu\left(\frac{\partial^2}{\partial \tilde{x}^2} + \frac{\partial^2}{\partial \tilde{z}^2}\right)\tilde{V}(\tilde{x},\tilde{z}) + \frac{\sigma}{\rho}\left[B_0\frac{\partial \tilde{\Phi}(\tilde{x},\tilde{z})}{\partial \tilde{x}} - B_0{}^2\tilde{V}_y(\tilde{x},\tilde{z})\right] = 0. \tag{2.39}$$

We use the dimensionless quantities by taking the values $L, \nu/L, B_0, \nu\sqrt{\rho\nu/\sigma}, \nu\sqrt{\rho\nu/\sigma}/L^2$ as the scales of length, velocity, magnetic field, potential and current, respectively.

To obtain equation (2.12), it is sufficient to apply operation of divergence to equation (2.14)

and use the equation of continuity $div\,\tilde{\vec{j}} = 0$ and equation (2.26):

$$0 = -\Delta\tilde{\Phi} + B_0 div\tilde{V}_y(\tilde{x},\tilde{z})\vec{e}_y\,, \tag{2.40}$$

i.e.

$$\Delta\tilde{\Phi} = B_0\frac{\partial\tilde{V}_y}{\partial\tilde{y}}\,. \tag{2.41}$$

Passing in formulae (2.41) to the dimensionless variables, we obtain equation (2.12).

To obtain pressure $\tilde{P}(\tilde{x},\tilde{z})$ we need to know the function $F_2(\tilde{x},\tilde{z})$, i.e. we should use a system of nonlinear equations (2.36) and (2.37). First, we can solve the linear system (2.11), (2.12) with the corresponding boundary conditions and obtain the functions $\tilde{V}_y(\tilde{x},\tilde{z})$ and $\tilde{\Phi}(\tilde{x},\tilde{z})$. After that we can obtain the induced magnetic field B^i, using equations $rotB^i = grad\tilde{\Phi}$, $divB^i = 0$. As a result, the right hand sides of equations (2.36) and (2.37) will be known functions and we get the function $\tilde{P}(\tilde{x},\tilde{z}) = F_2(\tilde{x},\tilde{z})$ from the system (2.36) and (2.37) up to an arbitrary constant.

2.2.2 THE PROBLEM IN THE CASE OF A NON UNIFORM EXTERNAL MAGNETIC FIELD

Assume that the external magnetic field can be represented in the form:

$$\vec{B^e} = \vec{B^i}_{\perp}(\tilde{x},\tilde{z}) = B_x(\tilde{x},\tilde{z})\vec{e}_x + B_z(\tilde{x},.\tilde{z})\vec{e}_z\,. \tag{2.42}$$

Since vector $\vec{B^e}$ does not depend on the variable y, the formula for $\vec{B^i}(\tilde{x},\tilde{z})$ has the same form as in section 2.2.1:

$$\vec{B^i}(\tilde{x},\tilde{z}) = B^i(\tilde{x},\tilde{z})\,\vec{e}_y\,. \tag{2.43}$$

In this section only the MHD equations and pressure $\tilde{P}(\tilde{x},\tilde{z})$ are changed.

We have

$$\tilde{\vec{V}} = \tilde{V}_y(\tilde{y},\tilde{z})\vec{e}_y\,, \tag{2.44}$$

$$\tilde{\vec{B}} = \vec{B}^i(\tilde{x},\tilde{z}) + \tilde{B}_x(\tilde{x},\tilde{z})\vec{e}_x + \tilde{B}_z(\tilde{x},\tilde{z})\vec{e}_z\,. \tag{2.45}$$

Consequently

$$\tilde{\vec{V}} \times \tilde{\vec{B}} = \tilde{V}_y\ (\tilde{x},\tilde{z})\left[-\tilde{B}_x(\tilde{x},\tilde{z})\vec{e}_z + \tilde{B}_z(\tilde{x},\tilde{z})\vec{e}_x \right], \tag{2.46}$$

$$\tilde{\vec{j}} \times \tilde{\vec{B}} = \sigma(-grad\tilde{\Phi} + \tilde{\vec{V}} \times \tilde{\vec{B}}) \times \tilde{\vec{B}}, \tag{2.47}$$

i.e.

$$\tilde{\vec{j}} \times \tilde{\vec{B}} = \sigma\left\{ \left(\frac{\partial\tilde{\Phi}}{\partial\tilde{z}} + B_x\tilde{V}_y \right)\tilde{B}^i\,\vec{e}_x + \left[\frac{\partial\tilde{\Phi}}{\partial\tilde{x}}B_z - \frac{\partial\tilde{\Phi}}{\partial\tilde{z}}B_x - \left(B_x{}^2 + B_z{}^2\right)\tilde{V}_y \right]\vec{e}_y + \left(B_z - \frac{\partial\tilde{\Phi}}{\partial\tilde{x}} \right)\tilde{B}^i\,\vec{e}_z \right\}. \tag{2.48}$$

Substituting (2.44), (2.45) and (2.48) into (2.13) and projecting the resulting equation on the y axis, we obtain:

$$0 = -\frac{1}{\rho}\frac{\partial\tilde{P}}{\partial\tilde{y}} + \nu\left(\frac{\partial^2}{\partial\tilde{x}^2} + \frac{\partial^2}{\partial\tilde{z}^2} \right)\tilde{V}_y + \frac{\sigma}{\rho}\left[\frac{\partial\tilde{\Phi}}{\partial\tilde{x}}B_z - \frac{\partial\tilde{\Phi}}{\partial\tilde{z}}B_x - (B_x{}^2 + B_z{}^2)\tilde{V}_y \right]. \tag{2.49}$$

As in section 2.2.1, it follows from (2.49) that

$$\frac{\partial\tilde{P}}{\partial\tilde{y}} = F_3(\tilde{x},\tilde{z}) \Rightarrow \tilde{P} = F_3(\tilde{x},\tilde{z})\,\tilde{y} + F_4(\tilde{x},\tilde{z}), \tag{2.50}$$

where F_3 and F_4 are arbitrary functions. Substituting (2.44), (2.45) and (2.50) into (2.13) and projecting the resulting equations on the x and z axes, respectively, we obtain:

$$0 = --\tilde{y}\frac{\partial F_3}{\partial\tilde{x}} - \frac{\partial F_4}{\partial\tilde{x}} + \sigma\left(\frac{\partial\tilde{\Phi}}{\partial\tilde{z}} + B_x\tilde{V}_y \right)\tilde{B}^i, \tag{2.51}$$

$$-\tilde{y}\frac{\partial F_3}{\partial\tilde{z}} - \frac{\partial F_4}{\partial\tilde{z}} + \sigma\left(\frac{\partial\tilde{\Phi}}{\partial\tilde{x}}B_z - \frac{\partial\tilde{\Phi}}{\partial\tilde{z}}B_x - \left|\vec{B}_\perp\right|^2\tilde{V}_y \right). \tag{2.52}$$

It follows from (2.51) and (2.52) that

$$\frac{\partial F_3}{\partial \tilde{x}} = 0, \frac{\partial F_3}{\partial \tilde{z}} = 0 \Rightarrow F_3 = C = const. \tag{2.53}$$

Consequently, equations (2.50)-(2.52) are of the form

$$\frac{\partial \tilde{P}}{\partial \tilde{y}} = C \Rightarrow \tilde{P}(\tilde{x}, \tilde{z}) = C\,\tilde{y} + F_4(\tilde{x}, \tilde{z}), \tag{2.54}$$

$$\frac{\partial F_4}{\partial \tilde{x}} = \sigma\left(\frac{\partial \tilde{\Phi}}{\partial \tilde{z}} + B_x \tilde{V}_y\right)\tilde{B}^i, \tag{2.55}$$

$$\frac{\partial F_4}{\partial \tilde{z}} = \sigma\left(\frac{\partial \tilde{\Phi}}{\partial \tilde{x}} B_z - \frac{\partial \tilde{\Phi}}{\partial \tilde{z}} B_x - \left|\vec{B}_\perp\right|^2 \tilde{V}_y\right). \tag{2.56}$$

As in section 2.2.1 the constant C = 0, i.e.

$$\tilde{P}(\tilde{x}, \tilde{z}) = F_4(\tilde{x}, \tilde{z}). \tag{2.57}$$

Equation (2.49) can be rewritten in the form

$$\nu\left(\frac{\partial^2}{\partial \tilde{x}^2} + \frac{\partial^2}{\partial \tilde{z}^2}\right)\tilde{V}_y + \sigma\left[\frac{\partial \tilde{\Phi}}{\partial \tilde{x}} B_z - \frac{\partial \tilde{\Phi}}{\partial \tilde{z}} B_x - \left(B_x^{\,2} + B_z^{\,2}\right)\tilde{V}_y\right] = 0. \tag{2.58}$$

To obtain the second equation it is sufficient to apply the operation of divergence to equation (2.14) and use the equation of continuity $div\vec{\tilde{j}} = 0$:

$$0 = -\Delta\tilde{\Phi} + div\left[\tilde{V}_y\left(B_z \vec{e}_x - B_x \vec{e}_z\right)\right], \tag{2.59}$$

or

$$\Delta\tilde{\Phi} = B_z \frac{\partial \tilde{V}_y}{\partial \tilde{x}} - B_x \frac{\partial \tilde{V}_y}{\partial \tilde{z}} + \tilde{V}_y\left(\frac{\partial B_z}{\partial \tilde{x}} - \frac{\partial B_x}{\partial \tilde{z}}\right). \tag{2.60}$$

The linear system (2.58)-(2.60) with corresponding boundary conditions on the boundary $\tilde{z} = 0$ has a unique solution. For a certain form of the given functions $B_x(\tilde{x}, \tilde{z})$ and $B_z(\tilde{x}, \tilde{z})$ one can find an analytic form of this solution. In general case, this solution may be obtained only by numerical methods. In this section we have considered the fully developed MHD flow in the direction of the y axis. The external magnetic field and the given external current has only x and z components, which do not depend on the variable y. The pressure gradient is absent in

the y-direction. It is proved using the symmetry of the flow in this case that induced magnetic field has only a y-component. The system of MHD equations for the velocity of the fluid and for the potential of the induced current is obtained. Also the equations for the x and z components of pressure gradient are obtained. It is also proved that the pressure of fluid in the given case is a function depending on the x and z variables.

2.3 ANALYTICAL SOLUTION OF THE MHD PROBLEM TO THE FLOW OVER ROUGHNESS ELEMENTS USING THE DIRAC DELTA FUNCTION

In the designing of the present reactor Tokamak the value of the Hartmann boundary layer in a strong magnetic field becomes commensurable with the size of roughness of the surface of a channel's wall. Therefore, there is a practical need to study the influence of roughness of the surface on the MHD flow of the conducting metal, which is planned to use in the system of the cooling of the reactor.

The MHD problem describing the flow of a conducting fluid in the half space arising due to roughness of the surface in the form $\tilde{z} = \tilde{\chi}_0 \tilde{f}(\tilde{x})$ with the conditions that the values $\left|\tilde{f}(\tilde{x})\right|$ and $\left|\tilde{f}'(\tilde{x})\right|$ are small is solved in [2]. These assumptions allow one to transfer the boundary condition for potential of the current $\tilde{\Phi}(\tilde{x},\tilde{z})$ from the surface $\tilde{z} = \tilde{\chi}_0 \tilde{f}(\tilde{x})$ to the plane $\tilde{z} = 0$ and neglect the term $\tilde{f}'(\tilde{x})\partial\tilde{\Phi}(\tilde{x},0)/\partial\tilde{x}$ in the boundary condition. Without this simplification one obtains an integral equation for an unknown function $\partial\tilde{\Phi}(\tilde{x},0)/\partial\tilde{x}$ which can be solved only numerically. In this section this problem is solved for the case when the roughness of surface $\tilde{z} = \tilde{\chi}_0 \tilde{f}(\tilde{x})$ has the rectangular form: $\tilde{z} = \tilde{\chi}_0$, if $\tilde{x} \in (-L, L)$ and $\tilde{z} = 0$, if $\tilde{x} \notin [-L, L]$. As a result the derivative $\tilde{f}'(\tilde{x})$ in the boundary condition is expressed through the Dirac delta function and instead of an integral equation for the function $\tilde{f}'(\tilde{x})\partial\tilde{\Phi}(\tilde{x},0)/\partial\tilde{x}$ an unknown constant $\partial\tilde{\Phi}(L,0)/\partial\tilde{x}$ appears in the process of solution. This fact allows one to solve this problem analytically and estimate the error due to the neglected term $\tilde{f}'(\tilde{x})\partial\tilde{\Phi}(\tilde{x},0)/\partial\tilde{x}$ in above mentioned boundary condition. In addition, the asymptotic of this problem in a strong magnetic field is obtained.

2.3.1 THE STATEMENT OF THE PROBLEM

The geometry of the flow is shown in Fig.1. The conducting fluid is located in the half space $\tilde{z} > 0,\ -\infty < \tilde{x}, \tilde{y} < +\infty$. The external magnetic field has the form

$$\vec{B} = B_0 \vec{e}_z . \tag{2.61}$$

The boundary $\tilde{z} = 0$ is not conducting. A steady current flows with the density $\vec{\tilde{j}} = j_0 \vec{e}_x$ in the direction of the x-axis. If the surface $\tilde{z} = 0$ is ideally smooth then the flow is absent because the electromagnetic force $\vec{F} = \vec{\tilde{j}} \times \vec{B}$ is constant and $rot\vec{F} = 0$. Suppose that roughness of the surface $\tilde{z} = 0$ has the rectangular form (see Fig.1):

$$\tilde{z} = \tilde{\chi}_0 \ \tilde{f}(\tilde{x}) = \tilde{\chi}_0 \left[\eta(\tilde{x} + L) - \eta(\tilde{x} - L)\right] = \begin{cases} \tilde{\chi}_0, & -L < \tilde{x} < L, \\ 0, & |\tilde{x}| > L, \end{cases} \tag{2.62}$$

where $\eta(\tilde{x})$ is the Heaviside step function:

$$\eta(\tilde{x}) = \begin{cases} 0, \ \tilde{x} < 0, \\ 1, \ \tilde{x} > 0. \end{cases} \tag{2.63}$$

In this case the full current is equal to $\vec{j} = \vec{j}_0 + \vec{j}(\tilde{x}, \tilde{z})$ and the flow of the fluid with the velocity $\vec{V} = \tilde{V}_y(\tilde{y}, \tilde{z})\vec{e}_y$ arises in the direction opposite to the $\tilde{y}$ axis (see Fig.1).

We will deduce the boundary condition for the potential $\tilde{\Phi}(\tilde{x}, \tilde{y})$ of an electrical field on the surface $\tilde{z} = \tilde{\chi}_0 \tilde{f}(\tilde{x})$. The normal component of the current on this surface must be equal to zero because the boundary $\tilde{z} = \tilde{\chi}_0 \tilde{f}(\tilde{x})$ is not conducting, i.e. it must be $\vec{j} \cdot \vec{n} = 0$ on the surface ($\vec{n}$ is the unit normal to the surface).

Using formula $\vec{n} = grad[\tilde{z} - \tilde{\chi}_0 \tilde{f}(\tilde{x})] / \sqrt{1 + \tilde{\chi}_0^{\,2} \tilde{f}'^2(\tilde{x})}$ we obtain

$$\vec{n} = \left[-\tilde{\chi}_0 \tilde{f}'(\tilde{x})\vec{e}_x + \vec{e}_z\right] / \sqrt{1 + \tilde{\chi}_0^{\,2} \tilde{f}'^2(\tilde{x})}\,, \tag{2.64}$$

where

$$\tilde{f}'(\tilde{x}) = \left[\delta(\tilde{x} + L) - \delta(\tilde{x} - L)\right], \tag{2.65}$$

and $\delta(\tilde{x})$ is the Dirac delta function.

Substituting $\vec{n}$ from (2.64) and $\tilde{\vec{j}} = \left(j_0 + \tilde{j}_x(\tilde{x},\tilde{z})\right)\vec{e}_x + \tilde{j}_z(\tilde{x},\tilde{z})\vec{e}_z$ into $\tilde{\vec{j}} \cdot \vec{n} = 0$ and using formula $\tilde{\vec{j}} = \sigma\left(grad\tilde{\Phi} + \tilde{\vec{V}} \times \tilde{\vec{B}} \right)$, i.e. $\tilde{j}_x = -\sigma\,\partial\tilde{\Phi}/\partial\tilde{x}$, $\tilde{j}_z = -\sigma\,\partial\tilde{\Phi}/\partial\tilde{z}$ on the surface, where $\tilde{\vec{V}} = 0$, we obtain the boundary condition for the potential $\tilde{\Phi}(\tilde{x},\tilde{z})$:

$$\tilde{z} = \tilde{\chi}_0 \tilde{f}(\tilde{x}): \quad -\sigma \frac{\partial\tilde{\Phi}}{\partial\tilde{z}} = \tilde{\chi}_0 \left[j_0 \tilde{f}'(\tilde{x}) \; -\sigma \frac{\partial\Phi}{\partial\tilde{x}} \tilde{f}'(\tilde{x}) \right], \tag{2.66}$$

where function $\tilde{f}'(\tilde{x})$ is given by (2.65).

The only approximation which is made in this section is the following: we transfer the boundary condition (2.66) from the surface $\tilde{z} = \tilde{\chi}_0 \tilde{f}(\tilde{x})$ to the plane $\tilde{z} = 0$, i.e. we only assume that the value $\tilde{\chi}_0 \left| \tilde{f}(\tilde{x}) \right|$ is small. As a result, we obtain the boundary condition for the potential in the form

$$\tilde{z} = 0: \quad \partial\tilde{\Phi}/\partial\tilde{z} = \tilde{\chi}_0 \left[- j_0 \sigma^{-1} + \partial\tilde{\Phi}/\partial\tilde{x} \right] \cdot \left[\delta(\tilde{x} + L) - \delta(\tilde{x} - L) \right]. \tag{2.67}$$

We do not neglect the term $\partial\tilde{\Phi}/\partial\tilde{x}$ in the boundary condition (2.67) and as a result we obtain the new coefficient in the solution used in paper [13].

We use the values of L, ν/L, B_0, $\nu\sqrt{\rho\nu/\sigma}/L$, $\nu\sqrt{\rho\nu\sigma}/L^2$ as measures of length, velocity, magnetic field, potential and current, respectively. Here σ, ρ, ν are, respectively, the conductivity, the density and the viscosity of the fluid. Then the MHD equations and the boundary conditions have the form (see [28]):

$$\Delta V_y - Ha^2 V_y + Ha \cdot \partial\Phi/\partial x = 0, \quad \Delta\Phi = Ha \cdot \partial V_y/\partial x \;, \tag{2.68),(2.69}$$

$$z = 0: V_y = 0, \partial\Phi/\partial z = \chi_0 \left[- A + F(x,0) \right] \cdot \left[\delta(x+1) - \delta(x-1) \right], \tag{2.70),(2.71}$$

$$\sqrt{x^2 + z^2} \to \infty: \quad V_y \to 0, \Phi \to 0, \tag{2.72}$$

where $\Delta = \partial^2/\partial x^2 + \partial^2/\partial z^2$, $Ha = B_0 L\sqrt{\sigma/\rho\nu}$ is the Hartmann number, $A = j_0 L^2/(\nu\sqrt{\rho\nu\sigma})$, $\chi_0 = \tilde{\chi}_0/L$ and $F(x,0) = \left.\dfrac{\partial\Phi}{\partial x}\right|_{z=0}$. (2.73)

2.3.2 THE SOLUTION OF PROBLEM (2.68)-(2.72)

In order to solve problem (2.68)-(2.72) we use the symmetry of this problem with respect to x: the function $V_y(x,z)$ is an even function, $\Phi(x,z)$ is an odd function with respect to x. This means that the functions $V_y(x,z)$ and $\Phi(x,z)$ satisfy additional boundary conditions:

$$z=0: \quad \frac{\partial V_y}{\partial x}=0,\ \Phi(x,0)=0. \tag{2.74}$$

Therefore, problem (2.68)-(2.72) can be solved by means of Fourier cosine and Fourier sine transforms (see [3]). Namely, we apply the Fourier cosine transform with respect to x to equation (2.68) and to V_y in boundary condition (2.70) and the Fourier sine transform to equation (2.69) and to $\partial\Phi/\partial z$ in boundary condition (2.71). The transforms are defined as follows:

$$V_y{}^c(\lambda,z)=\sqrt{\frac{2}{\pi}}\int_0^\infty V_y(x,z)\cos\lambda x dx, \tag{2.75}$$

$$\Phi^s(\lambda,z)=\sqrt{\frac{2}{\pi}}\int_0^\infty \Phi(x,z)\sin\lambda x dx. \tag{2.76}$$

We obtain the following system of ordinary differential equations for unknown functions $V_y{}^c(\lambda,z)$, $\Phi^s(\lambda,z)$:

$$-\lambda^2 V_y+\frac{d^2V_y{}^c}{dz^2}-Ha^2V_y{}^c+Ha\lambda\Phi^s=0, \tag{2.77}$$

$$-\lambda^2\Phi^s+\frac{d^2\Phi^s}{dz^2}+Ha\lambda V_y{}^c=0. \tag{2.78}$$

We also apply transforms (2.75) and (2.76) to boundary conditions (2.70) and (2.71):

$$z=0: \quad V_y{}^c=0, \quad \frac{d\Phi^s}{dz}=\chi_0\left[A-F(1,0)\right]\sqrt{\frac{2}{\pi}}\sin\lambda;\ z\to\infty: V_y{}^c,\Phi^s\to 0, \tag{2.79),(2.80}$$

$$\text{where} \quad F(1,0)=\frac{\partial\Phi}{\partial x} \text{ at } x=1,\ z=0 \tag{2.81}$$

is an unknown constant. The solution of the problem (2.77)-(2.80) has the form:

$$\Phi^s(\lambda,z)=\chi_0\sqrt{\frac{2}{\pi}}\left[-F(1,0)+A\right]\frac{\sin\lambda}{2\lambda^2}\left(k_1e^{k_2z}+k_2e^{k_1z}\right), \tag{2.82}$$

$$V^c(\lambda,z)=\chi_0\sqrt{\frac{2}{\pi}}[-F(1,0)+A]\frac{\sin\lambda}{2\lambda}\left(e^{k_1 z}-e^{k_2 z}\right), \tag{2.83}$$

where

$$k_1=-(\sqrt{\lambda^2+\mu^2}+\mu),\ k_2=-(\sqrt{\lambda^2+\mu^2}-\mu),\ 2\mu=Ha. \tag{2.84}$$

Applying the inverse Fourier sine and cosine transforms to formulae (2.82), (2.83), we obtain the solution of problem (2.68)-(2.72), containing unknown constant $F(1,0)$:

$$\Phi(x,z)=\frac{\chi_0}{\pi}[-F(1,0)+A]\int_0^\infty\left(k_1e^{k_2 z}+k_2e^{k_1 z}\right)\frac{\sin\lambda}{\lambda^2}\sin\lambda x d\lambda, \tag{2.85}$$

$$V_y(x,z)=\frac{\chi_0}{\pi}[-F(1,0)+A]\int_0^\infty\left(e^{k_1 z}-e^{k_2 z}\right)\frac{\sin\lambda}{\lambda}\cos\lambda x d\lambda. \tag{2.86}$$

The components j_x and j_z of the induced current density are obtained from the formula

$$\tilde{\tilde{j}}=\sigma\left[-grad\tilde{\Phi}(\tilde{x},\tilde{z})+\tilde{\tilde{V}}\times\tilde{\tilde{B}}\right], \tag{2.87}$$

where $\tilde{\tilde{V}}=\tilde{V}_y(\tilde{x},\tilde{z})\vec{e}_y$, $\tilde{\tilde{B}}=\tilde{B}_y^i(\tilde{x},\tilde{z})\vec{e}_{\mathbf{y}}+B_0\vec{e}_{\mathbf{z}}$. (2.88)

In the dimensionless quantities formula (2.87) has the form

$$\vec{j}=-grad\Phi(x,z)+Ha\vec{V}\times\vec{B}, \tag{2.89}$$

where $\vec{V}=V_y(x,z)\vec{e}_y$, $\vec{B}=B_y^i(x,z)\vec{e}_{\mathbf{y}}+\vec{e}_{\mathbf{z}}$. (2.90)

Substituting (2.90) into (2.89) we obtain

$$\vec{j}=-grad\Phi(x,z)+HaV_y(x,z)\vec{e}_{\mathbf{x}}. \tag{2.91}$$

It follows from (2.91) that

$$j_x=-\frac{\partial\Phi}{\partial x}+HaV_y(x,z),\quad j_z=-\frac{\partial\Phi}{\partial z}. \tag{2.92}$$

Using formulae (2.85), (2.86) and (2.84), we obtain

$$j_x=-D\int_0^\infty\left(k_1e^{k_1 z}+k_2e^{k_2 z}\right)\frac{\sin\lambda\cos\lambda x}{\lambda}d\lambda, \tag{2.93}$$

$$j_z = -D\int_0^{\infty}\left(e^{k_1 z} + e^{k_2 z}\right)\sin\lambda\sin\lambda x d\lambda\,, \tag{2.94}$$

$$D = \frac{\chi_0}{\pi}\left[A - F(1,0)\right]. \tag{2.95}$$

For the evaluation of unknown constants F(1,0) and D in formulae (2.85), (2.86), (2.93) and (2.94) it is necessary to use integral (2.85) and evaluate the limit

$$\mathrm{F}(1,0)= D\lim_{z\to+0}\int_0^{\infty}\left(k_1 e^{k_2 z} + k_2 e^{k_1 z}\right)\frac{\sin\lambda\cos\lambda}{\lambda}d\lambda\,. \tag{2.96}$$

Differentiation with respect to x under the integral sign in (2.85) is correct in the region $0 < z_0 \le z < +\infty, 0 \le x < +\infty$ because this integral and the corresponding integral (2.96) of partial derivative with respect to x of integrand in (2.85) is majorized in this region. However, if we substitute $z = 0$ under the integral sign in (2.96), we obtain the divergence of the integral, which converges only in the sense of Abel (see [3]):

$$I \equiv \int_0^{\infty}\sqrt{\lambda^2+\mu^2}\,\frac{\sin 2\lambda}{\lambda}d\lambda = \lim_{\delta\to+0}\int_0^{\infty} e^{-\delta\lambda}\sqrt{\lambda^2+\mu^2}\,\frac{\sin 2\lambda}{\lambda}d\lambda \tag{2.97}$$

or, after evident transformations

$$I \equiv \lim_{\delta\to+0}\int_0^{\infty} e^{-\delta\lambda}\frac{\mu^2}{\sqrt{\lambda^2+\mu^2}+\lambda}\frac{\sin 2\lambda}{\lambda}d\lambda + \lim_{\delta\to+0}\int_0^{\infty} e^{-\delta\lambda}\sin 2\lambda d\lambda. \tag{2.98}$$

The first integral on the right hand side of (2.98) converges in the usual sense, but the second integral converges only in the sense of Abel and equal to ½ (see [3]). However, such a method gives the solution, which tends to zero as Hartmann number Ha tends to infinity. The last fact contradicts to the physical sense of the problem. Therefore, there is a need to transform integral (2.85) to such a form that after passing to the limit as $z \to +0$ we would obtain the integral converging in the usual sense. For this purpose we use the formulae (see [74]):

$$\int_0^{\infty} e^{-z\sqrt{\lambda^2+\mu^2}}\cos a\lambda d\lambda = \frac{\mu z}{\sqrt{z^2+a^2}}K_1\left(\mu\sqrt{z^2+a^2}\right), \tag{2.99}$$

$$\int_0^{\infty}\sqrt{\lambda^2+\mu^2}\,e^{-z\sqrt{\lambda^2+\mu^2}}\cos a\lambda d\lambda = \frac{\mu}{\sqrt{z^2+a^2}}\left[\frac{\mu z^2}{\sqrt{z^2+a^2}}K_2\left(\mu\sqrt{z^2+a^2}\right) - K_1\left(\mu\sqrt{z^2+a^2}\right)\right], \tag{2.100}$$

where $a \geq 0$, $z > 0$ and $K_\nu(z)$ is the modified Bessel function of the second kind of order ν (ν=1, 2). As a result, we obtain (the details are found in [12]):

$$V_y(x,z) = -D \cdot \mu z \cdot sh\mu z \int_{x-1}^{x+1} \frac{K_1\left(\mu\sqrt{z^2+t^2}\right)}{\sqrt{z^2+t^2}} dt, \tag{2.101}$$

$$j_x(x,z) = D \cdot ch\mu z\left[F(1+x) - F(1-x)\right] + \mu V_y(x,z), \tag{2.102}$$

where

$$F(a) = \int_0^a \frac{\mu}{\sqrt{z^2+t^2}}\left[\frac{\mu z^2}{\sqrt{z^2+t^2}} K_2\left(\mu\sqrt{z^2+t^2}\right) - K_1\left(\mu\sqrt{z^2+t^2}\right)\right] dt. \tag{2.103}$$

Evaluating integral (2.94) we obtain

$$j_z(x,z) = D\mu z \cdot ch\mu z\left[\frac{K_1\left(\mu\sqrt{z^2+(1-x)^2}\right)}{\sqrt{z^2+(1-x)^2}} - \frac{K_1\left(\mu\sqrt{z^2+(1+x)^2}\right)}{\sqrt{z^2+(1+x)^2}}\right]. \tag{2.104}$$

We transform $\partial\Phi/\partial$x, using formulae (2.85), (2.99) and (2.100):

$$\left.\frac{\partial\Phi}{\partial x}\right|_{x=1} = -D\left\{ch\mu z \int_0^2 \frac{\mu}{\sqrt{z^2+t^2}}\left[\frac{\mu z^2}{\sqrt{z^2+t^2}} K_2\left(\mu\sqrt{z^2+t^2}\right) - K_1\left(\mu\sqrt{z^2+t^2}\right)\right] dt + \right.$$

$$\left. + \mu^2 z \cdot sh\mu z \int_0^2 \frac{1}{\sqrt{z^2+t^2}} K_1\left(\mu\sqrt{z^2+t^2}\right) dt\right\}. \tag{2.105}$$

The integrals on the right hand side of (2.105) diverge if $z = 0$. To overcome this difficulty, we perform the following transformation. First, we use the substitution

$$t = z\xi, \quad dt = zd\xi. \tag{2.106}$$

Then it follows from formula (2.105) that

$$\left.\frac{\partial\Phi}{\partial x}\right|_{x=1} = -D\left\{ch\mu z \int_0^{\frac{2}{z}} \frac{\mu}{\sqrt{1+\xi^2}}\left[\frac{\mu z}{\sqrt{1+\xi^2}} K_2\left(\mu z\sqrt{1+\xi^2}\right) - K_1\left(\mu z\sqrt{1+\xi^2}\right)\right] d\xi + \right.$$

$$\left. + \mu \cdot sh\mu z \int_0^{\frac{2}{z}} \frac{\mu z}{\sqrt{1+\xi^2}} K_1\left(\mu z\sqrt{1+\xi^2}\right) d\xi\right\}. \tag{2.107}$$

In order to pass to the limit as $z \to +0$ in (2.107) we use the formula

$$K_n(z) \approx \frac{1}{2}(n-1)!\left(\frac{2}{z}\right)^n,\ n = 1,2,3,\ldots \text{ at } z \to +0,$$

i.e. $$K_1(z) \approx \frac{1}{z},\ K_2(z) \approx \frac{2}{z^2} \text{ at } z \to +0. \tag{2.108}$$

As a result, we obtain from formula (2.107) that

$$\lim_{z\to+0}\left.\frac{\partial\Phi}{\partial x}\right|_{x=1} = -D\lim_{z\to+0}\frac{1}{z}\int_0^{\frac{2}{z}}\left[\frac{2}{\left(1+\xi^2\right)^2} - \frac{1}{1+\xi^2}\right]d\xi - D\lim_{z\to+0}\mu\cdot sh\mu z\int_0^{\frac{2}{z}}\frac{1}{1+\xi^2}d\xi. \tag{2.109}$$

The second limit on the right hand side of formula (2.109) is equal to zero, but the first limit gives undefined expression of the form $\frac{0}{0}$ because

$$\int_0^{\infty}\left[\frac{2}{\left(1+\xi^2\right)^2} - \frac{1}{1+\xi^2}\right]d\xi = \int_0^{\infty}\frac{2}{\left(1+\xi^2\right)^2}d\xi - \frac{\pi}{2} = 0. \tag{2.110}$$

Consequently, it follows from formula (1.109) that

$$\lim_{z\to+0}\left.\frac{\partial\Phi}{\partial x}\right|_{x=1} = -D\lim_{z\to+0}\frac{1}{z}\int_0^{\frac{2}{z}}\left[\frac{2}{\left(1+\xi^2\right)^2} - \frac{1}{1+\xi^2}\right]d\xi = = -D\lim_{z\to+0}\left[\frac{2}{\left(1+\frac{4}{z^2}\right)^2} - \frac{1}{1+\frac{4}{z^2}}\right]\left(-\frac{2}{z^2}\right) = -\frac{D}{2}. \tag{2.111}$$

It follows from (2.111) and (2.95) that

$$F(1,0) = -\frac{1}{2}D, \text{ i.e. } F(1,0) = -\frac{\chi_0}{2\pi}\left[A - F(1,0)\right] \tag{2.112}$$

We obtain the unknown constant F(1,0) from equation (2.112):

$$F(1,0) = -\frac{\chi_0}{2\pi}A\frac{1}{1-\frac{\chi_0}{2\pi}}. \tag{2.113}$$

Consequently, the coefficient D, which is the unknown coefficient in the (2.101), (2.102) and (2.104), is given by

$$D = \frac{\chi_0}{\pi}\left[A - F(1,0)\right] = \frac{\chi_0}{\pi}A\frac{1}{1-\frac{\chi_0}{2\pi}} > 0 \text{ if } \chi_0 < 2\pi. \tag{2.114}$$

We remind that $\chi_0 = \widetilde{\chi}_0 / L$ is the single small parameter in our problem. The inequality $\chi_0 < 2\pi$ gives the natural restriction at which the y-component of the velocity $V_y(x,z)$ in formula (2.86) is negative, that is, corresponds to the physical sense of this problem.

It is important to note that if we would neglect the term $\partial\Phi/\partial x$ in boundary condition (2.67), the way it was done in paper [2] for function $f(x)$ of arbitrary form, we obtain the same solution of this problem but at the condition that coefficient D would be equal to $D = A\chi_0/\pi$ instead of formula (2.114). It gives us the opportunity to evaluate the error which occurs if the term $\partial\Phi/\partial x$ is neglected in boundary condition (2.67). For example, if $\chi_0/2\pi = 0.1$, then the error δ is equal to $\delta = (1/0.9 - 1)\cdot 100\%$, i.e. $\delta = 11\%$.

2.3.3 THE ASYMPTOTIC ANALYSIS OF THE PROBLEM AND NUMERICAL RESULTS

It follows from formula (2.86) that at $Ha \to \infty$ we have $k_1 z \to -\infty$, $k_2 z \to 0$ (everywhere except the regions $0 \le z \le Ha^{-1}$ and $z > Ha$, respectively).
Consequently, at $Ha \to \infty$ in region $Ha^{-1} \le z \le Ha$ we obtain from formula (2.86) that

$$\lim_{Ha\to\infty} V_y(x,z) \equiv V_c = -\frac{\pi}{2}[\eta(1-x)+\eta(1+x)] = \begin{cases} -\dfrac{\pi D}{2}, & x \in (-1,1), \\ 0, & x \notin (-1,1), \end{cases} \qquad (2.115)$$

where V_c =constant is the core velocity.

The region $0 \le z \le Ha^{-1}$ is the Hartmann boundary layer, where the velocity of fluid is changed from zero to the velocity of the flow core V_c = constant, but the region $Ha < z < +\infty$ is the distant wake, where the velocity is changed from V_c to zero (see Figure 4).

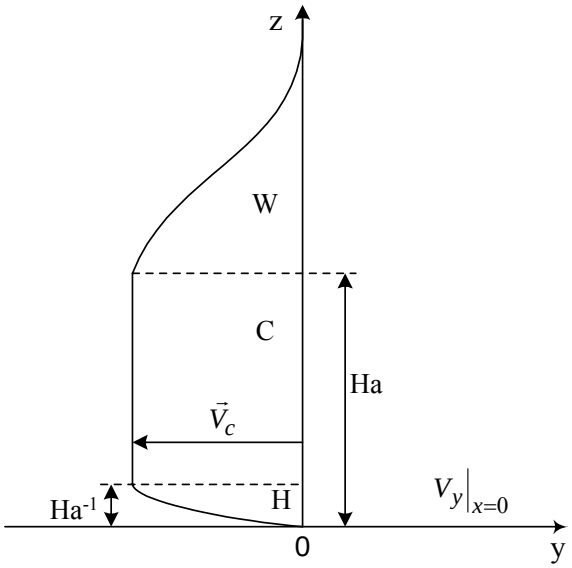

Figure 4. The regions of the flow in the cross-section $x = 0$ at $Ha \to \infty$:

H- the Hartmann layer, $0 < z < Ha^{-1}$;

C- the flow core, $Ha^{-1} < z < Ha$;

W- the distant wake, $Ha < z < +\infty$.

It is necessary to note that at large Hartmann numbers the velocity V_c in the core of flow is constant and does not depend on Ha. At $Ha \to +\infty$ only the height of core region $Ha^{-1} < z < Ha$ is increased. The asymptotic of the current's component $j_x(x,z)$ in the region $Ha^{-1} < z < +\infty$ is obtained from formula (2.93):

$$\lim_{Ha\to\infty} j_x = 0, \quad Ha^{-1} < z < +\infty. \tag{2.116}$$

The asymptotic of the current component $j_z(x,z)$ at $Ha \to +\infty$ is obtained from the exact formula (2.104). For this purpose we use the formula that holds when $\mu \to \infty$, $z > 0$, $l > 0$:

$$ch\mu z \approx 0.5 e^{\mu z}, \quad K_1(\mu l) \approx \sqrt{\frac{\pi}{\mu l}} e^{-\mu l}. \tag{2.117}$$

Then, according to (2.104), the component $j_z(x,z)$ exponentially tends to zero at $\mu \to \infty$ everywhere, except for the two regions, bounded by the parabolas:

$$\mu\sqrt{z^2 + (x-1)^2} - \mu z = 1 \text{ and } \mu\sqrt{z^2 + (x+1)^2} - \mu z = 1, \tag{2.118}$$

i.e. bounded by the parabolas:

$$z+\frac{1}{2\mu}=0.5\mu(x+1)^2 \quad \text{and} \quad z+\frac{1}{2\mu}=0.5\mu(x-1)^2. \qquad (2.119)$$

Furthermore, we can put $\frac{1}{2\mu}\approx 0$ at $\mu\to\infty$ in formula (2.119). Inside of the two regions, bounded by parabolas (2.119), the component $j_z(x,z)$ tends to infinity as $\mu\to\infty$ by the law

$$j_z \approx \sqrt{\mu / z}\,, \qquad (2.120)$$

since it follows from (2.104), (2.117), (2.118) that

$$\ell \equiv \sqrt{z^2+(1-x)^2} = (1+\mu z)/z \approx \mu,\ \ \mu l-\mu z=1, \qquad (2.121)$$

$$\mu z ch\mu z l^{-1}K_1(\mu l)\approx 0.5\mu e^{\mu(z-\ell)}(\pi/(2\mu z))^{0.5} = e^{-1}\left(\pi/8\right)^{0.5}\left(\mu/z\right)^{0.5} \qquad (2.122)$$

as $\mu\to\infty$.

The asymptotic of functions of the functions $V_y(x,z)$, $j_x(x,z)$ $j_z(x,z)$ are obtained from integrals (2.86), (2.93) and (2.94) by means of the formulae which hold at $\mu\to\infty$:

$$-k_1=\left(\sqrt{\lambda^2+\mu^2}-\mu\right)+2\mu=2\mu+\frac{\lambda^2}{\sqrt{\lambda^2+\mu^2}+\mu}\approx 2\mu+\frac{\lambda^2}{2\mu}, \qquad (2.123)$$

$$-k_2=\sqrt{\lambda^2+\mu^2}-\mu\approx\frac{\lambda^2}{2\mu},\ \ 2\mu=Ha. \qquad (2.124)$$

Substituting (2.123) and (2.124) into integrals (2.86), (2.93), (2.94) and using the Poisson integral (see [3]), we obtain the asymptotic formulae which hold for the whole region $0<z<+\infty$ as $Ha\to\infty$:

$$V_y(x,z)=-\frac{\pi}{4}D\left(1-e^{-zHa}\right)\psi(x,z), \qquad (2.125)$$

$$\psi(x,z)=erf\left[\beta\frac{1+x}{\sqrt{z}}\right]+erf\left[\beta\frac{1-x}{\sqrt{z}}\right],\ \beta=0.5\sqrt{Ha}\,, \qquad (2.126)$$

$$j_x=D\left\{\frac{\pi}{4}Hae^{-zHa}\psi(x,z)+\frac{\beta}{z\sqrt{\pi z}}\left(1+\frac{\pi}{4}e^{-zHa}\right)\left[(1+x)e^{\frac{-\beta^2(1+x)^2}{z}}+(1-x)e^{\frac{-\beta^2(1-x)^2}{z}}\right]\right\}, \qquad (2.127)$$

$$j_z = -\frac{1}{2} D\beta \sqrt{\frac{\pi}{z}\left(1+e^{-zHa}\right)}\left[e^{\frac{-\beta^2(1-x)^2}{z}} - e^{\frac{-\beta^2(1+x)^2}{z}} \right]. \qquad (2.128)$$

It can be seen that at $Ha \to \infty$ the following conclusion can be drawn from formula (2.125):

1) Component $V_y = \frac{-\pi}{2} D$ is constant in region $Ha^{-1} < z < Ha$.

2). Component V_y is changed from 0 to $V_y = \frac{-\pi}{2} D = V_c$ in region $0 < z < Ha^{-1}$.

3). Component V_y is changed from V_c to zero in region $Ha < z < +\infty$.

In addition, it follows from formula (2.125) that the component $V_y \to 0.5V_c$ as $Ha \to \infty$ on the lines $x = \pm 1$, $0 < z < +\infty$. That means that the two new boundary layers exist in the regions:

$$-\varepsilon < \beta \frac{1-x}{\sqrt{z}} < \varepsilon \text{ and } -\varepsilon < \beta \frac{1+x}{\sqrt{z}} < \varepsilon, \qquad (2.129)$$

where ε is some small positive number. In these regions component V_y is changed between $-V_c$ and zero. It is impossible to get these two new boundary layers from formula (2.86).

The following conclusions can be drawn from (2.128) that at $Ha \to \infty$:

1. Component j_z exponentially tends to zero everywhere except the two regions, lying inside parabolas (2.119), because in this case both exponents in the square brackets of formula (2.128) tend to zero.
2. Component j_z inside the region bounded by the first or second parabola in (2.119), where one of the exponents in the square brackets in (2.128) does not equal to zero, is given by $j_z \approx \sqrt{\mu / z}$, i.e. tends to infinity as $\mu \to \infty$.
3. Finally, we see from formula (2.127) that at $Ha \to \infty$ the current component $j_x(x,z)$ tends to zero everywhere except the region $0 < z < Ha^{-1}$ because in this region $\exp(-zHa) \neq 0$ and the function $\psi(x,z)$ tends to 2 everywhere except the two regions in formula (2.129).

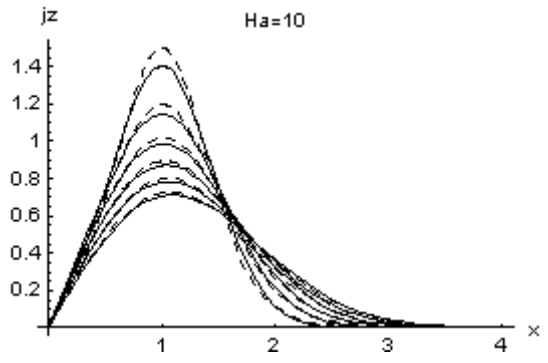

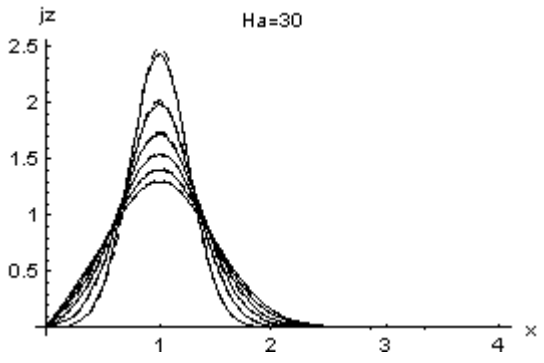

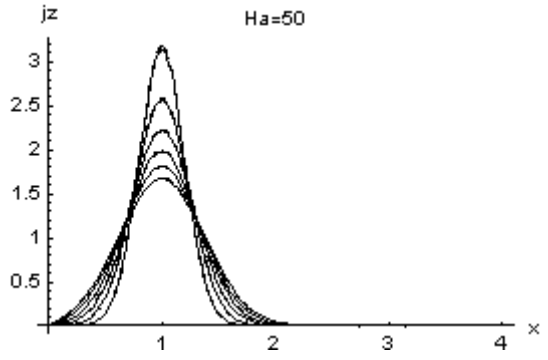

Figure 5. The graphs of the z -component of current by exact formula (2.128) (- - - - -) and by formula (2.104) ( ) from $z = 1$ (two upper lines) to $z = 3.5$ (two lower lines) through $\Delta z = 0.5$. Function $j_z(x, z)$ is odd with respect to x.

In order to estimate the range of Hartmann numbers at which the asymptotic formulae (2.125)-(2.128) are correct we compare the numerical results for the component $j_z(x, z)$, obtained by exact formula (2.104) and asymptotic formula (2.128). These numerical results for Hartmann numbers Ha =10 , 30 , 50 are shown in Fig. 5. For Hartmann numbers $Ha \geq 10$ the results obtained by exact formula (2.104) and asymptotic formula (2.128) practically coincide. Similar conclusions can be drawn by comparing the computed values of the functions $V_y(x, z)$ and $j_x(x, z)$ by exact formulae (2.86) , (2.93) and asymptotic formulae (2.125) , (2.127).

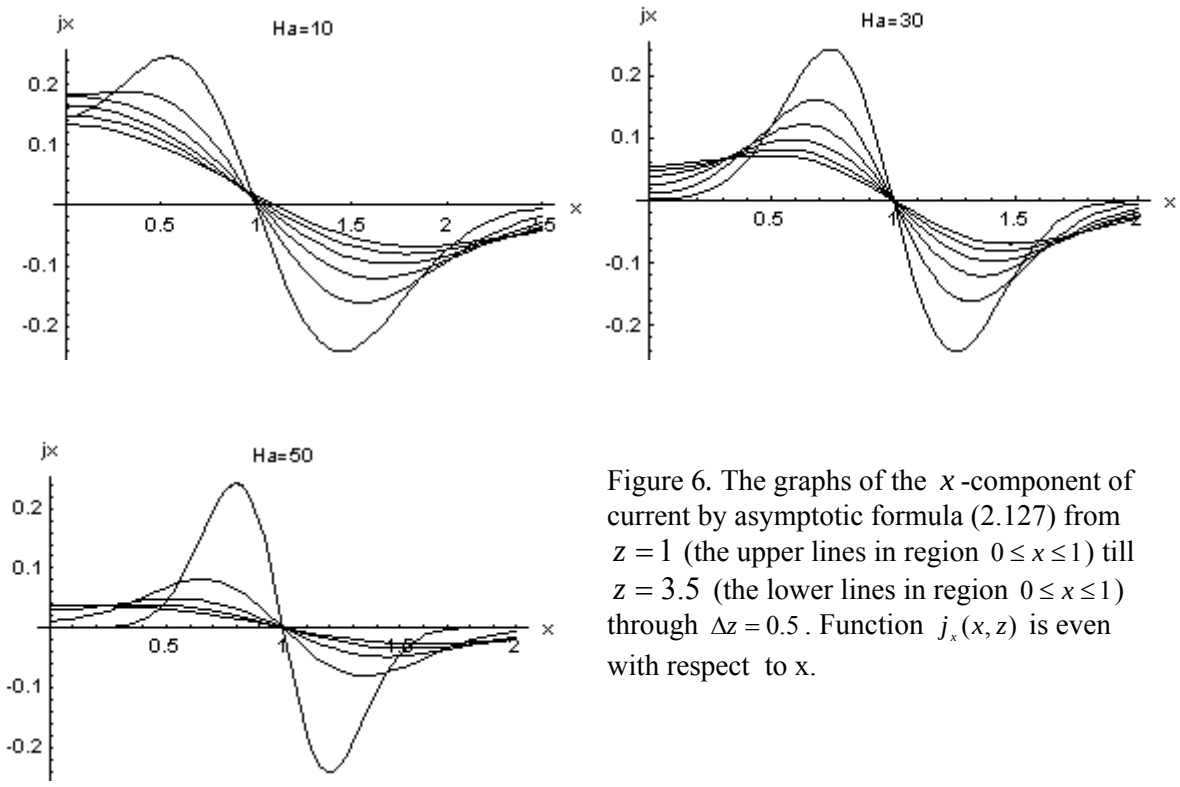

Figure 6. The graphs of the x-component of current by asymptotic formula (2.127) from $z = 1$ (the upper lines in region $0 \le x \le 1$) till $z = 3.5$ (the lower lines in region $0 \le x \le 1$) through $\Delta z = 0.5$. Function $j_x(x,z)$ is even with respect to x.

The numerical results of calculation of the current's component $j_x(x,z)$ by asymptotic formula (2.127) for Hartmann numbers Ha=10, 30 and 50 are shown in Fig. 6. We can see that the sign of the function $j_x(x,z)$ is changed in the neighbourhood of the line $x = 1,\ 0 < z < +\infty$. It means that the streamlines of current $\vec{j}(x,z)$ change their direction to the opposite in the neighbourhood of this line.

It follows from (2.128) that the full current through the cross section $z = z_0$=constant is equal to

$$\int_0^\infty j_z(x,z_0)dx = -\frac{\pi D}{2}\left(1+e^{-z_0 Ha}\right)erf\frac{Ha}{2z_0} \to -\frac{\pi D}{2} \text{ as } Ha \to \infty. \qquad (2.130)$$

The same full current flow can be obtained through the cross section $x = x_0,\ 0 < z < +\infty$. This result follows from (2.127) and also from the equation of continuity:

$$\int_0^\infty j_x(x_0,z)dz \to \frac{\pi D}{2} \text{ as } Ha \to \infty. \qquad (2.131)$$

One can see also from (2.127) that at $Ha \to \infty$ almost all of this full current flow through the cross section of Hartmann boundary layer $x = x_0 > 0,\ 0 \le z < Ha^{-1}$:

$$\int_0^{Ha^{-1}} j_x(x_0.z)dz = \frac{\pi D}{4} Ha \int_0^{Ha^{-1}} \psi(x_0, z) e^{-zHa} dz \approx \frac{\pi D}{2} Ha \int_0^{Ha^{-1}} e^{-zHa} dz = \frac{\pi D}{2}\left(1 - e^{-1}\right). \qquad (2.132)$$

The streamlines of current $\vec{j}(x,z)$ obtained by formula

$$\frac{dz}{dx} = \frac{j_z(x,z)}{j_x(x,z)} \qquad (2.133)$$

for Hartmann numbers Ha=5 and Ha=10 and for various values of initial conditions $z(0)$ are shown in Fig. 7. The package "Mathematica" is used for calculations. Since the function $j_x(x,z)$ is equal to zero in the neighbourhood of the point $x=1$ the results of calculations in Fig. 7 in region $0 \le x \le 1$ are shown . One can see from Fig. 7 that when Hartmann number increases then the full current is concentrated near the plane $z=0$.

For calculations of streamlines in region $1 \le x \le +\infty$ we use the differential equation

$$\frac{dx}{dz} = \frac{j_x(x,z)}{j_z(x,z)}. \qquad (2.134)$$

The streamlines of current in this region are shown in Fig. 8 for the same Hartmann numbers Ha=5 and Ha=10 . One can see from Fig. 8 that in the neighbourhood of point $x=1$ the streamlines change directions to the opposite.

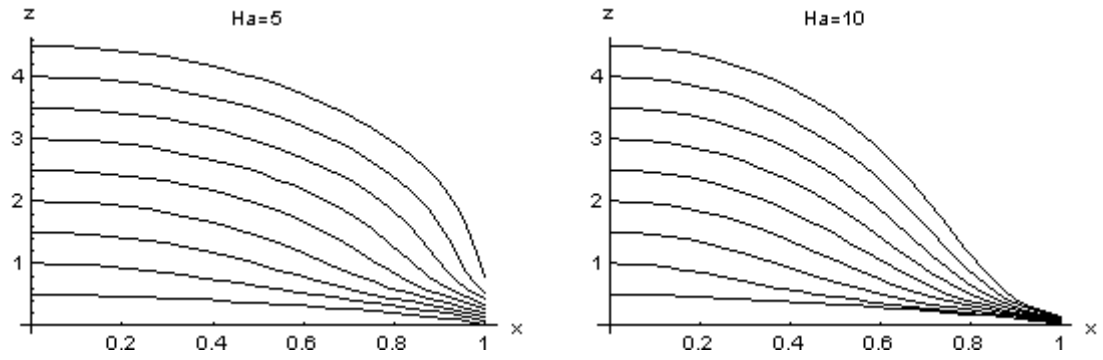

Figure 7. The streamlines of current $\vec{j}(x,z)$ in region $0 \le x \le 1$ at Ha=5 and at Ha=10.

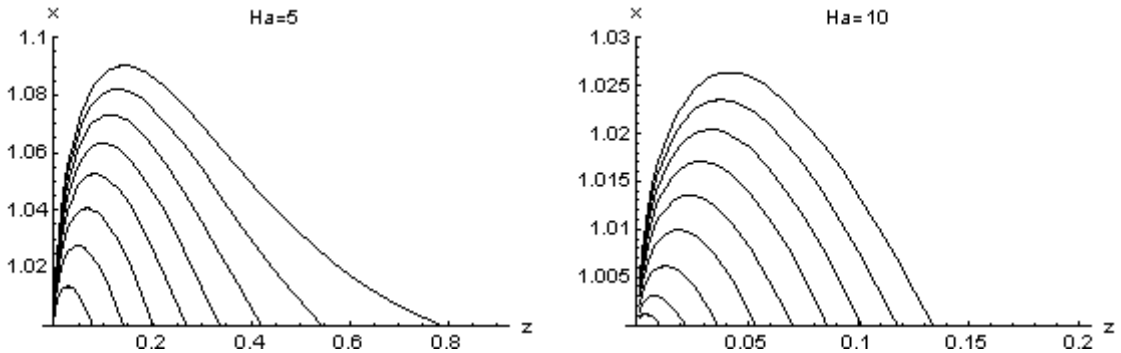

Figure 8. The streamlines of current $\vec{j}(x,z)$ in region $1 \le x \le +\infty$ at Ha=5 and at Ha=10.

CONCLUSIONS

1. The analytical solution of the two dimensional problem on the MHD flow in half space $z \ge 0$ due to the roughness of the boundary of special form is obtained. Roughness of constant rectangular cross section is located along the y - axis. In this case the external current flows parallel to x - axis and the external magnetic field is parallel to z - axis. The two dimensional MHD flow in the direction opposite to y - axis arises, only if the roughness of the boundary is present.

2. The analytical solution is obtained at the single approximate assumption that the height of roughness is small .The solutions for the y - component of the velocity of the fluid and for the x - component of the induced current are obtained in the form of improper integrals of elementary functions. On the other hand, the z - component of the induced current is expressed through the Bessel functions.

3. The asymptotic solution of the problem at Hartmann number $Ha \to \infty$ is obtained in the form of elementary functions. For Hartmann numbers $Ha \ge 10$ the exact and the asymptotic solutions practically coincide.

4. Several boundary layers for the velocity of the fluid and for the x - and z - components of the current at large Hartmann numbers are found.

5. The velocity of the fluid in the core at large Hartmann numbers is constant; that means it does not depend on Ha. Only the height of the core region $Ha^{-1} < z < Ha$ is increased with the increase of Hartmann number.

6. Using the package “Mathematica” the streamlines of electrical current are calculated. The induced current at large Hartmann numbers flow only in Hartmann boundary layer $0 < z < Ha^{-1}$ and along the lines $x = \pm 1$.

2.4 ANALYTICAL SOLUTION OF THE MHD PROBLEM TO THE FLOW OVER ROUGHNESS ELEMENTS IN THE FORM OF A STEP FUNCTION

In Section 2.3 the MHD problem on the flow of conducting fluid in the half space arising due to roughness of the surface of the form $\tilde{z} = \tilde{\chi}_0 \tilde{f}(\tilde{x})$ with the conditions that the values $\left|\tilde{f}(\tilde{x})\right|$ and $\left|\tilde{f}'(\tilde{x})\right|$ are small is solved. In this section similar problem for roughness of the form of a prism with constant cross-section bounded by step-function form is solved [13].

2.4.1 THE PROBLEM OVER ROUGHNESS ELEMENTS IN A STRONG MAGNETIC FIELD

In this section we assume that roughness of the surface $\tilde{z} = 0$ has the form of the step-function (see Fig.9):

$$\tilde{z} = \tilde{F}(\tilde{x}) = \begin{cases} \tilde{\chi}_1, & |\tilde{x}| < L_1 \\ \tilde{\chi}_0, & L_1 < |\tilde{x}| < L \\ 0, & |\tilde{x}| > L \end{cases} \tag{2.135}$$

or $\tilde{z} = \tilde{F}(\tilde{x}) = \tilde{\chi}_0 \ \tilde{f}_1(\tilde{x}) + (\tilde{\chi}_1 - \tilde{\chi}_0)\ \tilde{f}_2(\tilde{x})$, (2.136)

where $\tilde{f}_1(\tilde{x}) = \eta(\tilde{x} + L) - \eta(\tilde{x} - L)$, $\tilde{f}_2(\tilde{x}) = \eta(\tilde{x} + \tilde{L}_1) - \eta(\tilde{x} - \tilde{L}_1)$. (2.137)

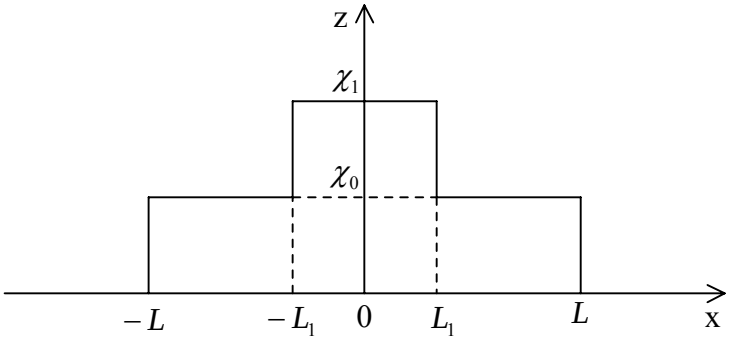

Figure 9. The constant cross-section of roughness.

We will deduce the boundary condition for the potential $\tilde{\Phi}(\tilde{x}, \tilde{z})$ of an electrical field on the surface $\tilde{z} = \tilde{F}(\tilde{x})$. The normal component of the current on this surface must be equal to zero

because the boundary $\tilde{z} = \tilde{\chi}_0 \tilde{f}(\tilde{x})$ is not conducting, i.e. it must be $\vec{j} \cdot \vec{n} = 0$ on the surface ($\vec{n}$ is the unit vector of the normal to the surface).

Using the formula $\vec{n} = grad[\tilde{z} - \tilde{F}(\tilde{x})] / \sqrt{1 + \tilde{F}^2(\tilde{x})}$ we obtain

$$\vec{n} = \left[\tilde{F}'(\tilde{x})\vec{e}_x + \vec{e}_z\right] / \sqrt{1 + \tilde{F}'^2(\tilde{x})}\,, \tag{2.138}$$

where

$$\tilde{F}'(\tilde{x}) = \tilde{\chi}_0\left[\delta(\tilde{x} + L) - \delta(\tilde{x} - L)\right] + (\tilde{\chi}_1 - \tilde{\chi}_0)\left[\delta(\tilde{x} + \tilde{L}_1) - \delta(\tilde{x} - \tilde{L}_1)\right], \tag{2.139}$$

and $\delta(\tilde{x})$ is the Dirac delta function.

Substituting the value of $\vec{n}$ from (2.138) and $\vec{\tilde{j}} = \left(j_0 + \tilde{j}_x(\tilde{x}, \tilde{z})\right)\vec{e}_x + \tilde{j}_z(\tilde{x}, \tilde{z})\vec{e}_z$ into $\vec{\tilde{j}} \cdot \vec{n} = 0$ and using formula $\vec{\tilde{j}} = \sigma\left[-grad\tilde{\Phi} + \vec{\tilde{V}} \times \vec{\tilde{B}}\right]$, i.e. $\tilde{j}_x = -\sigma\,\partial\tilde{\Phi}/\partial\tilde{x}$, $\tilde{j}_z = -\sigma\,\partial\tilde{\Phi}/\partial\tilde{z}$ on the surface where $\vec{\tilde{V}} = 0$, we obtain the boundary condition for the potential $\tilde{\Phi}(\tilde{x}, \tilde{z})$:

$$\tilde{z} = \tilde{F}(\tilde{x}): \quad -\sigma\frac{\partial\tilde{\Phi}}{\partial\tilde{z}} = \tilde{F}'(\tilde{x})\left[j_0 - \sigma\frac{\partial\tilde{\Phi}}{\partial\tilde{x}}\right], \tag{2.140}$$

where the function $\tilde{F}'(\tilde{x})$ is given by (2.139).

As in the previous section we transform the boundary condition (2.140) from the surface $\tilde{z} = \tilde{F}(\tilde{x})$ to the plane $\tilde{z} = 0$, i.e. we use the only assumption that the value $\left|\tilde{F}(\tilde{x})\right|$ is small. As a result, we obtain the boundary condition for the potential in the form

$$\tilde{z} = 0: \quad \partial\tilde{\Phi}/\partial\tilde{z} = \left[-j_0\sigma^{-1} + \partial\tilde{\Phi}/\partial\tilde{x}\right]\tilde{F}'(\tilde{x}). \tag{2.141}$$

We do not neglect the term $\partial\tilde{\Phi}/\partial\tilde{x}$ in boundary condition (2.140) and as a result, we obtain the new coefficient in the solution used in paper [2].

We use the values of L, ν/L, B_0, $\nu\sqrt{\rho\nu/\sigma}/L$, $\nu\sqrt{\rho\nu\sigma}/L^2$ as scales of length, velocity, magnetic field, potential and current, respectively. Here σ, ρ, ν are, respectively, the conductivity, the density and the viscosity of the fluid.

Then the MHD equations and the boundary conditions have the form (see [13]):

$$\Delta V_y - Ha^2 V_y + Ha \cdot \partial\Phi/\partial x = 0\,, \tag{2.142}$$

$$\Delta\Phi = Ha \cdot \partial V_y/\partial x\,, \tag{2.143}$$

$$z = 0 : V_y = 0 \tag{2.144}$$

$$\partial\Phi / \partial z = [-A + F(x,0)]F'(x), \tag{2.145}$$

$$F'(x) = \chi_0[\delta(x+1) - \delta(x+1)] + (\chi_1 - \chi_0)[\delta(x+L_1) - \delta(x-L_1)], \tag{2.146}$$

$$\sqrt{x^2 + z^2} \to \infty : \quad V_y \to 0, \Phi \to 0 , \tag{2.147}$$

where $\Delta = \partial^2 / \partial x^2 + \partial^2 / \partial z^2$, $Ha = B_0 L\sqrt{\sigma / \rho\nu}$ is the Hartmann number, $A = j_0 L^2 / (\nu\sqrt{\rho\nu\sigma})$, $\chi_0 = \widetilde{\chi}_0 / L$, $\chi_1 = \widetilde{\chi}_1 / L$ and

$$F(x,0) = \left.\frac{\partial\Phi}{\partial x}\right|_{z=0} . \tag{2.148}$$

2.4.2 The solution of the problem over roughness in a strong magnetic field

In order to solve problem (2.142)-(2.147) we use symmetry of this problem with respect to x: the function $V_y(x,z)$ is an even function, $\Phi(x,z)$ is an odd function with respect to x. This means that functions $V_y(x,z)$ and $\Phi(x,z)$ satisfy additional boundary conditions:

$$z = 0 : \quad \frac{\partial V_y}{\partial x} = 0, \Phi(x,0) = 0 . \tag{2.149}$$

Therefore, problem (2.142)-(2.147) can be solved by means of Fourier cosine and Fourier sine transforms (see [3]). We apply the Fourier cosine transform with respect to x to equation (2.142) and to V_y in boundary condition (2.144) and the Fourier sine transform to equation (2.143) and to $\partial\Phi / \partial z$ in boundary condition (2.145). The Fourier cosine and sine transforms of the functions $V_y(x,z)$ and $\Phi(x,z)$ are defined as follows:

$$V_y{}^c(\lambda, z) = \sqrt{\frac{2}{\pi}}\int_0^\infty V_y(x,z)\cos\lambda x dx , \tag{2.150}$$

$$\Phi^s(\lambda, z) = \sqrt{\frac{2}{\pi}}\int_0^\infty \Phi(x,z)\sin\lambda x dx . \tag{2.151}$$

As a result, we obtain the following system of ordinary differential equations for unknown functions $V_y{}^c(\lambda, z)$, $\Phi^s(\lambda, z)$:

$$-\lambda^2 V_y + \frac{d^2 V_y{}^c}{dz^2} - Ha^2 V_y{}^c + Ha\lambda\Phi^s = 0 , \tag{2.152}$$

$$-\lambda^2\Phi^s + \frac{d^2\Phi^s}{dz^2} + Ha\lambda V_y{}^c = 0\,. \tag{2.153}$$

We also apply transforms (2.150) and (2.151) to boundary conditions (2.144) and (2.145):

$$z = 0: \quad V_y{}^c = 0, \quad \frac{d\Phi^s}{dz} = \sqrt{2\pi}D_1 \sin\lambda + \sqrt{2\pi}D_2 \sin\lambda L_1; \tag{2.154}$$

$$z \to \infty : V_y{}^c, \Phi^s \to 0, \tag{2.155}$$

where $D_1 = \frac{\chi_0}{\pi}[A - F(1,0)], D_2 = \frac{\chi_1 - \chi_0}{\pi}[A - F(L_1,0),$ (2.156)

$$F(L_1,0) = \frac{\partial\Phi}{\partial x} \text{ at } x = L_1,\ z = 0,\ F(1,0) = \frac{\partial\Phi}{\partial x} \text{ at } x = 1,\ z = 0, \tag{2.157}$$

are unknown constants.

The solution of the problem (2.152)-(2.155) is represented in the form:

$$\Phi^s(\lambda, z) = \frac{1}{2\lambda^2}\left(k_1 e^{k_2 z} + k_2 e^{k_1 z}\right)\,[\sqrt{2\pi}D_1 \sin\lambda + \sqrt{2\pi}D_2 \sin\lambda L_1], \tag{2.158}$$

$$V^c(\lambda, z) = \frac{1}{2\lambda}\left(e^{k_1 z} - e^{k_2 z}\right)[\sqrt{2\pi}D_1 \sin\lambda + \sqrt{2\pi}D_2 \sin\lambda L_1], \tag{2.159}$$

where

$$k_1 = -(\sqrt{\lambda^2 + \mu^2} + \mu) \tag{2.160}$$

$$k_2 = -(\sqrt{\lambda^2 + \mu^2} - \mu), \tag{2.161}$$

and

$$2\mu = Ha\,. \tag{2.162}$$

Applying the inverse Fourier sine and cosine transforms to formulae (2.158) and (2.159), we obtain the solution of problem (2.142)-(2.147), containing unknown constants $F(1,0)$ and $F(L_1,0)$ as follows:

$$\Phi(x,z) = D_1\int_0^\infty \left(k_1 e^{k_2 z} + k_2 e^{k_1 z}\right)\frac{\sin\lambda}{\lambda^2}\sin\lambda x d\lambda +$$

$$+ D_2\int_0^\infty \left(k_1 e^{k_2 z} + k_2 e^{k_1 z}\right)\frac{\sin\lambda L_1}{\lambda^2}\sin\lambda x d\lambda\,, \tag{2.163}$$

$$V_y(x,z) = D_1\int_0^{\infty}\left(e^{k_1 z} - e^{k_2 z}\right)\frac{\sin\lambda}{\lambda}\cos\lambda x d\lambda +$$

$$+ D_2\int_0^{\infty}\left(e^{k_1 z} - e^{k_2 z}\right)\frac{\sin\lambda L_1}{\lambda}\cos\lambda x d\lambda. \qquad (2.164)$$

The components j_x and j_z of the induced current density are obtained using the formula:

$$\tilde{\vec{j}} = \sigma\left[-grad\tilde{\Phi}(\tilde{x},\tilde{z}) + \tilde{\vec{V}}\times\tilde{\vec{B}}\right], \qquad (2.165)$$

where

$$\tilde{\vec{V}} = \tilde{V}_y(\tilde{x},\tilde{z})\vec{e}_y, \qquad (2.166)$$

$$\tilde{\vec{B}} = \tilde{B}_y^i(\tilde{x},\tilde{z})\vec{e}_{\mathbf{y}} + B_0\vec{e}_{\mathbf{z}}. \qquad (2.167)$$

In the dimensionless quantities, formula (2.165) can be written in the form :

$$\vec{j} = -grad\Phi(x,z) + Ha\vec{V}\times\vec{B}, \qquad (2.168)$$

where

$$\vec{V} = V_y(x,z)\vec{e}_y, \qquad (2.169)$$

$$\vec{B} = B_y^i(x,z)\vec{e}_{\mathbf{y}} + \vec{e}_{\mathbf{z}}. \qquad (2.170)$$

Substituting (2.169) and (2.170) into (2.168) we obtain:

$$\vec{j} = -grad\Phi(x,z) + HaV_y(x,z)\vec{e}_{\mathbf{x}}. \qquad (2.171)$$

It follows from (1.168), (1.169) and (1.170) that

$$j_x = -\frac{\partial\Phi}{\partial x} + HaV_y(x,z) \qquad (2.172)$$

and

$$j_z = -\frac{\partial\Phi}{\partial z}. \qquad (2.173)$$

Now using formulae (2.160), (2.161), (2.162), (2.163) , (2.164) and (2.172) we get:

$$j_x = -D_1\int_0^{\infty}\left(k_1e^{k_1 z} + k_2e^{k_2 z}\right)\frac{\sin\lambda\cos\lambda x}{\lambda}d\lambda - D_2\int_0^{\infty}\left(k_1e^{k_1 z} + k_2e^{k_2 z}\right)\frac{\sin\lambda L_1\cos\lambda x}{\lambda}d\lambda, \qquad (2.174)$$

$$j_z = -D_1\int_0^{\infty}\left(e^{k_1 z} + e^{k_2 z}\right)\sin\lambda\sin\lambda x d\lambda \; - D_2\int_0^{\infty}\left(e^{k_1 z} + e^{k_2 z}\right)\sin\lambda L_1\sin\lambda x d\lambda. \qquad (2.175)$$

For the evaluation of unknown constants $F(1,0), F(L_1,0)$ or D_1, D_2 in formulae (2.163), (2.164) (2.174) and (2.175) it is necessary to use integral (2.163) and evaluate the limit as follows:

$$F(1,0) = D_1 \lim_{z\to+0}\int_0^\infty \left(k_1 e^{k_2 z} + k_2 e^{k_1 z}\right)\frac{\sin\lambda\cos\lambda}{\lambda}d\lambda + D_2 \lim_{z\to+0}\int_0^\infty \left(k_1 e^{k_2 z} + k_2 e^{k_1 z}\right)\frac{\sin\lambda L_1\cos\lambda}{\lambda}d\lambda \tag{2.176}$$

In addition, a similar limit for $F(L_1,0)$ should be evaluated. Note that the partial derivatives with respect to x of (2.163) can be calculated under the integral sign in (2.163) in the region $0 < z_0 \le z < +\infty, 0 \le x < +\infty$. This integral is majorized in this region. However, if we substitute $z = 0$ under the same integral sign in (2.176), we obtain the divergent integral. In fact this integral converges only in the sense of Abel (see [3]). For example, for the first integral on the right hand side in (2.176), we obtain:

$$I \equiv \int_0^\infty \sqrt{\lambda^2+\mu^2}\,\frac{\sin 2\lambda}{\lambda}d\lambda = \lim_{\delta\to+0}\int_0^\infty e^{-\delta\lambda}\sqrt{\lambda^2+\mu^2}\,\frac{\sin 2\lambda}{\lambda}d\lambda \tag{2.177}$$

or, after evident transformations

$$I \equiv \lim_{\delta\to+0}\int_0^\infty e^{-\delta\lambda}\frac{\mu^2}{\sqrt{\lambda^2+\mu^2}+\lambda}\frac{\sin 2\lambda}{\lambda}d\lambda + \lim_{\delta\to+0}\int_0^\infty e^{-\delta\lambda}\sin 2\lambda d\lambda. \tag{2.178}$$

The first integral on the right hand side of (2.178) converges in the usual sense, but the second integral converges only in the sense of Abel and equal to ½ (see [3]). However, such method gives the solution which tends to zero as the Hartmann number Ha tends to infinity. But this fact contradicts the physical sense of the problem. Therefore, it is necessary to transform integral (2.163) to such a form that after passing to the limit as $z \to +0$ we would obtain the convergence of this integral in the usual sense.

For this purpose we use the following formulae:

$$\int_0^\infty e^{-z\sqrt{\lambda^2+\mu^2}}\cos a\lambda d\lambda = \frac{\mu z}{\sqrt{z^2+a^2}}K_1\left(\mu\sqrt{z^2+a^2}\right), \tag{2.179}$$

$$\int_0^\infty \sqrt{\lambda^2+\mu^2}\,e^{-z\sqrt{\lambda^2+\mu^2}}\cos a\lambda d\lambda = \frac{\mu}{\sqrt{z^2+a^2}}\left[\frac{\mu z^2}{\sqrt{z^2+a^2}}K_2\left(\mu\sqrt{z^2+a^2}\right) - K_1\left(\mu\sqrt{z^2+a^2}\right)\right], \tag{2.180}$$

where $a \ge 0$, $z > 0$ and $K_\nu(z)$ is the modified Bessel function of the second kind of order ν (ν=1, 2). As a result, we obtain (for the details see [6] and [7]):

$$V_y(x,z) = -\mu z \cdot sh\mu z\left[D_1\int_{x-1}^{x+1}\frac{K_1\left(\mu\sqrt{z^2+t^2}\right)}{\sqrt{z^2+t^2}}dt + D_2\int_{x-L_1}^{x+L_1}\frac{K_1\left(\mu\sqrt{z^2+t^2}\right)}{\sqrt{z^2+t^2}}dt\right], \tag{2.181}$$

$$j_x(x,z) = ch\mu z\{D_1\left[F(1+x)-F(1-x)\right] + D_2[F(L_1+x)-F(L_1-x)]\} + \mu V_y(x,z), \tag{2.182}$$

where

$$F(a)=\int_0^a \frac{\mu}{\sqrt{z^2+t^2}}\left[\frac{\mu z^2}{\sqrt{z^2+t^2}}K_2\left(\mu\sqrt{z^2+t^2}\right)-K_1\left(\mu\sqrt{z^2+t^2}\right)\right]dt\,. \tag{2.183}$$

The evaluation of integral (2.175) gives:

$$j_z(x,z)=\mu z\cdot ch\mu z\left[D_1G(x,z,1)+D_2G(x,z,L_1)\right], \tag{2.184}$$

$$G(x,z,L_1)=\frac{K_1\left(\mu\sqrt{z^2+(L_1-x)^2}\right)}{\sqrt{z^2+(L_1-x)^2}}-\frac{K_1\left(\mu\sqrt{z^2+(L_1+x)^2}\right)}{\sqrt{z^2+(L_1+x)^2}}. \tag{2.185}$$

We transform $\partial\Phi/\partial x$, using formulae (2.175), (2.179), and (2.180) :

$$\left.\frac{\partial\Phi}{\partial x}\right|_{x=1}=-D_1\left\{ch\mu z\int_0^2\frac{\mu}{\sqrt{z^2+t^2}}\left[\frac{\mu z^2}{\sqrt{z^2+t^2}}K_2\left(\mu\sqrt{z^2+t^2}\right)-K_1\left(\mu\sqrt{z^2+t^2}\right)\right]dt+\right.$$

$$\left.+\mu^2 z\cdot sh\mu z\int_0^2\frac{1}{\sqrt{z^2+t^2}}K_1\left(\mu\sqrt{z^2+t^2}\right)dt\right\}-$$

$$-D_2\left\{ch\mu z\int_{L_1-1}^{L_1+1}\frac{\mu}{\sqrt{z^2+t^2}}\left[\frac{\mu z^2}{\sqrt{z^2+t^2}}K_2\left(\mu\sqrt{z^2+t^2}\right)-K_1\left(\mu\sqrt{z^2+t^2}\right)\right]dt+\right.$$

$$\left.+\mu^2 z\cdot sh\mu z\int_{L_1-1}^{L_1+1}\frac{1}{\sqrt{z^2+t^2}}K_1\left(\mu\sqrt{z^2+t^2}\right)dt\right\}. \tag{2.186}$$

The integrals on the right hand side of formula (2.186) diverge if $z=0$.

In order to overcome this difficulty, we perform the following transformation. First, we use the following substitution:

$$t=z\xi,\quad dt=zd\xi\,. \tag{2.187}$$

It follows from formula (2.186) that

$$\left.\frac{\partial\Phi}{\partial x}\right|_{x=1}=-D_1\left\{ch\mu z\int_0^{\frac{2}{z}}\frac{\mu}{\sqrt{1+\xi^2}}\left[\frac{\mu z}{\sqrt{1+\xi^2}}K_2\left(\mu z\sqrt{1+\xi^2}\right)-K_1\left(\mu z\sqrt{1+\xi^2}\right)\right]d\xi+\right.$$

$$\left.+\mu\cdot sh\mu z\int_0^{\frac{2}{z}}\frac{\mu z}{\sqrt{1+\xi^2}}K_1\left(\mu z\sqrt{1+\xi^2}\right)d\xi\right\}-$$

$$- D_2 \left\{ ch\mu z \int_{\frac{L_1-1}{z}}^{\frac{L_1+1}{z}} \frac{\mu}{\sqrt{1+\xi^2}} \left[\frac{\mu z}{\sqrt{1+\xi^2}} K_2\left(\mu z\sqrt{1+\xi^2}\right) - K_1\left(\mu z\sqrt{1+\xi^2}\right) \right] d\xi \right.$$

$$\left. + \mu \cdot sh\mu z \int_{\frac{L_1-1}{z}}^{\frac{L_1+1}{z}} \frac{\mu z}{\sqrt{1+\xi^2}} K_1\left(\mu z\sqrt{1+\xi^2}\right) d\xi \right\}. \qquad (2.188)$$

In order to pass to the limit in (2.186) as $z \to +0$ we use the following formula :

$$K_n(z) \approx \frac{1}{2}(n-1)!\left(\frac{2}{z}\right)^n, \; n = 1,2,3,... \text{ at } z \to +0,$$

i.e. $$K_1(z) \approx \frac{1}{z}, \; K_2(z) \approx \frac{2}{z^2} \text{ at } z \to +0. \qquad (2.189)$$

As a result, we obtain from formula (2.188) that

$$\lim_{z\to+0} \left.\frac{\partial\Phi}{\partial x}\right|_{x=1} = -D_1 \lim_{z\to+0} \frac{1}{z} \int_0^{\frac{2}{z}} \left[\frac{2}{\left(1+\xi^2\right)^2} - \frac{1}{1+\xi^2} \right] d\xi - D_1 \lim_{z\to+0} \mu \cdot sh\mu z \int_0^{\frac{2}{z}} \frac{1}{1+\xi^2} d\xi -$$

$$- D_2 \lim_{z\to+0} \frac{1}{z} \int_{\frac{L_1-1}{z}}^{\frac{L_1+1}{z}} \left[\frac{2}{\left(1+\xi^2\right)^2} - \frac{1}{1+\xi^2} \right] d\xi - D_2 \lim_{z\to+0} \mu \cdot sh\mu z \int_{\frac{L_1-1}{z}}^{\frac{L_1+1}{z}} \frac{1}{1+\xi^2} d\xi. \qquad (2.190)$$

The second and the last limits on the right hand side of formula (2.190) are equal to zero, but the first and the third limits give undefined expressions of the form $\frac{0}{0}$ and that is mainly because of the following equality :

$$\int_0^{\infty} \left[\frac{2}{\left(1+\xi^2\right)^2} - \frac{1}{1+\xi^2} \right] d\xi = \int_0^{\infty} \frac{2}{\left(1+\xi^2\right)^2} d\xi - \frac{\pi}{2} = 0. \qquad (2.191)$$

Consequently, from formula (2.190) we obtain:

$$\lim_{z\to+0}\left.\frac{\partial\Phi}{\partial x}\right|_{x=1} = -D_1\lim_{z\to+0}\frac{1}{z}\int_0^{\frac{2}{z}}\left[\frac{2}{\left(1+\xi^2\right)^2}-\frac{1}{1+\xi^2}\right]d\xi - \quad D_2\lim_{z\to+0}\frac{1}{z}\int_{\frac{L_1-1}{z}}^{\frac{L_1+1}{z}}\left[\frac{2}{\left(1+\xi^2\right)^2}-\frac{1}{1+\xi^2}\right]d\xi =$$

$$= -D_1\lim_{z\to+0}\left[\frac{2}{\left(1+\frac{4}{z^2}\right)^2}-\frac{1}{1+\frac{4}{z^2}}\right]\left(-\frac{2}{z^2}\right) - D_2\lim_{z\to+0}\left[\frac{2}{\left(1+\frac{(L_1+1)^2}{z^2}\right)^2}-\frac{1}{1+\frac{(L_1+1)^2}{z^2}}\right]\left(-\frac{L_1+1}{z^2}\right) +$$

$$D_2\lim_{z\to+0}\left[\frac{2}{\left(1+\frac{(L_1-1)^2}{z^2}\right)^2}-\frac{1}{1+\frac{(L_1-1)^2}{z^2}}\right]\left(-\frac{L_1-1}{z^2}\right) = -\frac{D_1}{2}+\frac{2D_2}{1-L_1{}^2}. \qquad (2.192)$$

It follows from (2.156) and (2.192) that

$$F(1,0) = -\frac{1}{2}D+\frac{2D_2}{1-L_1{}^2}. \qquad (2.193)$$

Similarly, for $F(L_1,0)$ we obtain:

$$F(L_1,0) = \frac{2D_1}{1-L_1{}^2}-\frac{D_2}{2L_1}. \qquad (2.194)$$

We remind that [see formula (2.156)]

$$D_1 = \frac{\chi_0}{\pi}[A-F(1,0)],\ \ D_2 = \frac{\chi_1-\chi_0}{\pi}[A-F(L_1,0)]. \qquad (2.195)$$

Consequently, formulae (2.193) and (2.194) represent the system of two equations for the two unknown constants $F(1,0)$ and $F(L_1,0)$, i.e. for the two unknown constants D_1 and D_2.

Substituting these constants into formulae (2.163), (2.164), (2.174) and (2.175), we obtain the solution of problem (2.142)-(2.147).

Chapter 3
EVALUATION OF IMPROPER INTEGRAL

The solutions of certain problems about MHD flow of conducting fluid in the half space are expressed in terms of improper integrals of the product of some meromorphic function and the function $\exp(-a\sqrt{\lambda^2+b^2})\cos\lambda\cos\lambda x$. Here $a>0$ and $b>0$ are some parameters, $x>0$ is the x-coordinate in Cartesian coordinate system (see [6], [7]). It is difficult to calculate these integrals numerically since the integrands are strongly oscillating at large x.

In this chapter these integrals are transformed into integrals of monotone functions using the convolution theorem for product of two Fourier cosine transforms.

3.1 THE TRANSFORMATION OF INTEGRAL OF PRODUCT OF A MEROMORPHIC FUNCTION AND THE FUNCTION $\exp(-a\sqrt{\lambda^2+b^2})\cos\lambda\cos\lambda x$

We consider the improper integral of the form

$$\int_0^\infty \frac{P_n(\lambda^2)}{Q_m(\lambda^2)} e^{-a\sqrt{\lambda^2+b^2}} \frac{\cos\lambda\cos\lambda x}{\lambda^2-\frac{\pi^2}{4}}\,d\lambda, \tag{3.1}$$

where $P_n(\lambda^2)$, $Q_m(\lambda^2)$ are polynomials of degrees n and m, respectively, $m\geq n$, $a>0$, $b>0$, $x>0$ are some positive parameters. The point $\lambda=\pi/2$ is the removable singularity of the integrand in (3.1), because $\cos\lambda=0$ at $\lambda=\pi/2$ in the numerator of the integrand. At large x the integrand in formula (3.1) strongly oscillates so that it is difficult to calculate of this integral numerically.

We suppose that all zeros of polynomial $Q(\lambda^2)$ are simple and have the form: ${\lambda_k}^2=-{a_k}^2$, $k=1,2,\cdots 3,...,n$.

Let

$$F_c(\lambda)=\sqrt{\frac{2}{\pi}}\int_0^\infty f(x)\cos\lambda x dx \tag{3.2}$$

be the Fourier cosine transform of the function $f(x)$.

We use the following

Theorem (see [4]):

If $F_c(\lambda)$ and $\Phi_c(\lambda)$ are the Fourier cosine transforms of functions $f(x)$ and $\varphi(x)$, respectively, then

$$\int_0^\infty F_c(\lambda)\Phi_c(\lambda)\cos\lambda x d\lambda = \frac{1}{2}\int_0^\infty \varphi(\xi)\left[f(|x-\xi|) + f(x+\xi)\right]d\xi\,. \tag{3.3}$$

We define the functions $F_c(\lambda)$ and $\Phi_c(\lambda)$ by the formulae:

$$\frac{P_n(\lambda^2)}{Q_m(\lambda^2)}\frac{\cos\lambda}{\lambda^2-\frac{\pi^2}{4}} = \Phi_c(\lambda), \quad e^{-a\sqrt{\lambda^2+b^2}} = F_c(\lambda)\,. \tag{3.4}$$

To obtain the functions $\varphi(x)$, $f(x)$ it is necessary to evaluate the integrals:

$$I_1 = \sqrt{\frac{2}{\pi}}\int_0^\infty \frac{P_n(\lambda^2)}{Q_m(\lambda^2)}\frac{\cos\lambda\cos\lambda x\, d\lambda}{\lambda^2-\frac{\pi^2}{4}} = \varphi(x), \tag{3.5}$$

$$I_2 = \sqrt{\frac{2}{\pi}}\int_0^\infty e^{-a\sqrt{\lambda^2+b^2}}\cos\lambda x\, d\lambda = f(x)\,. \tag{3.6}$$

For evaluation of I_2 we use the integral known in the literature:

$$\int_0^\infty \frac{e^{-a\sqrt{\lambda^2+b^2}}}{\sqrt{\lambda^2+b^2}}\cos\lambda x\, d\lambda = K_0(b\sqrt{a^2+x^2}), \tag{3.7}$$

where $K_0(z)$ is the modified Bessel function of order 0 of the second kind.

Differentiating formula (3.7) with respect to a we calculate I_2:

$$I_2 = \sqrt{\frac{2}{\pi}}\int_0^\infty e^{-a\sqrt{\lambda^2+b^2}}\cos\lambda x\, d\lambda = \sqrt{\frac{2}{\pi}}\frac{K_1(b\sqrt{a^2+x^2})}{\sqrt{a^2+x^2}} = f(x) \tag{3.8}$$

where $K_1(z)$ is the modified Bessel function of order 1 of the second kind.

For evaluation of integral I_1 we use the residue theorem (from [4]):

$$I_1 = \sqrt{\frac{2}{\pi}}\frac{1}{2}\mathrm{Re}\left\{\left(2\pi i\sum_{k=1}^{m}\operatorname*{Res}_{a_k i} + \pi i \operatorname*{Res}_{\pi/2}\right)\frac{P_n(z^2)}{Q_m(z^2)}\left[e^{iz(1-x)} + e^{iz(1+x)}\right]\right\}, \tag{3.9}$$

where

$$\operatorname*{Res}_{z_0}\frac{\varphi(z)}{\psi(z)} = \frac{\varphi(z_0)}{\psi'(z_0)}\,. \tag{3.10}$$

It is assumed here that $\varphi(z)$ and $\psi(z)$ are analytic functions at point z_0 and in some small neighbourhood where $\psi(z_0)=0$, $\psi'(z_0)\neq 0$. It follows from (3.9), (3.10) that

$$I_1=\sqrt{\frac{2}{\pi}}\frac{\pi}{2}\sum_{k=1}^{m}\frac{P_n(-a_k^2)}{Q_m{}'(-a_k^2)}\left[e^{-a_k|1-x|}\,\mathrm{sign}(1-x)+e^{-a_k(1+x)}\right]+$$

$$+\frac{1}{2}\frac{P_n\left(\frac{\pi^2}{4}\right)}{Q_m{}'\left(\frac{\pi^2}{4}\right)}\left[\sin\left(\frac{\pi}{2}|1-x|\right)sign(1-x)+\sin\left(\frac{\pi}{2}|1+x|\right)\right]=\varphi(x), \qquad (3.11)$$

where $sign(1-x)$ means the sign of $(1-x)$.

Substituting (3.8) and (3.11) into (3.3), using (3.1) and (3.4) and taking into account that $|1-x|^2=(1-x)^2$, we transform integral (3.1) into integral of non-oscillating function:

$$\int_0^\infty\frac{P_n(\lambda^2)}{Q_m(\lambda^2)}e^{-a\sqrt{\lambda^2+b^2}}\cos\lambda\cos\lambda x d\lambda=$$

$$=\frac{ab}{\pi}\int_0^\infty\varphi(\xi)\left[\frac{K_1\left(b\sqrt{(x-\xi)^2+a^2}\right)}{b\sqrt{(x-\xi)^2+a^2}}+\frac{K_1\left(b\sqrt{(x+\xi)^2+a^2}\right)}{b\sqrt{(x+\xi)^2+a^2}}\right]d\xi, \qquad (3.12)$$

where $\varphi(\xi)$ is given by formula (3.11).

Similarly, we can transform each integral of the form

$$\int_0^\infty F_c(\lambda^2)e^{-b\sqrt{\lambda^2+a^2}}\cos\lambda\cos\lambda x\,d\lambda \qquad (3.13)$$

into the right-hand side of formula (3.12) under the condition, that integral (3.13) converges and

$$\sqrt{\frac{2}{\pi}}\int_0^\infty\varphi(x)\cos\lambda x\,dx=F_c(\lambda^2) \qquad (3.14)$$

Let us consider the integral

$$\int_0^\infty\frac{e^{-z\sqrt{\lambda^2+\mu^2}}}{\frac{\pi^2}{4}-\lambda^2}\cos\lambda\cos\lambda x d\lambda,\ (z\geq 0,\ x\geq 0), \qquad (3.15)$$

with oscillatory function $\cos\lambda x$ at large x.

Here $x>0$, $z>0$ are some positive parameters. It follows from

(3.4), (3.8), (3.11) that:

$$\Phi_c(\lambda)=\frac{\cos\lambda}{\frac{\pi^2}{4}-\lambda^2},\quad F_c(\lambda)=e^{-z\sqrt{\lambda^2+\mu^2}} \tag{3.16}$$

$$I_1=\sqrt{\frac{2}{\pi}}\int_0^\infty \frac{\cos\lambda\cos\lambda x}{\frac{\pi^2}{4}-\lambda^2}d\lambda=\sqrt{\frac{2}{\pi}}\cos\left(\frac{\pi}{2}x\right)\eta(1-x)=\varphi(x), \tag{3.17}$$

where

$$\eta(1-x)=\begin{cases}1, & |x|<1\\ 0, & |x|>1\end{cases} \tag{3.18}$$

is the Heaviside step function,

$$I_2=\sqrt{\frac{2}{\pi}}\int_0^\infty e^{-z\sqrt{\lambda^2+\mu^2}}\cos\lambda x d\lambda=\sqrt{\frac{2}{\pi}}\frac{\mu z}{\sqrt{z^2+x^2}}K_1\left(\mu\sqrt{z^2+x^2}\right)=f(x). \tag{3.19}$$

Substituting (3.16), (3.17) and (3.19) into (3.3) we obtain:

$$\int_0^\infty \frac{e^{-z\sqrt{\lambda^2+\mu^2}}}{\frac{\pi^2}{4}-\lambda^2}\cos\lambda\cos\lambda x d\lambda=$$

$$=\frac{2\mu z}{\pi}\int_0^1\left[\frac{K_1\left(\mu\sqrt{z^2+(x-\xi)^2}\right)}{\sqrt{z^2+(x-\xi)^2}}+\frac{K_1\left(\mu\sqrt{z^2+(x+\xi)^2}\right)}{\sqrt{z^2+(x+\xi)^2}}\right]\cos\frac{\pi}{2}\xi\, d\xi. \tag{3.20}$$

Integral (3.20) can be easily evaluated using package "Mathematica" for all values of the parameters $x\ge 0$ and $z\ge 0$. As it can be seen from formula (3.20), the advantages of these transformations are:

1. The parameter x goes from an argument of oscillatory function cosine into the argument of the monotone Bessel function K_1;
2. The limits of the integration are changed to the limits in the bounded region $0\le\xi\le 1$.

3.2 APPLICATIONS TO SOME MHD PROBLEMS

The integrals (3.12) and (3.20) are used to evaluate or transform the solution of problems about MHD flows arising due to roughness of the surface (see [12], [13]).

Consider the following problem.

A conducting fluid is located in the half space $\tilde{z} > 0, -\infty < \tilde{x}, \tilde{y} < +\infty$. The external magnetic field has the form

$$\vec{B}^e = B_0 \vec{e}_z . \tag{3.21}$$

The boundary $\tilde{z} = 0$ is not conducting. A steady current flows with the density $\vec{j} = j_0 \vec{e}_x$ in the direction of the x axis. If the surface $\tilde{z} = 0$ is ideally smooth then the flow is absent. Suppose that roughness on the surface $\tilde{z} = 0$ has the form

$$\tilde{z} = \tilde{\chi}_0 \tilde{f}(\tilde{x}) \eta\left(L - |\tilde{x}|\right), \quad -\infty < \tilde{y} < +\infty , \tag{3.22}$$

where the height of the surface $\tilde{\chi}_0$ is small and $\eta(L - |x|)$ is the Heaviside step function (see Fig.10)) where the particular case of $\tilde{f}(\tilde{x})$ given by formula $\tilde{z} = \tilde{\chi}_0 \cos(\pi\tilde{x} / 2L) \cdot \eta(L - |x|)$). In this case the full current is equal to $\vec{j} = \vec{j}_0 + \vec{j}(\tilde{x},\tilde{z})$ and the flow of the fluid with the velocity $\vec{V} = V_y(y,z)\vec{e}_y$ arises in the direction opposite to the $\tilde{y}$ axis (see Fig.10).

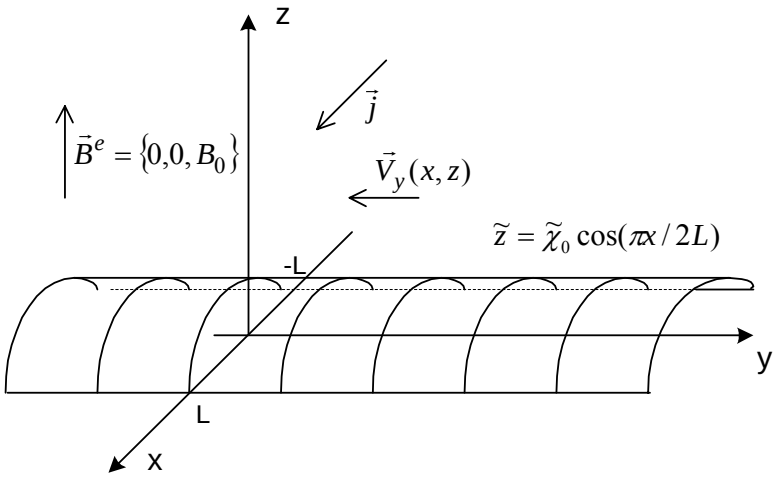

Figure 10. The geometry of the flow in the case of full current.

In the dimensionless quantities the MHD equations and boundary conditions, which we transform from the surface $\tilde{z} = \tilde{f}(\tilde{x})$ to the surface $\tilde{z} = 0$ at the condition that $\tilde{\chi}_0$ is small, have the form (see [2]):

$$\Delta V_y - Ha^2 V_y + Ha \cdot \partial\Phi / \partial x = 0 , \tag{3.23}$$

$$\Delta\Phi = Ha \cdot \partial V_y / \partial x , \tag{3.24}$$

$$z = 0 : V_y = 0 , \partial\Phi / \partial z = \chi_0 \left[- A + F(x,0) \right] \cdot \left(df / dx \right), \tag{3.25}$$

$$\sqrt{x^2 + z^2} \to \infty : \quad V_y \to 0, \Phi \to 0 , \tag{3.26}$$

where $\Delta = \partial^2/\partial x^2 + \partial^2/\partial z^2$, $\Phi(x,z)$ is the potential of current, $Ha = B_0 L\sqrt{\sigma/\rho\nu}$ is the Hartmann number, $A = j_0 L^2/(\nu\sqrt{\rho\nu\sigma})$, $\chi_0 = \tilde{\chi}_0/L$ and σ, ρ, ν are, respectively, the conductivity, the density and the viscosity of the fluid and

$$F(x,0) = \left.\frac{\partial\Phi}{\partial x}\right|_{z=0}. \tag{3.27}$$

Problem (3.23) – (3.26) is solved in [2] when the product $F(x,0)df/dx$ is neglected in boundary condition (3.25), i.e. at the assumption that this product is also small. If the function $f(x)$ is given by

$$f(x) = \chi_0 \cos(\pi x/2)\cdot\eta(1-|x|) \tag{3.28}$$

then the solution has the form

$$V_y(x,z) = 0.5A\chi_0\int_0^\infty \left(e^{k_1 z} - e^{k_2 z}\right)\frac{\cos\lambda\cos\lambda x}{\pi^2/4-\lambda^2}d\lambda, \tag{3.29}$$

$$\Phi(x,z) = -0.5A\int_0^\infty \left(k_1 e^{k_2 z} + k_2 e^{k_1 z}\right)\frac{\cos\lambda\sin\lambda x}{\lambda\left(\lambda^2-\pi^2/4\right)}d\lambda, \tag{3.30}$$

where $k_1 = -(\sqrt{\lambda^2+\mu^2}+\mu)$, $k_2 = -(\sqrt{\lambda^2+\mu^2}-\mu)$, $\mu = 0.5Ha$. (3.31)

It follows from (3.30) that the components of current $\vec{j} = -grad\Phi + HaV_y(x,z)\vec{e}_x$ have the form

$$j_x = -0.5A\chi_0\int_0^\infty \left(k_1 e^{k_1 z} + k_2 e^{k_2 z}\right)\frac{\cos\lambda\cos\lambda x}{\lambda^2-\pi^2/4}d\lambda, \tag{3.32}$$

$$j_z = -0.5A\chi_0\int_0^\infty \left(e^{k_1 z} + e^{k_2 z}\right)\frac{\lambda\cos\lambda\sin\lambda x}{\lambda^2-\pi^2/4}d\lambda. \tag{3.33}$$

We can transform $V_y(x,z)$, j_x and j_z using integral (3.20):

$$V_y(x,z) = -\frac{2\mu z}{\pi}A\chi_0\,\mathrm{sh}\,\mu z\int F(x,z,\xi)\cos\frac{\pi}{2}\xi d\xi, \tag{3.34}$$

where

$$F(x,z,\xi) = \frac{K_1\left(\mu\sqrt{z^2+(x-\xi)^2}\right)}{\sqrt{z^2+(x-\xi)^2}} + \frac{K_1\left(\mu\sqrt{z^2+(x+\xi)^2}\right)}{\sqrt{z^2+(x+\xi)^2}}, \tag{3.35}$$

$$j_x = \frac{2}{\pi} A\chi_0 \mu \left\{ ch\mu z \int_0^1 \frac{\partial}{\partial z}\left[zF(x,z,\xi)\right]\cos\frac{\pi}{2}\xi d\xi \right\} - \mu z sh\mu z \int_0^1 F(x,z,\xi)\cos\frac{\pi}{2}\xi d\xi \qquad (3.36)$$

$$j_z = -A\chi_0 ch\mu z \int_0^1 \frac{\partial F(x,z,\xi)}{\partial x}\cos\frac{\pi}{2}\xi d\xi . \qquad (3.37)$$

Integrals (3.34), (3.36), (3.37) are more suitable for calculations using package "Mathematica", than integrals (3.29), (3.32), (3.33).

In paper [13] the problem (3.23) – (3.26) is solved taking into account the product $F(x,0)df/dx$ in boundary condition for the case where

$$f(x) = \chi_0\left[\eta(x+1) - \eta(x-1)\right]. \qquad (3.38)$$

Then

$$f'(x) = \left[\delta(x+1) - \delta(x-1)\right], \qquad (3.39)$$

where $\delta(\widetilde{x})$ is the Dirac delta function.

In this case the solution of the problem (3.23) – (3.26) has the form:

$$V_y(x,z) = D\int_0^\infty \left(e^{k_1 z} - e^{k_2 z}\right)\frac{\sin\lambda}{\lambda}\cos\lambda x d\lambda , \qquad (3.40)$$

$$\Phi(x,z) = D\int_0^\infty \left(k_1 e^{k_2 z} + k_2 e^{k_1 z}\right)\frac{\sin\lambda}{\lambda^2}\sin\lambda x d\lambda , \qquad (3.41)$$

where

$$D = \frac{\chi_0}{\pi}\frac{A}{1-\chi_0/\pi} . \qquad (3.42)$$

Components of current $\vec{j} = -grad\Phi + HaV_y(x,z)\vec{e}_x$ have the form

$$j_x = -D\int_0^\infty \left(k_1 e^{k_1 z} + k_2 e^{k_2 z}\right)\frac{\sin\lambda\cos\lambda x}{\lambda} d\lambda , \qquad (3.43)$$

$$j_z = -D\int_0^\infty \left(e^{k_1 z} + e^{k_2 z}\right)\sin\lambda\sin\lambda x d\lambda . \qquad (3.44)$$

In order to transform the given solution it is necessary to use the integral which we obtain by differentiating formula (3.28) with respect to parameter a and substituting $a = z$, $b = \mu$, $x = a$:

$$\int_0^\infty \sqrt{\lambda^2+\mu^2}\, e^{-z\sqrt{\lambda^2+\mu^2}}\cos a\lambda\, d\lambda = \frac{\mu}{\sqrt{z^2+a^2}}\left[\frac{\mu z^2}{\sqrt{z^2+a^2}}K_2\left(\mu\sqrt{z^2+a^2}\right) - K_1\left(\mu\sqrt{z^2+a^2}\right)\right] \qquad (3.45)$$

where $K_2(z)$ is the modified Bessel function of second kind.

Substituting $a = t$ in (3.45) and integrating with respect to t from $t = 0$ to $t = a$, we obtain:

$$\int_0^\infty \sqrt{\lambda^2 + \mu^2}\, e^{-z\sqrt{\lambda^2+\mu^2}}\, \frac{\sin a\lambda}{\lambda}\, d\lambda = F(a), \tag{3.46}$$

where

$$F(a) = \int_0^a \frac{\mu}{\sqrt{z^2+t^2}} \left[\frac{\mu z^2}{\sqrt{z^2+t^2}} K_2\left(\mu\sqrt{z^2+t^2}\right) - K_1\left(\mu\sqrt{z^2+t^2}\right) \right] dt. \tag{3.47}$$

Similar transformations with formula (3.28) gives:

$$\int_0^\infty e^{-z\sqrt{\lambda^2+\mu^2}}\, \frac{\sin a\lambda}{\lambda}\, d\lambda = \mu z \int_0^a \frac{K_1(\mu\sqrt{z^2+t^2})}{\sqrt{z^2+t^2}}\, dt. \tag{3.48}$$

Using formulae (3.46), (3.48) we transform integrals (3.39), (3.43) to the form of integrals of non-oscillatory functions:

$$V_y(x,z) = -D\mu z\, sh\mu z \int_{x-1}^{x+1} \frac{K_1(\mu\sqrt{z^2+t^2})}{\sqrt{z^2+t^2}}\, dt, \tag{3.49}$$

$$j_x(x,z) = Dch\mu z\left[F(1+x) - F(1-x)\right] + \mu V_y(x,z), \tag{3.50}$$

where $F(a)$ is given by formula (3.47). Using formula (3.28) one can evaluate integral (3.44):

$$j_z(x,z) = D\mu z\, ch\mu z \left[\frac{K_1\left(\mu\sqrt{z^2+(1-x)^2}\right)}{\sqrt{z^2+(1-x)^2}} + \frac{K_1\left(\mu\sqrt{z^2+(1+x)^2}\right)}{\sqrt{z^2+(1+x)^2}} \right]. \tag{3.51}$$

Formula (3.51) allows one to obtain the asymptotic of the component $j_z(x,z)$ at $\mu = 0.5Ha \to \infty$. We now use the formulae which hold at $\mu \to \infty$, $z > 0$, $l > 0$:

$$ch\mu z \approx 0.5e^{\mu z}, \quad K_1(\mu l) \approx \sqrt{\frac{\pi}{2\mu l}}\, e^{-\mu l}. \tag{3.52}$$

Then, according to (3.51), component $j_z(x,z)$ decreases at $\mu \to \infty$ everywhere, except two regions bounded by the parabolas:

$$\mu\sqrt{z^2+(x-1)^2} - \mu z = 1; \quad \mu\sqrt{z^2+(x+1)^2} - \mu z = 1, \tag{3.53}$$

i.e. by parabolas

$$z+\frac{1}{2\mu}=0.5\mu(x+1)^2;\qquad z+\frac{1}{2\mu}=0.5\mu(x-1)^2 \tag{3.54}$$

and we can replace $1/2\mu\approx 0$ at $\mu\to\infty$ in formula (3.54). Inside the regions bounded by parabolas (3.54), the component $j_z(x,z)$ tends to infinity in accordance with formula:

$$j_z\approx\sqrt{\mu/z}\,, \tag{3.55}$$

and it follows from (3.51) – (3.53) that:

$$l\equiv\sqrt{z^2+(1-x)^2}=(1+\mu z)/\mu\approx z\,,$$

$$\mu z\,\mathrm{ch}\,\mu z l^{-1}K_1(\mu l)\approx\mu\frac{1}{2}e^{\mu(z-l)}\sqrt{\frac{\pi}{2\mu z}}=e^{-1}\sqrt{\frac{\pi}{8}}\sqrt{\frac{\mu}{z}}\quad .$$

The convolution theorem for product of two Fourier cosine transforms can be used for transformation of one class of integrals containing oscillatory functions to integrals of monotonic functions. These results are applied for transformation of solution of some MHD problems arising in half space $z\geq 0$ as a result of roughness of the surface $z=0$. The various boundary layers for induced current in a strong magnetic field are found in this problem.

Chapter 4
CORROSION OF EUROFER STEEL AND MAGNETIC CONFINEMENT OF PLASMA IN REACTORS

Search of new energy sources draws the increasing attention of scientists of many countries and that is why they are trying to drag and control the fusion of **D-T** (Deutrium-Tritium) plasma inside of a Tokamak reactor (Tokamak is a device used in nuclear fusion research for magnetic confinement of plasma and it consists of a complex system of magnetic fields that confine the plasma in a hollow doughnut-shaped container). The **D-T** reaction and its related use in reactors are briefly described below.

During my seven year staying period in Riga, Latvia (one of the main MHD application centers currently existing in Europe), I have had access to some interesting sites related to MHD study such as the Physics Institute in Salaspils where I have seen the three recently planned experimental sessions (each 2000 hours long) which have been successfully completed. New results concerning the profile of corrosion are obtained. I had the opportunity to participate in some PAMIR MHD International Conferences (4^{th} and 5^{th} and the 7^{th} PAMIR International Conferences). This led to the writing of Chapter 4 illustrating the mentioned above (see [1], [32], [34], [35], [36], [37], [40], [49], [56] and [64])

4.1 Deuterium-Tritium reaction and its use in reactors.

During this century, the world's population will double from six billion people and it will rise to ten billions by 2050. More importantly, a lot more energy will be used than we use today, energy consumption will probably be two times higher by the middle of the century with an even stronger increase in electricity consumption (see Table 1 below).

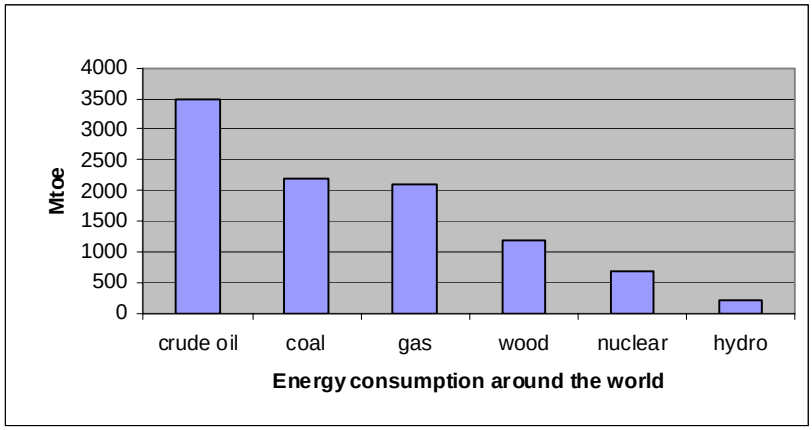

Table 1. Energy consumption by the year 2007 [Mtoe (Million Tonnes Of Oil Equivalent)]
(The exact values are respectively 3500, 2200, 2100, 1200, 700, and 200)

Fusion is the nuclear process that powers the sun and other stars. Under the very high temperature conditions, hydrogen atom becomes separated into its fundamental components-electrons and nuclei, and form a new state of matter called "Plasma". Finally the nuclei fuse produces Helium and gives energy. Scientists from all European member states and G8 countries associated with the EURATOM fusion program have been trying to reproduce this process on Earth. The fusion of Deutrium and Tritium, two Hydrogen isotopes would need a temperatue of 100 million ºC. This procedure can be done inside of a reactor using a Magnetic confinement that consists of heating on the Plasma by Joule effect and by injection of energetic particle beams and radio-frequency waves into the plasma and its thermal isolation from the material walls by strong magnetic fields [1], [32], [33], [57], [49].

Mainly, three types of liquid metal blankets are proposed for this purpose:

1) (SCLL), the Self-Cooled Lithium-Lead blanket

2) (WCLL), the Water-Cooled Lithium-Lead blanket

3) (HCLL), the Helium-Cooled Lithium-Lead blanket [1], [33], [57], [49].

EUROFER-97 steel has been tested as the best structural materials of the blanket in a reactor. It is supposed to be used as the basic construction material for the production of the HCLL **(Helium-Cooled Lithium-Lead**) Blanket (see Fig. 11 below).

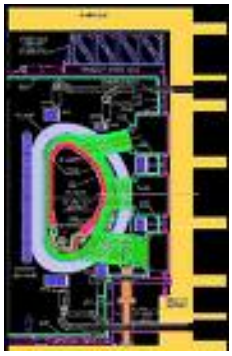

Figure 11. HCLL Blanket image.

4.1.1 The Deuterium-Tritium (D-T) reaction and its products

The reaction is represented by the following relation

$$ {}^{2}_{1}\mathrm{H} + {}^{3}_{1}\mathrm{H} \rightarrow {}^{4}_{2}\mathrm{He} + {}^{1}_{0}\mathrm{n} + 17.6\ \mathrm{MeV} \qquad (4.1) $$

and is simply represented in Fig. 12 below.

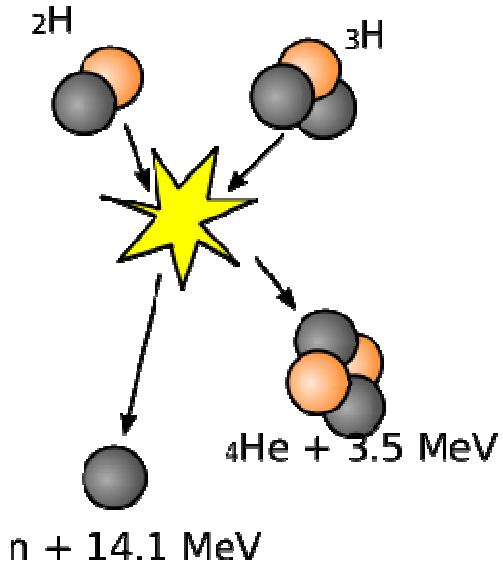

Figure 12. Deuterium-Tritium (D-T) reaction and its products

The fusion energy (17.6 MeV) appears as kinetic energy of neutrons (14.1 MeV) that need to be saved inside of a reactor using lead, and of Alphas (3.5MeV) that are evacuated as ashes from the chimney of a certain reactor [1], [36], [37], and [64].

Deutrium is generously present in seawater but Tritium is a radioactive element rarely existent naturally on Earth. However it can be bred inside the reactor using the reaction of the neutrons in a blanket containing lithium, an abundant light metal in the nature as:

Li6 + n ---- T + He4 + 4.8 MeV (4.2)

Li7 + n ---- T + He4 – 2.5 MeV (4.3)

Ten grams of deuterium which can be extrated from 500 litres of water and 15 gr of tritium produced from 30 gr the lithium would produce enough fuel for the lifetime electricity needs of a person in an industrialised country. In other words, these two resources are practically available. This is another advantage of D-T Fusion (see [1], [32], [39], [35], [49], [55], [56], [64]).

4.1.2 Progress of the D-T plasmas confinement inside of reactors.

Europe, the world leader in this field, has already undertaken several research and development projects dealing with fusion (as an example, we mention the **JET** project (the Joint European Torus)). The largest Tokamak in the world will be constructed in Culham (UK). Despite the progress continuously achieved on JET, it is clear that a larger and more powerful device would be necessary to demonstrate the feasibility of nuclear fusion energy on a reactor scale. The future of fusion lies on **ITER** (The International Thermonuclear Experimental Reactor) whose purpose is to produce a detailed, complete, and fully integrated engineering design of ITER and all technical data necessary for future decisions and results that come out of ITER (see [1], [23], [33], [34], [37], [57], [49], [64]).

ITER will be constructed using the results of **JET** with the same concepts and the same Toroidal shape but on a much larger scale (see Fig. 13 below).

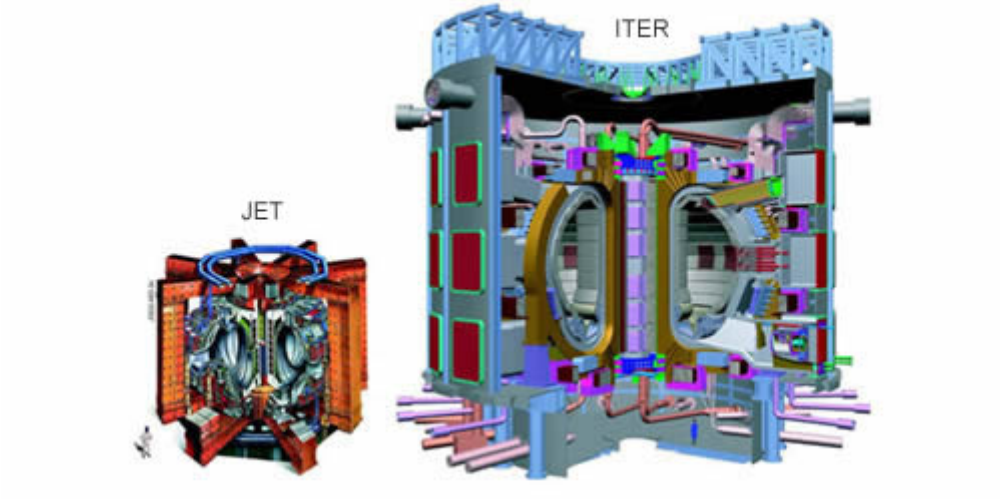

Figure 13. The relative sizes of JET and ITER devices (see [1]).

The plasma volume of **JET** and **ITER** are 100 m^2 and 800 m^2, respectively. In the case of **JET**, losses of energy are compensated by a source of outside energy. One of the advantages of **ITER** that it will not depend on power supply from the outside. The deuterium-tritium (D-T) experiments on the Tokamak Fusion Test Reactor (TFTR) have yielded unique information on the confinement, heating and alpha particle physics of reactor scale D-T plasmas as well as the first experience with tritium handling and D-T neutron activation in an experimental environment. Toroidal and poloidal field coils are used and these generate strong magnetic field (typically about 5 tesla, which is about 100,000 times the earth's magnetic field) that confines the plasma and stops it touching the walls of the vacuum vessel. The D-T plasmas produced and studied in TFTR have peak fusion power of 10.7 MW with central fusion power densities of 2.8 MWm^{-3} which is similar to the 1.7 MWm^{-3} fusion power densities projected for 1,500 MW operation of (ITER). Detailed alpha particle measurements have confirmed alpha confinement and heating of the D-T plasma by alpha particles as expected. Advanced Tokamak operating modes have been produced in TFTR which have the potential to double the fusion power to ~20 MW which would also allow the study of alpha particle effects under conditions very similar to those projected for ITER. TFTR is also investigating two new innovations, alpha channeling and controlled transport barriers, which have the potential to significantly improve the standard advanced Tokamak.

This strategy included three steps beyond JET [35], [36], [37], [61]:

1) ITER is a liquid lithium self-cooled breeding blanket aiming at demonstrating the controlled burn of deuterium-tritium plasmas with steady state as an ultimate goal on a scale of a power

plant and of a number of key technologies. ITER project will be ready approximately by the end of year 2050 in Caradache, south of France.

2) DEMO is the water cooled blanket reactor aiming at the final demonstration of all the relevant technologies, tritium self-sufficiency and electricity production. The design of DEMO suppose to start in 2035s and its operation in 2060s. A steady-state Tokamak is minimized to have 5.8 m of major radius with 2.3 GW of fusion power with energy amplification Q exceeding 30.

3) PROTO is the first proto-type power station with complete reactor and ancillary systems that would include all the remaining technological developments as well as generating electricity on a commercial scale, under the assumption that its design and construction would be started in 2050s and its operation in 2070s (see [1], [33], [35], [49], [49], [57], [64]).

4.1.3 Major reasons of the use of fusion energy

Maybe at the end of this century, fusion would be considered as a new reliable long-term energy source that becomes a part of humans' lives due to such important reasons:

1. The fuels are abundant everywhere and for a much cheaper price in comparison to the present price.

2. The fusion process is very clean since it does not contribute to the greenhouse effect, to the spread of acid rain, or to radioactive particles that could take many years to remove.

3. D-T fusion power station can be made very safe due to two main reasons:

(i) a large uncontrolled release of energy would be impossible since the amounts of deuterium and tritium fuels inside the reactor will be very small;

(ii) the fusion reactions can be stopped in a very short time if an accident occurs, since the fuels are introduced inside the reactor while they are burned.

4.2 Analysis of MHD Phenomena Influence on the Corrosion of EUROFER Steel in the Pb-17Li Flow

In the second part of this thesis (section 2.2) the MHD flow of a conducting fluid located in the half space $\tilde{z} > 0, -\infty < \tilde{x}, \tilde{y} < +\infty$ with the roughness of the surface in the form $\tilde{z} = \tilde{\chi}_0 \cos(\pi\tilde{x}/2L)$ is considered. The external magnetic field is $B^c = B_0 e_z$. Corrosion of EUROFER steel in the Pb-17Li flow can be considered as a consequence of roughness on the surface of the walls where the Hartmann surfaces flows are perpendicular to the flow as well. Roughness is modelled by the formula

$$Z = Z(y) = \chi_0 \cos \alpha y \,, \qquad (4.4)$$

where χ_0 is the amplitude, $\alpha = \pi a / L$ characterizes the scale, L is the width of hills and depressions, and Ha is the Hartmann number. The value a=3 mm is chosen as a typical dimension. Here $v = 1.1 \times 10^{-7} m^2 / s$; $\sigma = 0.73 \times 10^6 S / m$ and thus for the mass transfer problem $D_{Fe} = (6.4) \times 10^{-9} m^2/s$ more than $6 \times 10^{-9} m^2/s$ as it was assumed in [1], [55], and [56]) .

Despite the fact that corrosion of steel in the Pb-17Li flow is a small but important part of the reactor work, we notify the importance and newest results obtained on the corrosion process in the Physics Institute in Latvia [55], [56]. For instance, the first experimental 2000 hours' session for investigating the influence of magnetic field on the corrosion of EUROFER steel in the flow of Pb-17Li has been successfully completed. During the whole session the following conditions were maintained at the experimental facility: the minimum temperature in the cold part of the loop T_{min} = (350 ± 20) ^{0}C; the temperature in the test section T_{TS} = (550 ± 10) ^{0}C; the mean flow velocity in the test section U_{mean} = (5 ± 0.5) cm/s; the magnetic field strength B = 1.7 T. The residue of the melt in a pure Li melt at the temperature of 400^{0}C was washed off from the samples removed from the test section and the samples were further weighed. These measurements showed that mass losses for corroded samples located in the zone with a magnetic field are approximately over two times greater when compared with those located in the zone outside the magnetic field (B = 0). This fact shows a significant intensification of the corrosion by the magnetic field. Moreover, it should be stressed that due to insufficient heat isolation of the test section the temperature of the molten metal varied over the length of the test section: at the zone where B = 0 (inlet) it was by ~ 15 °C higher than at the test section (outlet) with the magnetic field where T = 550 °C. This experiment was performed on different samples with flow velocities of 2,5 cm/s and 5cm/s and magnetic current of 0, 1,5 and 1.7 T. Results gained in these investigations demonstrated essential influence of magnetic field on the corrosion processes both in the intensity of corrosion and its character (see Fig. 14).

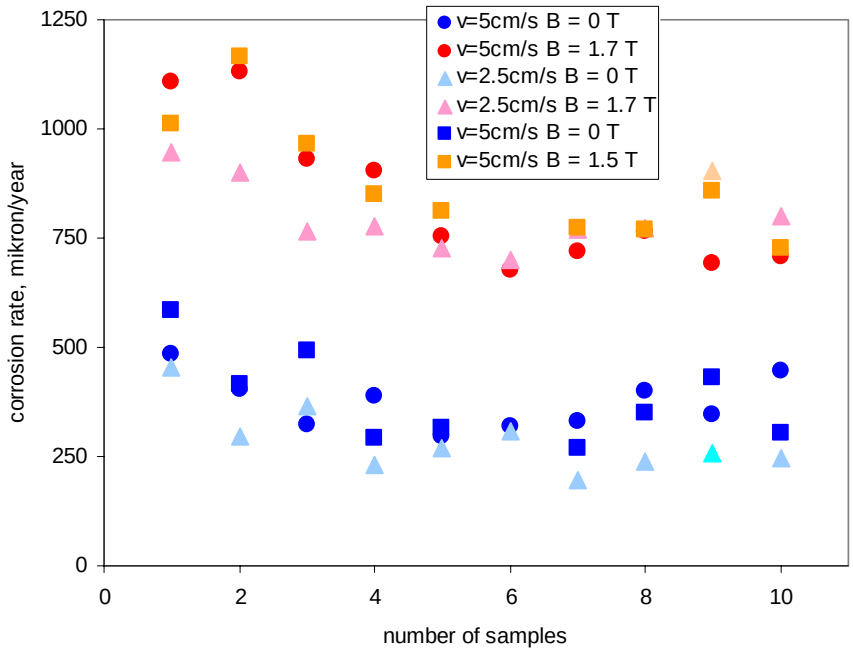

Figure 14. Comparison of corrosion rate of EUROFER samples in magnetic field and without magnetic field.

Visual observations of the test samples showed sufficient distinctions in relief on the sample surfaces. In particular, samples suffering corrosion from the zone with B = 0 are rather smooth and, on the contrary, the sample surfaces from the zone exposed to the magnetic field resemble a regular enough wave-like pattern with furrows oriented in the melt flow direction. Such pattern is typical only of the Hartmann (perpendicular to the magnetic field) walls. The side walls remain rather smooth. The same can be attributed to the outer sample surfaces, which exhibit traces of corrosion caused by the EUROFER interaction with the melt that penetrated the gaps between the samples and the outer channel.

The second experimental (2000 hours' session) has been completed successfully and showed that the magnetic field not only generally enhanced the corrosion rate, but showed that magnetic field badly influences corrosion. In the case for samples located in zone ($\boldsymbol{B}$ = 0) all inner surfaces of samples being subjected to the Pb-17Li flow were maintained sufficiently smooth, then in zone with magnetic field ($\boldsymbol{B}$ = 1.7 T) all Hartman surfaces of samples were covered with grooved structure oriented in the flow direction (see [1], [49], [55], [56], [64]). The presence of a magnetic field led to the appearance of regular wave-like patterns on the corroding surfaces perpendicular to the magnetic field, which were oriented in the melt flow direction and that the corrosion processes on the EUROFER surfaces washed over by Pb-17Li and were determined by the surface orientation about the magnetic field direction ([55], [56]), (see also Fig. 15 below).

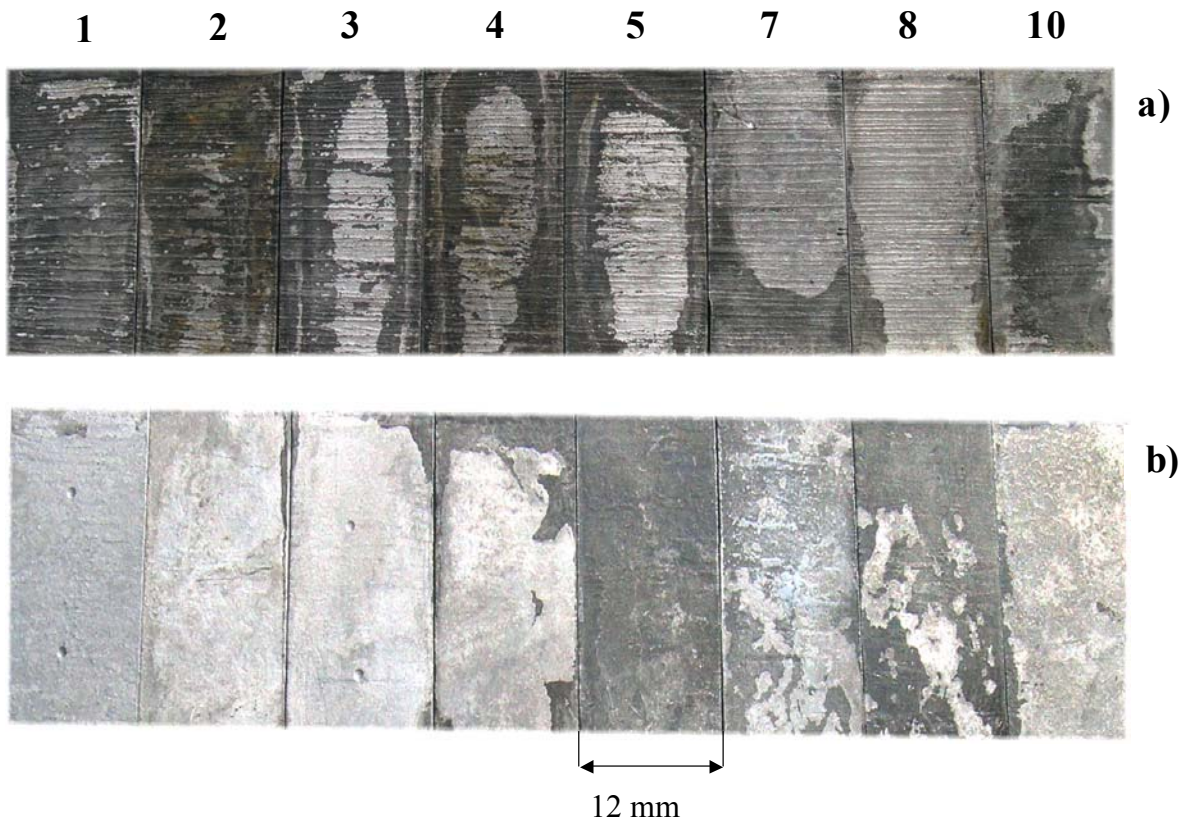

Figure 15. Surface relief of EUROFER samples subjected to corrosion in Pb17Li during 2000 hours.

Moreover, in the third experimental session [56] the corrosion rate h_0 caused by Pb-17Li on the EUROFER steel was investigated and its results of the corrosion rate are shown in Table below).

Corrosion rate h_0 without and with magnetic field.

N	B_0=0	B_0=1.8T
	h_0, μ meter/year	
1	523	967
2	458	877
3	381	694
4	293	846
5	388	726

Table 2. Corrosion rate of EUROFER steel by Pb-17Li flow [55], [56]

There is a hope that before the end of this century, scientists with all the technologies and studies available, would be able to achieve success of the ITER project. This will provide the physical and technological basis for the construction of a demonstration electrically generating power plant in the future like DEMO and PROTO . Then a new clean and cheap source of energy would be a part of humans' life (see [1], [9], [28], [32]-[37] , [40] , [49] , [51], [55] , [56] , [62] , [70] and [73]).

Chapter 5

Ginzburg-Landau equation for stability analysis of shallow water in a weakly non-linear regime

Losses due to turbulent friction are often described in hydraulics by means of empirical (or semi-empirical) formulas like Chezy of Manning's formulas [66]. In particular, the Chezy formula is used to represent the bottom friction force $\vec{F}$ in the form

$$\vec{F} = \frac{\rho g A c_f}{h} \vec{v}|\vec{v}|,$$

where ρ is the density of the fluid, g is the acceleration due to gravity, A is the cross-sectional area, h is water depth, c_f is the friction (or roughness) coefficient, $\vec{v}$ is the velocity vector and $\vec{F}$ is the friction force. The coefficient c_f is estimated by means of several empirical formulas which can be found in the literature. One example is Colebrook formula [66] which relates c_f to the Reynolds number of the flow.

Chezy formula is effectively used by hydraulic engineers for many years to estimate the "lumped" effect of friction in a turbulent flow. Examples include computation of flow rate and losses in channels or pipes and design of open channels. Chezy formula is also widely used in cases where more detailed knowledge of the flow field is required [50]. The coherent structures in wake flows are believed to appear as a final product of hydrodynamic instability of the flow [45]. Classical method of analysis of hydrodynamic stability is the linear stability analysis [26]. Linear theory can be used to find the value of the parameters of the problem for which a particular flow becomes unstable. However, the development of instability beyond the threshold cannot be described by the linear theory. Methods of weakly nonlinear theory have been applied in the past to different flows [8, 10, 14-16, 19, 22, 23, 26, 43, 44, 47, and 67] and usually lead to amplitude evolution equations for the most unstable mode. One of such equations is the complex Ginzburg-Landau equation. Weakly nonlinear theory is applied to quasi-two-dimensional flows in [22] with Rayleigh friction (internal friction is assumed to be linearly related to the velocity distribution). It is concluded in [22] that small variations of linear stability characteristics (in particular, small variations in the base flow profile) led to large changes in the Landau constant (the Landau constant is the real part of one of the coefficients of the Ginzburg-Landau equation).

5.1 Shallow flows behind obstacles

Wake flows are quasi-two-dimensional flows behind obstacles (such as islands) in which

the horizontal components of the velocity vector are much larger than the vertical component. A typical measure of shallowness of the flow is the ratio of the transverse length scale of the flow, D, and water depth, H. The flow is assumed to be shallow if the ratio D/H is large enough: $D/H >> 1$. An excellent example of shallow wake flow is discussed in [19] where the leaking oil from the tanker Argo Merchant shows a von Karman vortex street flow pattern. Experimentally observed coherent structures in shallow wakes are believed to appear as a result of flow instability [19], [44]. Linear stability of shallow flows is studied experimentally in [19], [44], [45]. It is shown in [19] that three different flow regimes can be observed in shallow wake flows: steady bubble, unsteady bubble and vortex street. It was found in [19] and [44] that flow patterns behind obstacles depend on shallow wake stability parameter $S = c_f b/H$, where c_f is the bottom friction coefficient and b is length scale (the diameter of the cylinder in [19]).

Theoretical investigation of linear stability of shallow wake flows is performed in [19], [44], [45]. Linear stability analyses confirm that the stability characteristics of shallow water flows depend on the magnitude of the stability parameter S. In particular, a flow becomes more stable as the parameter S increases.

The linear stability theory can be used to determine when a particular flow becomes unstable. The "fate" of the disturbance just above the threshold cannot be predicted by the linear theory. Methods of weakly nonlinear theory are often applied to describe the evolution of the most unstable linear mode when the flow becomes unstable [26], and [67]. Relatively simple amplitude evolution equations such as the complex Ginzburg-Landau equation (CGLE) are used in the literature to analyze spatio-temporal dynamics of complex flows [10], [67]. The popularity of the CGLE is based on the following factors: (1) the model is relatively simple but includes such physical effects as nonlinearity and diffusion, (2) the CGLE is a scalar equation, (3) the CGLE can be derived (in some cases) from the equations of motion, (4) the coefficients of the CGLE can be obtained in closed form (in terms of integrals containing the characteristics of the corresponding linear stability problem), (5) the CGLE can exhibit a rich variety of solutions depending on the values of its coefficients.

In many applications the CGLE (or the Landau equation) is used as a phenomenological model equation. In such cases the coefficients of the CGLE are obtained from experimental data.

On the other hand, the CGLE can be derived from the equations of motion. Examples include weakly nonlinear analyses of plane Poiseuille flow [67] and problems related to generation of waves by wind [10], shallow flows behind obstacles such as islands [44], and [45], rapidly decelerated flows in pipes [43] and channels [46].

Despite the fact that the CGLE was successfully applied in practice to model spatio-temporal dynamics of complex flows [44], [45], other sources in the literature suggest that the

use of weakly nonlinear theory should be limited. One such an example is introduced in paper [22] where linear and weakly nonlinear theory is applied to the stability analysis of quasi-two-dimensional shear flows such as shallow water flows. It is assumed in [22] that the term representing friction in fluid system is of the form $\vec{f}_R = -\lambda_R \vec{u}$, where λ_R is the coefficient of Rayleigh friction and $\vec{u}$ is the velocity vector. The authors compared their theoretical predictions from the linear stability analysis with experimental data. Reasonable agreement was found. On the other hand, it is found in [22] that the Landau constant (the real part of one of the coefficients of the CGLE) is quite sensitive to the shape of the base flow velocity profile. As a result, it is concluded in [22] that it would be impossible to compare directly the theory with experiments since it would be difficult to determine the base flow velocity profile with accuracy up to the third derivative (as it is required by a weakly nonlinear theory). In particular, it is found in [22] that the values of the Landau constant differ by a factor of 3 for two base flow velocity profiles whose linear stability characteristics differ by not more than 20%.

In the present section, linear and weakly nonlinear stability of a one-parametric family of shallow wake flows is investigated [15] and [16]. The parameter used in the study represents a slow longitudinal variation of shallow wake flow behind obstacles such as islands. In contrast to [22] where the internal friction is linearly related to the velocity distribution, a nonlinear Chezy formula [66] is used to model bottom friction. The base flow profile used in [19] is adopted in our study. Calculations show that the Landau constant as well as other coefficients of the CGLE are not so sensitive to the shape of the base flow profile. Thus, it is plausible to assume that the CGLE can be used to describe spatio-temporal dynamics of shallow wake flows.

5.2 Linear stability analysis

Consider the base flow of the form

$$\vec{U} = (U(y),0) \tag{5.1}$$

where

$$U(y) = 1 - \frac{2R}{1-R}\frac{1}{\cosh^2(\alpha y)}. \tag{5.2}$$

The base flow (5.2) is suggested in [19] after careful analysis of available experimental data for deep water flows behind circular cylinders. The profile (5.2) is also adopted in the present study. The parameter R is the velocity ratio: $R = (U_m - U_a)/(U_m + U_a)$, where U_m is the wake centerline velocity and U_a is the ambient velocity, and $\alpha = \sinh^{-1}(1)$. It is shown in [44] that

under the rigid-lid assumption the linear stability of wake flows in shallow water is described by the following eigenvalue problem:

$$\varphi_1''(U-c+SU)+SU_y\varphi_1'+\left(k^2-U_{yy}-k^2U-\frac{S}{2}kU\right)\varphi_1=0 \tag{5.3}$$

$$\varphi_1(\pm\infty)=0, \tag{5.4}$$

where the perturbed stream function of the flow, $\psi(x,y,t)$, is assumed to be of the form

$$\psi(x,y,t)=\varphi_1(y)\exp[ik(x-ct)]+c.c. \tag{5.5}$$

Here $\varphi_1(y)$ is the amplitude of the normal perturbation, k is the wavenumber, c is the wave speed of the perturbation, and $c.c.$ means "complex conjugate". The linear stability of the base flow (5.2) is determined by the eigenvalues, $c_m=c_{rm}+ic_{im}$, $m=1,2,...$ of the eigenvalue problem (5.3), (5.4). The flow (5.2) is linearly stable if $c_{im}<0$ for all m and linearly unstable if $c_{im}>0$ for at least one value of m.

The linear stability problem (5.3), (5.4) is solved by means of a pseudospectral collocation method based on Chebyshev polynomials. The computational procedure is briefly described below (details of the numerical method can be found in [44]). The interval $-\infty<y<+\infty$ is mapped onto the interval $-1<r<1$ by means of the transformation $r=\frac{2}{\pi}\arctan y$. The solution to (5.3), (5.4) is sought in the form

$$\varphi_1(r)=\sum_{k=0}^{N}a_k(1-r^2)T_k(r), \tag{5.6}$$

where $T_k(r)$ is the Chebyshev polynomial of degree k. The collocation points r_j are

$$r_j=\cos\frac{\pi j}{N},\ j=0,1,...,N. \tag{5.7}$$

The derivatives are transformed by the chain rule:

$$\begin{aligned}\frac{d\varphi_1}{dy}&=\frac{2}{\pi}\cos^2\frac{\pi r}{2}\frac{d\varphi_1}{dr},\\ \frac{d^2\varphi_1}{dy^2}&=\frac{4}{\pi^2}\cos^4\frac{\pi r}{2}\frac{d^2\varphi_1}{dr^2}-\frac{4}{\pi}\sin\frac{\pi r}{2}\cos^3\frac{\pi r}{2}\frac{d\varphi_1}{dr}\end{aligned} \tag{5.8}$$

Substituting (5.6), (5.8) into (5.3), (5.4) and evaluating the function $\varphi_1(r)$ and its derivatives at the collocation points (5.7) we obtain the following generalized eigenvalue problem:

$$(B-\lambda C)a=0 \tag{5.9}$$

where B and C are complex-valued matrices and

$a=(a_1a_2...a_N)^T$.

Problem (5.9) is solved numerically by means of the IMSL routine DGVCCG. The critical values of the stability parameters k, S and c for different values of R are given in Table 3 (here $S_c = \max_k S$ **).**

R	k	S_c	c
-0.3	0.892	0.11819	0.69814
-0.4	0.909	0.15689	0.65964
-0.5	0.926	0.19548	0.62394
-0.6	0.944	0.23409	0.59083
-0.7	0.962	0.27286	0.55925
-0.8	0.980	0.31189	0.52882

Table 3. Critical values of of the stability parameter S .

5.3 Weakly nonlinear analysis

Following [67], in this section the main steps of the derivation of the amplitude evolution equation for the most unstable mode are briefly described. Consider the two-dimensional shallow water equations of the form :

$$\frac{\partial u}{\partial x}+\frac{\partial v}{\partial y}=0, \tag{5.10}$$

$$\frac{\partial u}{\partial t}+u\frac{\partial u}{\partial x}+v\frac{\partial u}{\partial y}+\frac{\partial p}{\partial x}+\frac{c_f}{2H}u\sqrt{u^2+v^2}=0, \tag{5.11}$$

$$\frac{\partial v}{\partial t}+u\frac{\partial v}{\partial x}+v\frac{\partial v}{\partial y}+\frac{\partial p}{\partial y}+\frac{c_f}{2H}v\sqrt{u^2+v^2}=0, \tag{5.12}$$

where u and v are the depth-averaged velocity components in the x and y directions, respectively, H is water depth, p is the pressure.

Suppose that

$$u=\frac{\partial \psi}{\partial y},\ v=-\frac{\partial \psi}{\partial x}, \tag{5.13}$$

where $\psi(x,y,t)$ is the stream function of the flow. Eliminating the pressure and using (5.13) one can rewrite the system (5.10) – (5.12) in the form

$$\begin{aligned}&(\Delta\psi)_t+\psi_y(\Delta\psi)_x-\psi_x(\Delta\psi)_y+\frac{c_f}{2h}\Delta\psi\sqrt{\psi_x^2+\psi_y^2}\\&+\frac{c_f}{2h\sqrt{\psi_x^2+\psi_y^2}}\left(\psi_y^2\psi_{yy}+2\psi_x\psi_y\psi_{xy}+\psi_x^2\psi_{xx}\right)=0\end{aligned} \tag{5.14}$$

Consider a perturbed solution to (4.14) of the form

$$\psi = \psi_0(y) + \varepsilon\psi_1(x,y,t) + \varepsilon^2\psi_2(x,y,t) + \ldots \qquad (5.15)$$

The parameter ε describes a small deviation of the shallow wake stability parameter S from the critical value S_c:

$$S = S_c(1-\varepsilon^2) \qquad (5.16)$$

Weakly nonlinear theory is applicable in a small neighborhood of the critical point (see Fig. 16):

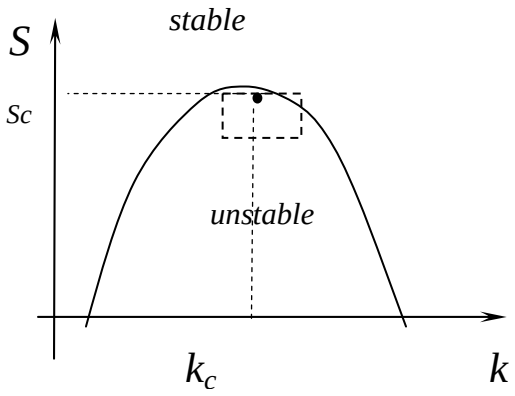

Figure 16. Neighborhood of the critical point in a weakly nonlinear Region in the (k,S)-plane (shown as dashed rectangle) where weakly nonlinear theory is applicable.

The amplitude evolution equation for the most unstable mode is derived by means of the method of multiple scales. Following [67], the following slow time and longitudinal variables are introduced:

$$\tau = \varepsilon^2 t, \quad \xi = \varepsilon(x - c_g t), \qquad (5.17)$$

where c_g is the group velocity.

The function ψ_1 in [15] is sought in the form

$$\psi_1(x,y,t) = A(\xi,\tau)\varphi_1(y)\exp[ik(x-ct)] + c.c. \qquad (5.18)$$

where A is a slowly varying amplitude.

The linear stability problem (5.3), (5.4) is obtained by substituting (5.15) – (5.18) into (5.14), collecting the terms containing ε and using (5.5). Collecting the terms containing ε^2 the following equation is obtained:

$$
\begin{aligned}
&L\psi_2 = c_g(\psi_{1xx\xi} + \psi_{1yy\xi}) - 2\psi_{1x\xi t} - \psi_{0y}(3\psi_{1xx\xi} + \psi_{1yy\xi}) \\
&-\psi_{1y}(\psi_{1xxx} + \psi_{1yyx}) + \psi_{1x}(\psi_{1xxy} + \psi_{1yyy}) + \psi_{1\xi}\psi_{0yyy} \\
&-S[(\psi_{1xx} + \psi_{1yy})\psi_{1y} + 2\psi_{1x\xi}\psi_{0y} + \psi_{1yy}\psi_{1y} - 2\psi_{0y}\psi_{0yy} \\
&+2\psi_{1x}\psi_{1xy}]
\end{aligned}
\tag{5.19}
$$

Here

$$
\begin{aligned}
&L\psi = \psi_{xxt} + \psi_{yyt} + \psi_{0y}(\psi_{xxx} + \psi_{yyx}) - \psi_{0yyy}\psi_x \\
&+\frac{c_f}{2h}\Big[(\psi_{xx} + 2\psi_{yy})\psi_{0y} + 2\psi_y\psi_{0yy}\Big].
\end{aligned}
$$

Similarly, the equation of order ε^3 has the form

$$
\begin{aligned}
&L\psi_3 = c_g(\psi_{2xx\xi} + 2\psi_{1x\xi\xi} + \psi_{2yy\xi}) - \psi_{1xx\tau} - \psi_{1yy\tau} - 2\psi_{2x\xi t} \\
&-\psi_{1\xi\xi t} - 3\psi_{0y}(\psi_{2xx\xi} + \psi_{1x\xi\xi}) - \psi_{1y}(\psi_{2xxx} + 3\psi_{1xx\xi}) \\
&-\psi_{2y}(\psi_{1xxx} + \psi_{1yyx}) - \psi_{1y}(\psi_{2yyx} - \psi_{1\xi yy}) - \psi_{0y}\psi_{2\xi yy} \\
&+\psi_{2x}\psi_{1xxy} + \psi_{1\xi}\psi_{1xxy} + \psi_{1x}\psi_{2xxy} + 2\psi_{1x}\psi_{1xy\xi} + \psi_{1x}\psi_{2yyy} \\
&+\psi_{2x}\psi_{1yyy} + \psi_{1\xi}\psi_{1yyy} + \psi_{2\xi}\psi_{0yyy} \\
&-S[\psi_{2y}(\psi_{1xx} + \psi_{1yy}) + 2\psi_{2yy}\psi_{1y} + 1.5\psi_{1xx}\psi_{1x}^2/\psi_{0y} \\
&+\psi_{2xx}\psi_{1y} + 2\psi_{1x\xi}\psi_{1y} + 2\psi_{0y}\psi_{2x\xi} + \psi_{1\xi\xi}\psi_{0y} - \psi_{1xx}\psi_{0y} \\
&-2\psi_{0yy}\psi_{1y} - 2\psi_{0y}\psi_{1yy} + \psi_{1yy}\psi_{2y} - \psi_{1y}\psi_{2yy} + 2\psi_{1x}\psi_{2xy} \\
&+2\psi_{1x}\psi_{1yy} + 2\psi_{2x}\psi_{1xy} + 2\psi_{1\xi}\psi_{1xy}]
\end{aligned}
\tag{5.20}
$$

The function ψ_2 is sought in the form

$$
\begin{aligned}
&\psi_2 = AA^*\varphi_2^{(0)}(y) + A_\xi\varphi_2^{(1)}(y)\exp[ik(x-ct)] \\
&+A^2\varphi_2^{(2)}(y)\exp[2ik(x-ct)] + c.c.
\end{aligned}
\tag{5.21}
$$

The function $\varphi_2^{(0)}(y)$ is the solution of the following boundary value problem

$$
\begin{aligned}
&2S[u_{0y}\varphi_{2y}^{(0)} + u_0\varphi_{2yy}^{(0)}] = ik[\varphi_{1y}\varphi_{1yy}^* - \varphi_{1y}^*\varphi_{1yy} \\
&+\varphi_1\varphi_{1yyy}^* - \varphi_1^*\varphi_{1yyy}] - S[k^2\varphi_1\varphi_{1y}^* + k^2\varphi_1^*\varphi_{1y} \\
&+2\varphi_{1y}^*\varphi_{1yy} + 2\varphi_{1yy}^*\varphi_{1y}],
\end{aligned}
\tag{5.22}
$$

$$
\varphi_2^{(0)}(\pm\infty) = 0. \tag{5.23}
$$

The function $\varphi_2^{(1)}(y)$ satisfies the equation

$$
\begin{aligned}
&(iku_0 - ikc)\varphi_{2yy}^{(1)} + (ik^3 c - ik^3 u_0 - iku_{0yy})\varphi_2^{(1)} \\
&+S[2u_0\varphi_{2yy}^{(1)} + 2u_{0y}\varphi_{2y}^{(1)} - k^2 u_0 \varphi_2^{(1)}] \\
&= (c_g - u_0)\varphi_{1yy} + [-2k^2 c + 3k^2 u_0 + u_{0yy} - k^2 c_g \\
&-iku_0 S]\varphi_1,
\end{aligned}
\tag{5.24}
$$

$$
\varphi_2^{(1)}(\pm\infty) = 0. \tag{5.25}
$$

The function $\varphi_2^{(2)}(y)$ is the solution of the boundary value problem

$$
\begin{aligned}
&2(iku_0 - ikc)\varphi_{2yy}^{(2)} + (8ik^3 c - 8ik^3 u_0 - 2iku_{0yy})\varphi_2^{(2)} \\
&+S[2u_0\varphi_{2yy}^{(2)} + 2u_{0y}\varphi_{2y}^{(2)} - 4k^2 u_0 \varphi_2^{(2)}] \\
&= ik(\varphi_1\varphi_{1yyy} - \varphi_{1y}\varphi_{1yy}) - S(2\varphi_{1y}\varphi_{1yy} - 3k^2\varphi_1\varphi_{1y}),
\end{aligned}
\tag{5.26}
$$

$$
\varphi_2^{(2)}(\pm\infty) = 0. \tag{5.27}
$$

The amplitude evolution equation for A is obtained from the solvability condition for equation (5.20) and has the form of the complex Ginzburg-Landau equation (the equation is derived in detail in [44]):

$$
\frac{\partial A}{\partial \tau} = \sigma A + \delta \frac{\partial^2 A}{\partial \xi^2} - \mu |A|^2 A \tag{5.28}
$$

The coefficients of equation (5.28) are given by

$$
\sigma = \frac{\sigma_1}{\gamma},\ \delta = \frac{\delta_1}{\gamma},\ \mu = \frac{\mu}{\gamma}, \tag{5.29}
$$

where

$$
\gamma_1 = \int_{-\infty}^{+\infty} \varphi_1^a(\varphi_{1yy} - k^2\varphi_1)dy, \tag{5.30}
$$

$$
\sigma_1 = S\int_{-\infty}^{+\infty} \varphi_1^a(2u_0\varphi_{1yy} + 2u_{0y}\varphi_{1y} - k^2 u_0\varphi_1)dy, \tag{5.31}
$$

$$
\begin{aligned}
\delta_1 = &\int_{-\infty}^{+\infty} \varphi_1^a[\varphi_{2yy}^{(1)}(c_g - u_0) + \varphi_2^{(1)}(-k^2 c_g - 2k^2 c \\
&+3k^2 u_0 + u_{0yy} - 2iku_0 S) + \varphi_1(2ikc_g + ikc \\
&-3iku_0 - US)]dy,
\end{aligned}
\tag{5.32}
$$

$$\mu_1 = \int_{-\infty}^{+\infty} \varphi_1^a \{6ik^3\varphi_2^{(2)}\varphi_{1y}^* - 2ik\varphi_{1y}^*\varphi_{2yy}^{(2)} + 3ik^3\varphi_1^*\varphi_{2y}^{(2)}$$
$$+ik^3\varphi_1(\varphi_{2y}^{(0)} + \varphi^{*(0)}_{2y}) - ik\varphi_{1yy}(\varphi_{2y}^{(0)} + \varphi^{*(0)}_{2y})$$
$$+ik\varphi_{2y}^{(2)}\varphi_{1yy}^* - ik\varphi_1^*\varphi_{2yyy}^{(2)} + ik\varphi_1(\varphi_{2yyy}^{(0)} + \varphi_{2yyy}^{*(0)}) \qquad (5.33)$$
$$+2ik\varphi_{1yyy}^*\varphi_2^{(2)} - 2S[-k^2\varphi_1(\varphi_{2y}^{(0)} + \varphi^{*(0)}_{2y})$$
$$+3k^2\varphi_1^*\varphi_{2y}^{(2)} - 1.5k^4\varphi_1^2\varphi_1^*/u_0 + 2\varphi_{1yy}(\varphi_{2y}^{(0)} + \varphi^{*(0)}_{2y})$$
$$+2\varphi_{1yy}^*\varphi_{2y}^{(2)} + 2\varphi_{1y}(\varphi_{2yy}^{(0)} + \varphi^{*(0)}_{2yy}) + 2\varphi_{2yy}^{(2)}\varphi_{1y}^*]\}dy$$

In addition, one needs to calculate the adjoint eigenfunction φ_1^a of the linear stability problem:

$$(iku_0 + 2Su_0)(\varphi_1^a)'' + (2iku_{0y} + 2Su_{0y})(\varphi_1^a)'$$
$$-(ik^3u_0 + u_0k^2S)\varphi_1^a + ikc[(\varphi_1^a)'' - k^2\varphi_1^a] = 0 \qquad (5.34)$$

$$\varphi_1^a(\pm\infty) = 0\,. \qquad (5.35)$$

The group velocity c_g is given by

$$c_g = \frac{I_1}{I_2}, \qquad (5.36)$$

where

$$I_1 = \int_{-\infty}^{+\infty} [u_0\varphi_{1yy} - \varphi_1(3k^2u_0 + u_{0yy}$$
$$-2k^2c - 2iku_0S)]\varphi_1^a dy$$

$$I_2 = \int_{-\infty}^{+\infty} \varphi_1^a(\varphi_{1yy} - k^2\varphi_1)dy\,.$$

Solving boundary value problems (5.22) – (5.27), calculating φ_1^a and c_g and evaluating integrals in (5.30) – (5.33) numerically, the coefficients of the CGLE (5.28) are obtained for different values of R. The results are summarized in Table 4.

R	σ	δ	μ
-0.3	0.063 + 0.004i	0.060 – 0.206i	4.673 + 13.294i
-0.4	0.078 + 0.003i	0.090 – 0.195i	3.796 + 10.938i
-0.5	0.090 + 0.000i	0.115 – 0.184i	3.895 + 10.119i
-0.6	0.100 – 0.003i	0.136 – 0.172i	4.375 + 10.109i
-0.7	0.109 – 0.007i	0.153 – 0.161i	5.149 + 10.590i
-0.8	0.116 – 0.012i	0.167 – 0.152i	6.302 + 11.448i

TABLE 4
Coefficents of the CGLE (5.28)

One of the major conclusions drawn from weakly nonlinear analysis applied to quasi-two-dimensional flows in [22] was the effect of strong dependence of the Landau constant μ_r on the form of the base flow profile. Calculations presented in [22] showed that the values of the Landau constant differed by a factor of 3 for two base flow velocity profiles whose linear stability characteristics differed by only 20%. As a result, it was concluded in [22] that it would be impossible to apply methods of weakly nonlinear theory in practice since the base flow profile cannot be determined very precisely in experiments. In other words, it was concluded in [22] that the problem of determination of the Landau constant from weakly nonlinear theory is ill-posed so that small variations of the base flow profile lead to large changes in the Landau constant.

The calculations presented in Table 3 and 4 in our paper demonstrate that the coefficients of the CGLE are not so sensitive to the variation of the parameter R of the base flow profile (5.2) as claimed in [22]. In fact, not only the Landau constant is not so sensitive to the changes in the profile (5.2) but all the coefficients of the CGLE do not vary too much.

CONCLUSIONS

The thesis is devoted to the analysis of factors that influence the structure and stability of magnetohydrodynamic (MHD) flows and shallow water flows. In particular, the effects of wall resistance on the flow can be described locally (taking into account roughness of the boundary) or globally (using semi-empirical formulas describing the effect of internal friction). Roughness of the bolundary can occur as a result of corrosion. Experimental results demonstrated essential influence of magnetic field on the corrosion process both in the intensity of corrosion and its character. Therefore, it is important from a practical point of view to analyze the effect of roughness on the structure of magnetohydrodynamic flows. This effect is evaluated in the thesis by solving the system of magnetohydrodynamic equations analytically (using the Fourier transform). Several forms of surface roughness are considered in the thesis. Analytical solutions are found and velocity distribution is analyzed numerically for different Hartmann numbers. Asymptotical solution for high Hartmann numbers is also found. The solutions are found in terms of integrals containing oscillatory functions. These integrals are transformed in the thesis to integrals containing non-oscillatory functions.

Global effect of internal friction is usually taken into account by using empirical resistance formulas like Chezy formula to estimate the “lumped” effect of turbulent flows for the computation of flow rate and losses in channels or pipes and design of open channels. These formulas contain empirical friction coefficients that are directly related to the Reynolds number of the flow and the roughness of the boundary. The coherent structures in wake flows behind obstacles are believed to appear as a final product of hydrodynamic instability of the flow. Methods of weakly nonlinear stability theory have been applied in the past to different flows and usually lead to amplitude evolution equations for the most unstable mode. One of such equations is the complex Ginzburg-Landau equation. Weakly nonlinear theory applied to quasi-two-dimensional flows with Rayleigh friction (internal friction is assumed to be linearly related to the velocity distribution) led to the conclusion that the coefficients of the amplitude evolution equation (Ginzburg-Landau equation) for the most unstable mode strongly depend on the shape of the base flow profile. As a result it was concluded in the literature that weakly nonlinear models cannot be used for such cases since it is impossible to determine experimentally the base

flow velocity distribution with high accuracy and, therefore, one cannot use reliable values of the coefficients of the Ginzburg- Landau equation. It is shown in the thesis that if a nonlinear formula is used to model bottom friction then the coefficients of the Ginzburg-Landau equation are not sensitive to the base flow velocity distribution.

Literature review is presented in the Chapter 1. In addition, the structure of the thesis and the main results are discussed.

In Chapter 2 we state the principles of MHD flows and then we describe the influence of the surface roughness on the MHD flow of a conducting metal and state the governing equations. Since MHD flow problems are widely studied in channels of various forms and different boundary conditions, the results of such studies have direct applications in different fields of magnetohydrodynamics [29], [38], and [58]. Since magnetohydrodynamics studies the motion of electrically conducting fluids in the presence of magnetic fields, it is obvious that the magnetic field influences the fluid motion. Usually in MHD problems electromagnetic force is added to the equation of motion and the magnetic field (through Ohm's law) changes the fluid motion. We describe some MHD flow problems in ducts over the roughness elements in a strong magnetic field and analytical solutions of such problems are obtained using the Dirac delta function (see [3], [4], [6], [7], [12], [13], [17], [18]).

Asymptotic analysis of these problems is performed for the case of strong magnetic fields and graphs of the z-components of the current are shown for different Hartmann numbers. Different boundary layers for the field velocity and for the z-components of the currents at large Hartmann numbers are analyzed. The MHD problem for fully developed flow is solved for the cases of a uniform and non-uniform external magnetic field where the surface roughness is taken into account. The distribution of fluid velocity, induced current with its potential and external magnetic field are derived (see the following references for the analysis of similar problems [2], [5], [11]-[13], [17], [18], [21], [30], [31], [42], [50], [53], [54], [57], [59], [65], [69]).

Chapter 3 is devoted to the calculation of some classes of improper oscillatory integrals. It is shown that oscillatory integrals in some cases can be transformed to integrals of non-oscillatory functions. Such integrals have direct applications to MHD flows analyzed in the thesis. These results are applied in order to transform the solution of some MHD problems arising in half space $z \geq 0$ as a result of roughness of the surface $z = 0$ for various boundary layers (see [3], [4], [6], [7], [17], [72], [74]).

During my seven year stay in Riga, Latvia (one the main MHD application centers in Europe), I had the opportunity to visit some interesting sites related to MHD study such as the Physics Institute in Salaspils where I have seen the three recently planned experimental sessions (each 2000 hours long) which have been finished successfully. Results gained in these investigations demonstrated essential influence of magnetic field on the corrosion processes both in the intensity of corrosion and its character. New results concerning the profile of corrosion are obtained [55] and [56]. Such studies have an important implication on how to confine and control the burning D-T plasmas by a strong drag of magnetic fields inside a reactor [1], [9], [55], [56], [70] and [73]. In addition, I had the opportunity to participate in some PAMIR MHD International Conferences (4^{th} , 5^{th} and 7^{th} PAMIR International Conferences) . As a result of these activities Chapter 4 of the thesis describing practical aspects related to the effect of surface roughness on MHD flows ([1], [9], [32]-[37], [39], [40], [48], [49], [55]-[57], [60], [64], [68], [70] and [73]) is written.

Chapter 5 is devoted to the analysis of shallow water flow in a weakly nonlinear regime using the complex Ginzburg-Landau equation (CGLE). It is shown in the previous studies [22] related to weakly nonlinear analysis of quasi-two-dimensional flows (shallow water flow is one of the examples considered in [22]) that the values of the Landau's constant differ by a factor of 3 for two different velocity profiles with linear stability characteristics (differing by not more that 20%). In other words, the Landau's constant was found to be quite sensitive to the shape of the base flow profile. In Chapter 5 the bottom friction is modeled by a nonlinear Chezy formula [66]. The analysis of data presented in Table 3 and Table 4 shows that for a one-parametric family of shallow wake flows the changes in the linear stability characteristics resulted in even smaller changes in the coefficients of the CGLE. As a result, it is plausible to conclude that the complex Ginzburg-Landau equation can be used for the analysis of shallow wake flows in a weakly nonlinear regime (see [8], [10], [14]-[16], [19], [22], [26], [43]-[47], and [67]) for the application of weakly nonlinear models to different flows in fluid mechanics.

Appendix 1

NOMENCLATURE

List of Latin Symbols

A The cross-sectional area

$\mathbf{B}^{e} = \mathrm{B}_0\mathbf{e}_z$ .the form of the external magnetic field

B_0 The potential of the magnetic field

$\vec{B}$ Complex-valued amplitude magnetic induction vector

$\vec{\tilde{B}}$ Magnetic induction vector, $\vec{\tilde{B}} = \vec{B}e^{jwt}$

c Euler conctant, c = 0.577215…

C The flow core, $Ha^{-1} < z < Ha$;

c.c. Complex conjugate

c_f The friction (or roughness) coefficient,

$\mathbf{C}_r$ The Chromium element (Atomic Number 24)

CGLE The Complex Ginzburg-Landau Equation

$\vec{E}$ Complex-valued amplitude electric field vector

$\vec{\tilde{E}}$ Electric field vector $\vec{\tilde{E}} = \vec{E}e^{jwt}$

EFDA The European Fusion Development Agreement

$\mathrm{erf}(x) = \frac{2}{\sqrt{\pi}}\int_0^x e^{-\xi^2}\,d\xi$ The probability integral. (Gauss error function)

$\vec{F}$ The bottom friction force of water flows

$\vec{f}_R = -\lambda_R\vec{u}$ the friction in fluid system g The acceleration due to gravity

$K_\nu(z)$ The modified Bessel function of the second kind of order ($\nu = 1, 2$)

h The water depth

H The Hartmann layer, $0 < z < Ha^{-1}$;

Ha The Hartmann number

ITER The International Thermonuclear Experimental Reactor

j Imaginary unit, $j = \sqrt{-1}$

L Length scale

Li The Lithium element (Atomic number 3)

Pb The lead element (Atomic number 82)

Ni The Nickel element (Atomic number 28)

Nu The Nusselt number

$\vec{n}$ The unit normal vector to the surface

Re The Reinholds number

S The stability parameter

S_c The critical stability value

Si The Silicon Element (Atomic number 14)

T The temperature in Kelvin.

$\vec{u}$ & $\vec{v}$ Velocity vectors

v The velocity scale

V_c The core velocity constant

X Real part of Z

Y Imaginary part of Z

$Y_\nu(s)$ Bessel function of the second kind of order ν

W The distant wake, $Ha < z < +\infty$.

$\tilde{z} = \tilde{\chi}_0 \tilde{f}(\tilde{x})$ The roughness of the surface of a channel's wall

List of Greek Symbols

$\Gamma(x)$ Euler Gamma function

Δ Laplacian , $\Delta f(x,y,z) = \frac{\partial^2 f}{\partial x^2} + \frac{\partial^2 f}{\partial y^2} + \frac{\partial^2 f}{\partial z^2}$

$$\Delta f(r,\phi,z) = \frac{1}{r}\frac{\partial}{\partial r}\left(r\frac{\partial f}{\partial r}\right) + \frac{1}{r^2}\frac{\partial^2 f}{\phi^2} + \frac{\partial^2 f}{\partial z^2}$$

$\delta(\tilde{x})$ The Dirac delta function

λ_R The coefficient of Rayleigh friction

μ_0 Magnetic constant

ρ Density of fluid

ν The Viscosity of fluid

$\tilde{\rho}$ Charge density

σ Conductivity

ψ Scalar electric potential intensity

$\widetilde{\psi}$ Scalar electric potential, $\widetilde{\psi} = \psi e^{jwt}$

ω Frequency

$\eta(\widetilde{x}) = \begin{cases} 0, \widetilde{x} < 0, \\ 1, \widetilde{x} > 0. \end{cases}$ The Heaviside step function

ϕ Potential of current

$$V_y{}^c(\lambda, z) = \sqrt{\frac{2}{\pi}} \int_0^\infty V_y(x, z) \cos \lambda x dx$$ The Fourier cosine transform

$\Phi^s(\lambda, z) = \sqrt{\frac{2}{\pi}} \int_0^\infty \Phi(x, z) \sin \lambda x dx$. The Fourier sine transforms

Coordinate systems

(x,y,z) Cartesian coordinates, $x,y,z \in \Re$

(r, ϕ ,z) Cylindrical polar coordinates , $r \geq 0,\ 0 \leq \phi \leq 2r,\quad z \in \Re$

(ρ, θ, ϕ) Spherical coordinates , $\rho \geq 0$, $0 \leq \theta \leq 2\pi$, $0 \leq \phi \leq \pi$,

Classes of definite integrals

$$\int_0^\infty \frac{P_n(\lambda^2)}{Q_m(\lambda^2)} e^{-a\sqrt{\lambda^2+b^2}} \frac{\cos\lambda \cos\lambda x}{\lambda^2 - \frac{\pi^2}{4}} d\lambda , \quad I_1 = \sqrt{\frac{2}{\pi}} \int_0^\infty \frac{P_n(\lambda^2)}{Q_m(\lambda^2)} \frac{\cos\lambda \cos\lambda x \, d\lambda}{\lambda^2 - \frac{\pi^2}{4}} = \varphi(x),$$

Appendix 2

LIST OF FIGURES AND TABLES

REFERENCES

[1] Abdou.M., Sawan M. Physics and technology conditions for attaining tritium self sufficiency for the DT fuel cycle, Fusion Engineering & Design, vol. 81, pp. 1131-1144 (2006).

[2] Antimirov M.Ya., Lielausis O.A., Ligere E.S. Shishko A.Ya. Linear approximation to the flow over roughness elements in a strong magnetic field, Fifth International Pamir Conference on Fundamental and Applied MHD, Volume 1. Ramatuelle, France, (2002).

[3] Antimirov M.Ya., Kolyshkin, A.A. Vaillancourt, R. Applied Integral Transforms. AMS, Providence (1993).

[4] Antimirov M.Ya. , Kolyshkin, A.A. Vaillancourt, R. Complex variables. Academic Press (1998).

[5] Antimirov M.Ya., Chaddad I.A. Solution of the flow over the roughness elements of special shape in a strong magnetic field, Magnetohydrodynamics, vol. 41, no. 1, pp. 3 – 17 (2005).

[6] Antimirov.M.Ya, Dzenite I. Evaluation of new classes of Definite Integrals, Scientific Proceedings at Riga Technical University,5th series: Computer Science,43rd thematic Issue, vol., pp 32-39, Riga, RTU (2001).

[7] Antimirov.M.Ya, Dzenite I. Evaluation of new classes of definite integrals, Proceeding of the 3rd European Congress of Mathematics, ECM , Barcelona (SPAIN), July 10-15 (2000).

[8] Aranson L.S., Cramer L. The world of the complex Ginzburg-Laundau equation, Review of Modern Physics vol. 74, pp. 99-143 (2002).

[9] Benamati G., Fazio G, .Ricapito C: Mechanical and corrosion behavior of EUROFER 97 steel exposed to Pb-17Li. Journal of Nuclear Materials, vol. 307-311, 2, pp.1379-1383 (2002).

[10] Blennerhassett P.J. On the generation of waves by wind, Philosophical transactions of the Royal Society of London, Ser. A Mathematical and Physical Sciences, vol. 298, pp 451-494 (1980).

[11] Buikis A, Kalis H. Numerical modeling of heat transfer in magnetohydrodynamic flows in a finite cylinder, Computational Methods in Applied Mathematics , vol.2. No.3, pp.243-259 (2002).

[12] Chaddad I.A., Antimirov M.Ya. Solution of a problem to the flow over the roughness elements of a special form in a strong magnetic field , 5th Pamir International conference, Fundamental and applied MHD, Poster session 1, June 27 – July 1, Riga, Latvia (2005).

[13] Antimirov M.Ya., Chaddad I. A. Analytical solution of the MHD problem to the flow over the roughness elements using the Dirac Delta function, Scientific Proceedings at Riga Technical University,5th series: Computer Science, 46th thematic issue,vol.13, pp. 123 – 136, Riga, RTU (2004).

[14] Chaddad I. A., Kolyshkin A.A. Ginzburg-Landau model: an amplitude evolution equation for shallow wake flows, Proceedings of World Academy of Science, Engineering and Technology, vol. 28, pp. 1 – 5. April (2008).

[15] Chaddad, I. A., Kolyshkin A. A Ginzburg-Landau model: an amplitude evolution equation for shallow wake flows, International conference on Mathematics and Statistics, Rome, Italy, April 25 – 27 (2008).

[16] Chaddad I. A., Kolyshkin A. Ginzburg-Landau model: an amplitude evolution equation for shallow wake flows, International Journal of Mathematical, Physical and Engineering Sciences, vol. 2, no. 3, pp. 126 – 130 (2008).

[17] Ligere E.S., Chaddad I. The transformation of one class of integrals containing oscillating functions and its application to some MHD problems, Proceeding of Riga Technical University, 5th series: Computer Science, 45th issue, vol.7, pp. 70 – 78, Riga, (2003).

[18] Chaddad.I.A. On the form of magnetic field of fully developed MHD equations. Proceeding of Riga Technical University,6th series: Computer Science, 46th issue, vol.9, pp. 113 – 122, Riga, RTU (2004).

[19] Chen D., Jirka G.H. Absolute and convective instabilities of plane turbulent wakes in shallow water, Journal of Fluid Mechanics, vol. 338, pp. 157-172 (1997).

[20] Cross M.C., Honenberg P.C . Pattern formation outside of equilibrium, Reviews of Modern Physics, vol. 65, pp. 851-1112 (1993).

[21] Davidson P.A. An introduction to magnetohydrodynamics, Cambridge University Press, (2001).

[22] Dolzhanskii F.V. Krymov V.A., Manin D. Yu. Stability and vortex structures of quasi-two-dimentional shear flows, Soviet Physics Uspekhi, vol. 33, pp. 495-520 (1990).

[23] Dufrenoy T, Rodi W. Developments in computational modelling of turbulent flows. In 'ERCOFTAC'. Workshop on numerical simulation of unsteady flows. Cambridge Univ. Press, pp. 1-76 (1996).

[24] Drazin, P.G and Reid W.H. Hydrodynamic stability (second edition), Cambridge University Press (2004).

[25] EFDA (European Fusion Development Agreement) The European Fusion Research Programme:Strategic outlook for infrastructure towards DEMO. EFDA associates and F4E (2008).

[26] Fedderson F. Weakly nonlinear shear waves, Journal of Fluid Mechanics, vol. 372, pp. 71-91 (1998).

[27] Gazzola F., Secchi P. Some results about Stationary Navier-Stokes equations with a pressure dependent viscosity, Proceedings of the International Conference on Navier- Stokes. Equations, Theory and Numerical Methods, Varenna 1997, pp. 131-137 (1998).

[28] Gelfgat YM., Lielausis O.A., Shcherbinin E.V. Liquid metal under influence of electromagnetic forces, Riga (1975) (In Russian).

[29] Hartmann J. Theory of the laminar flow of an electrically conductive liquid in a homogenous magnetic field, Mat.fys. medd. K. Danske videnskab. Selskab, bd. 15, no. 7 (1937).

[30] Hunt, J.C.R., Stewartson K. Magnetohydrodynamic flow in a rectangular ducts II, Journal of Fluid Mechanics, vol. 23, pp 563-581 (1964).

[31] Hunt, J.C.R., Moreau R. Liquid metal magnetohydrodynamics with strong magnetic fields: a report on Euromech 70, Journal of Fluid Mechanics, vol. 78, pp.261-288 (1976).

[32] Ihle H., Wu C. Chemical thermodynamics of fusion reactor breeding materials and their interaction with tritium, Nuclear.Materials, vol.130, No.3, pp. 454-464 (1985).

[33] ITER Physics basis, Nuclear Physics Documentation vol.47, Number 6 pp. S1-414 (2007).

[34] ITER EDA Agreement and Protocol 2. Documentation series Number 5.IAEA Vienna (1999).

[35] ITER special working group report on task 1 results. ITER Council proceeding (1998).

[36] Shimomura, Y., Spears, W. Review of the ITER project, IEEE Transactions on Applied Superconductivity, vol. 14, pp. 1369 -1375 (2004).

[37] ITER Council proceeding: ITER DEMO Documentation series Number 20. IAEA Vienna (2007).

[38] Jackson J.D. Classical electrodynamics, Wiley (1986).

[39] Jeffrey. P., Freidberg Plasma Physics and Fusion energy, Cambridge University Press (2006).

[40] Kallenrode M.-B., An Introduction to Plasmas and Particles in the Heliosphere and Magnetospheres. (Second Edition) Springer (2001).

[41] Metallurgical technologies, energy conversion, and magnetohydrodynamic flows, Progress in Astronautics and Aeronautics, vol. 148, Published by AIAA (1993).

[42] Sterl A. Numerical simulation of liquid-metal MHD flows in rectangular ducts, Journal of Fluid Mechanics , vol. 216, pp. 161 - 191 (1990).

[43] Kolyshkin A.A., Ghidaoui M.S. A quasi-steady approach to the stability of time-dependent flows in pipes, Journal of Fluid Mechanics vol. 465, pp. 301-330 (2002).

[44] Kolyshkin A.A., Ghidaoui M.S. Stability analysis of shallow wake flows, Journal of Fluid Mechanics, vol. 494, pp.355-377 (2003).

[45] Kolyshkin A.A., Nazarovs S. Influence of averaging coefficients on weakly nonlinear stability of shallow flows, IASME transactions, Issue 1, vol.2, pp. 86-91 (2005).

[46] Kolyshkin A.A., Vaillancourt, R., and Volodko, I. Weakly nonlinear analysis of rapidly decelerated flow, IASME transactions. Issue 7, vol. 2, pp. 1157-1165 (2005).

[47] Kolyshkin A.A. Chaddad I.A. Ginzburg- Landau equation for stability of water flow in a weakly nonlinear regime, Scientific Proceedings at Riga Technical University,5th series: Computer Science,49th thematic issue, vol. 33, pp. 58-64, Riga, RTU (2007).

[48] KYOTO Protocol to the United Nations framework convection on climate change By United States Congress. House. Committee on Science United Nations Framework Convention on ClimateChange (2007).

[49] Leavenworth H.W., Clealy R.E. The solubility of Ni, Cr, Fe, Ti and Mo in lithium. Acta Metallurgica, vol.9, no.5, p.519-520 (2002).

[50] Lorrain P., Lorrain F., Haule S. Magneto-fluid dynamics. Fundamentals and case studies of natural phenomena. Springer (2006).

[51] Max-Plank Institute for Plasma Physics- Research for Energy of the Future. Vol.2 Issue3. Berlin (2005).

[52] Micheal I. Study of MHD problems in liquid metal blankets of fusion reactors, KFK-3839, Karlsruhe Nuclear Research Center (1984).

[53] Moreau R. Magnetohydrodynamics , Kluwer (1990).

[54] Muller U., Buhler L. Magnetofluiddynamics in channels and containers, Springer (2001).

[55] Platacis.E, Shishko.A, Bucenieks.I., Krishbergs R., Lipsbergs G, Zik A., & Muktepāvela F., Assessement of Magnetic field effects on EUROFER Corrosion in Pb.17 Li at 550°C, EFDA, Final report TTBC-006-D1, Salaspils, Latvia (2006).

[56] Platacis.E, Shishko.A, Bucenieks.I., Krishbergs R. Analysis of the strong magnetic field influence on the Corrosion of EUROFER steel in Pb.17 Li flows, Salaspils, LATVIA (2008).

[57] Porleon L., Miyazaki,K. Reed C. Present understanding of MHD and heat transfer phenomena for liquid metal blankets. Report 8 ANL/TD/CP--83938; CONF-940664-27, Washington, DC , USA (1998).

[58] Priest E, Forbes T. MHD Theory and Applications, Cambridge University Press (2000).

[59] Ramos J.I, Picologlu Numerical simulation of liquid metal MHD in rectangular ducts. Physics of Fluids 29, pp.34-42 (1996).

[60] Ramos J. Report of of the PROTO Project on joint implementastion of ITER : Documentation series. Number 20. IAEA Vienna (2007).

[61] Schultz B. Thermophysical properties of the Li17Pb83 alloy, Fusion Engineering and Design activities . vol. 14, Issues 3-4, pp.199-205 (2005).

[62] Shimomura Y. Large eddy simulation of magnetohydrodynamic turbulent channel flows

under a uniform magnetic field, Physics of Fluids A, vol. 3, pp. 3098 -3106 (1991).

[63] Shimomura Y. ITER: opportunities of burning plasma studies, Burning Plasma Science Workshop, San Diego, USA, May 1 – 3, (2001).

[64] Simon N., Terlain A., Flament T. The compatibility of martensitic sttels with liquid Pb 17 – Li, Journal of Nuclear Materials, vol. 254 . pp 185-194 (1998).

[65] Singh B., Lal J. Heat transfer in an MHD channel flow with boundary conditions of the third kind, Applied Scientific Research, vol. 48, no. 1, pp. 11 - 33 (1991) .

[66] Streeter V.L., Wylie E.B., Bedford K.W. Fluid Mechanics (9th edition) McGraw Hill (1998).

[67] Stewartson, K. & Stuart J.T. A nonlinear instability theory for a wave system in plane Poiseuille flow. Journal of Fluid Mechanics, vol. 48, pp. 529-545 (1971).

[68] Stott G., PeterE. Diagnostics for thermonuclear Fusion reactors part 2, Proceedings of the International School of Plasma Physics "Piero Caldirola" Workshop on Diagnostics for Experimental Fusion Reactors, held September 4-12, in Varenna, Italy (1997).

[69] Valdmanis J., Shishko A., & Krishbergs R. MHD flow pattern near the rough Hartmann wall subjected to corrosion process, 4th International conference of electromagnetic proceeding of materials, France (2007).

[70] Levinton, F.M., Batha, S., Yamada, M., Zarnstroff, M.C. Q-profile measurements in the Tokamak fusion test reactor, Physics of Fluids B, vol. 5, pp. 2554- 2559 (1993).

[71] Antimirov M. Ya., Kremenetsky V.N. Magnetohydrodynamical flow of a flat submerged jet into semi-space in a strong magnetic fields . Magnitnaya Gidrodinamika, 32(1):56-62, (in Russian) (1996).

[72] Ditkin V.A., Proudnikov A. P. Integral transforms and operational calculus, Moscow , FizMatGiz (1979) (In Russian).

[73] Gryaznov G.M., Evtikhin V.A., Zavyalsky L.P. et al. Material science of liquid metal systems for thermonuclear reactors, Energoizdat Publishing House, Moscow, (In Russian) / (1989).

[74] Prudnikov A.P., Brychkov Yu.A., Marichev O.I. Integrals and Series, Science journal, Moscow, Nauka, (1981) (In Russian).

[75] Vatazin A.B., Lubimov G.A., Regirer S.A. Magnetohydrodynamic flows in channels, Moscow, Nauka, (1970) (In Russian).